SHORT TERM WEATHER FORECASTING TECHNIQUES FOR HEAVY RAINFALL

LL Dyson · J van Heerden · HG Marx

WRC Report No. 1011/1/02

Water Research Commission

Short Term Weather Forecasting Techniques for Heavy Rainfall

LL Dyson • J van Heerden • HG Marx

Report to the Water Research Commission
by
Department of Geography, Geoinformatics and Meteorology
University of Pretoria

WRC Report No: 1011/1/02
ISBN NO 1-86845-937-3

November 2002

ACKNOWLEDGEMENTS

The project team would like to thank the Water Research Commission, especially Dr G C Green, who provided the support which made this project possible.

The project steering committee gave invaluable guidance and support. The following persons all served on the steering committee:

Dr GC Green (Chairman)
Ms E Banitz (De Coning)
Mr DB du Plessis
Dr D Terblanche
Mrs CM Smit (Secretary)
Mr H Maaren
Mr C Turner
Mr J van Heerden
Mr OA van der Westhuizen
Ms U Wium (Secretary)
Mr KE Estie
Mr C Swiegers
Prof GGS Pegram
Mr J Taljaard

The University of Pretoria (UP) provided most of the infrastructure, which made the project run smoothly. The support and encouragement of Prof S A de Waal (Department of Geology, UP) is gratefully acknowledged as is the encouragement of Prof K S O Beavon (Department of Geography, Geoinformatics and Meteorology, UP).

Special thanks go to the management of the South African Weather Service who allowed some of their personnel to actively participate in this research project. The South African weather forecasters and especially those in the central forecasting office are acknowledged for their support, the sharing of their knowledge, the endurance of criticism and above all their eagerness to learn. A special dedication goes to Mr E P Scholz, who, despite his more than 30-years of forecasting experience is the first and most willing to test and employ new techniques which may improve the forecasting of rainfall.

The project team herby acknowledge, with sincere thanks, the contribution and support of the following people

Mr W Tennant (SAWS)
Ms M Mittermaier (SAWS)
Ms C De Villiers (SAWS)
Prof WJR Alexander (UP)
Mr L Banitz (SAWS)
Ms C Bruyere (SAWS)
Ms K Marais (SAWS)
Mr ITH Deyzel (SAWS)
Ms G Swart (SAWS)
Ms E Stewart (SAWS)

The Project Team consisted of:

Prof J van Heerden (UP)
Mr L Masimini (UP)
Ms LL Dyson (UP)
Ms L Clark (UP)
Ms HG Pienaar (UP & SAWS)
Ms H Kenyon (UP)

Collaborators:

Mr ER Poolman (SAWS)

Prof J van Heerden expresses his personal gratitude to the team members and collaborators for their dedication.

EXECUTIVE SUMMARY

Abstract

The project set out to develop a computer-based quantitative precipitation forecast system for South Africa. The aims also included research on past heavy rainfall events, evaluation of their predictability and the classification of associated systems according to their dynamical characteristics. The project succeeded in developing systems that delineate heavy rainfall from tropical and coastal zone baroclinic systems. A further product, an operational verification system to evaluate the quality of Eta rainfall prognoses, became operational at the SAWS in September 2001.

Introduction

Serious floods happen over South Africa. Recent examples are the devastating floods over the Northern Province of South Africa during February 2000, the famous Kwazulu-Natal floods of September 1987, the Free State floods of February 1988 and 1996, to name but a few. These caused loss of life and damage to infrastructure easily amounting to R 1000 million. The tools available to the weather forecaster are at present still unable to provide accurately predicted rainfall amounts. Pinpointing the exact area where the heavy rainfall will be concentrated is very difficult. This is so in spite of all the recent advances in Numerical Weather Prediction (NWP) models.

The atmospheric flow field plus the many dynamical parameters derived from NWP models are complex and it is beyond the human mind to integrate them all. The project set out to test these parameters against the occurrence of heavy rainfall. In this way those combinations of dynamical parameters consistently associated with heavy rainfall over South Africa could be identified. The mechanisms responsible for heavy rainfall could subsequently be determined and products developed to delineate areas where heavy rainfall occurs.

Considering the operational environment under which weather forecasts are prepared it was considered imperative to produce a product that is easily accessible to the forecaster. The final product must also be applicable in a flood management environment.

Aims of the Project

The aims of the FORFLOOD Project detailed in the original contract, but slightly modified during the Steering Committee meetings, can be subdivided into the main objective and secondary goals:

The main objective of this project was to research the atmospherical circulation in order to:

- Make available a Quantitative Precipitation Forecast (QPF) for input into an envisaged DWAF/Weather Service River Flow Project by improving forecasting techniques and developing a new forecasting system for the period 6 to 48-hours ahead.

In order to achieve this main goal, secondary research aims of the project were listed:

- Devise a method to classify weather systems into Baroclinic, Tropical or Tropical-Temperate using synoptic data.
- Classify all past heavy rainfall events in South Africa as Baroclinic, Tropical or Tropical-Temperate.
- Evaluate all past forecasts issued for these heavy rainfall events.

Major Results and Achievements

For the first time, in southern Africa, a system is available which reliably delineates areas where heavy rainfall can be expected with a good degree of accuracy. This system is based on meteorological dynamics but depends on the accuracy of the data fields generated by NWP models. The analysis and integration performed by the heavy rainfall identification system is easily accomplished in the short time available to the meteorologist in the operational environment and empowers him/her to make predictions, which would otherwise be beyond the capacity of any meteorologist.

The heavy rainfall identification system is made of three independent sub-systems:

The first of these is MITS (model for the identification of tropical weather systems), which determines whether a weather system is tropical. It also delineates the area where rainfall from convective weather systems will develop.

The second, THERIS (tropical heavy rainfall identification system) is a powerful, unique system for isolating heavy rainfall forced by continental tropical weather systems. THERIS runs on both digital forecast data from numerical models and archived analysis data. THERIS should also perform well north of South Africa.

BARCOZ (baroclinic rainfall system for the coastal zone) isolates areas where heavy rainfall can be expected from typical baroclinic weather systems. Most important amongst these were the cut-off low-pressure systems. The research revealed new parameters: Convergence of the gradient of the moisture flux by the southeastern (meridional) component of the wind. These new parameters are referred to as SEC (MC). When SEC was applied with upward motion under specified conditions, BARCOZ was able to isolate heavy rain from baroclinic systems.

The results of the heavy rainfall identification systems are assimilated by a Geographical Information System (GIS) and are available for publication on the World Wide Web.

During the development of MITS, THERIS and BARCOZ it became clear that synoptic scale data do not have the resolution to resolve some of the severe and important smaller scale rainfall events. The systems were very successful in isolating areas of heavy rain but were unable to explain severe events such as the Port Elizabeth flood in 1968 or the very heavy rainfall along the escarpment.

Ongoing research on the geographical and spatial characteristics of widespread rain indicated that the frequency and magnitude of these systems changed, probably during the long period with above normal rainfall of the 1970's. The research also indicated that the relationship between the frequency of occurrence of these systems and the southern oscillation index (SOI) is tenuous at best.

In the quest to evaluate past forecasts of heavy rainfall the project team failed to get a record of past rainfall forecasts from the SAWS, apart from a short period of some 4 years. The historic rainfall forecasts were unavailable to the project team, lost or irretrievable. The forecasts, which were available, formed the basis of research on the reliability of rainfall forecasts over the Vaal Dam catchment. Research to test the accuracy of SAWS rainfall forecasts over the Vaal Dam catchment indicated that forecasters tended to err on the conservative side. The project also evaluated the Eta model rainfall prognoses statistically against rainfall figures computed from radar reflectivity data as well as conventional rainfall gauge data. Verifying the Eta model predictions against gauge data became operational at the SAWS in September 2001. Over the 6-month operational period results show that the model tends to over-predict rainfall. The model fared well with identifying rainfall areas but the rainfall totals were not simulated equally well. It is recommended that the verification method be expanded to include all available real-time and countrywide rainfall data.

The project has made a significant contribution to the understanding and recognition of situations, which give rise to heavy rainfall over South Africa and to the prediction of heavy rainfall events. In doing so the major objectives of the project have been met.

Recommendations

The systems developed are powerful and provide tools, to the meteorologist, not available before. Urgent operational implementation is recommended parallel with an evaluation programme. The operational system is very user friendly but the project team can assist with on site training of weather forecasters. The systems, especially MITS and THERIS should work equally well in countries north of South Africa. The WRC should consider making these systems available to the weather services of these countries. The SAWS has extended a formal invitation to the project team to install the systems: MITS, THERIS and BARCOZ on their computers.

Unfortunately the preparation of a proper quantitative precipitation forecast proved impossible. Uncertainty about the accuracy of the NWP rainfall prevented the creation of a first guess rainfall field. These NWP generated rainfall fields should serve as a basis in the creation of a QPF. It is recommended that the SAWS upgrade their models to small resolution regional models.

The project determined that the high South African topography and especially the escarpment modify rainfall significantly. Further research to address this factor is recommended.

A possible side benefit, of the Vaal Dam catchment rainfall forecast verification might be that the SAWS will again look at the way rainfall forecasts are worded. It is also recommended that the Eta precipitation verification method, developed during this project, be expanded to include all available rainfall data.

Conclusions

This project was very cost effective which delivered an important tool for forecasting heavy rain. It provided the opportunity for capacity building as well as the training of forecasters both local and abroad. Several research papers were published or are in the process of publication. The University of Pretoria awarded an MSc (Meteorology) degree, to the Principle Researcher, for research during this project. Several previously disadvantaged students participated and benefited from this project.

The support of the Water Research Commission made the research possible. The SAWS provided data, guidance and allowed some of their staff to participate in the project.

TABLE OF CONTENT

KEY WORDS AND DEFINITIONS

ACC: The hit rate or percentage correct.

Adiabatic: Refers to a process in which a parcel of air is moved vertically in the atmosphere without any energy or mass transfer into or out of the parcel.

Advection: Transported by the atmospheric winds. Generally in the horizontal plane

Ageostrophic: Atmospheric flow across to the isobars (or contours)

Anti-cyclonic: Anti clockwise rotation of the wind (in the Southern Hemisphere)

BARCOZ : A coastal zone heavy rainfall identification system for baroclinic weather systems

Baroclinic: Weather systems which possess vertical wind shear. An atmosphere where the density depends on pressure and temperature.

Barotrophic: Weather systems with no vertical wind shear. Density is a function of pressure alone.

Catchment: Also referred to as a river's drainage area

Cold front: A narrow sloping layer with a vertical extent of at least three kilometres over which the temperature changes by at least 3 degrees Celsius. This zone separates advancing cold air of polar origin from tropical air. Normally moving eastwards and associated with cloud and rain.

Components of the horizontal wind: The horizontal air motion divided into two components. An east west component (along latitude lines) referred to as the 'x' component, denoted by 'u', sign positive eastwards. The second component is in the north-south direction (along meridians) referred to as the 'y' component, denoted by 'v', sign positive northward.

Conditional instability: Explains the condition of the atmosphere when the temperature lapse rate is less than dry adiabatic but greater than saturated adiabatic.

Continental circulation: Refers to atmospheric circulation over the continents.

Contours: Iso-lines of atmospheric geopotential on a constant pressure level. Generally used to delineate (define, isolate) pressure systems in the upper air.

Convective, convection: Upward motion in the atmosphere forced by unequal heating of the surface.

Convergence: Normally the convergence of the horizontal wind or the convergence of the wind along a constant pressure surface. Computed as the divergence but in this case $D < 0$.

Coriolis force (parameter): When a particle moves on the rotating earth it experience a deflecting force perpendicular to its direction of motion acting to deflect the particle to the left in the southern hemisphere. Coriolis parameter: $f = 2\Omega \sin\phi$ with Ω the angular velocity of the earth and ϕ the latitude. In the Southern Hemisphere $f < 0$.

Cut-off low (COL): Low pressure system in upper troposphere isolated from the mid-latitude westerlies, north of 40 S which is cold cored and has a closed circulation from the upper troposphere to the surface.

Cyclogenesis: The process of development (intensification) and eventual decay of a mid-latitude low-pressure system with associated cold and warm fronts.

Cyclonic circulation: Clockwise rotation of the wind around a low pressure system (Southern Hemisphere).

Divergence (D): Normally referred to as the divergence of the horizontal wind or along a constant pressure surface. Outflow or air from a point by the divergent component of the wind. $D = \nabla_p \bullet \mathbf{V} > 0$.

Dry adiabatic lapse rate (DALR): Rate at which an unsaturated parcel of air will cool if it is displaced vertically and adiabatically. DALR = 1K/100m.

El Nino Southern Oscillation (ENSO): Global scale atmospheric and oceanic circulation and temperature oscillation best measured over the tropical Pacific Ocean. Above normal sea surface temperatures prevail over the eastern Pacific Ocean accompanied by a eastward shift of the convection zones. Below normal rains over continental southern Africa often occur during El-Nino years.

Equivalent potential temperature: The temperature that a parcel of air will attain if the parcel is first moved upward till all the water vapour have been condensed and removed from the parcel and then brought down to the 1000 hPa level while heating at the dry adiabatic lapse rate. The entire process takes place under adiabatic conditions.

Eta model: A limited area numerical weather prediction model referred as the Eta model.

ETS: The Equitable Threat Score.

FAR : The false alarm ratio.

FBI : The Frequency Bias Index.

Geopotential: The geopotential energy per unit mass at a pressure level z metre above sea level.

Geopotential height: Expressed as geopotential metre (gpm). Defined as the geopotential ($\Phi = \int gdz$) divided by constant gravitational acceleration ($g=9.8\ ms^2$). Used commonly when discussing the synoptic circulation patterns on pressure levels.

Geostationary satellite (Meteosat): A satellite placed in the equatorial plane at a distance above the surface of the earth (35000 km) and at the specific angular velocity to ensure that the satellite remains at the same position above the equator. Meteosat provides half-hourly images of the earth in three spectral bands.

Geostrophic wind: Approximation of the horizontal wind on the synoptic scale. Assuming that the flow remains frictionless and constant in a straight line. The flow is tangent to the isobars (contours) and the only two forces acting are the pressure gradient force and the Coriolis force which are equal and opposing. $\mathbf{V}_g = \mathbf{k} \times (f^{-1}\rho^{-1})\nabla p$ or $\mathbf{V}_g = \mathbf{k} \times (f^{-1})\nabla\Phi$ in pressure coordinates.

Heat low: A shallow continental low pressure system which develop because of intense heating of the surface by solar radiation. It is principally a daytime and summer feature.

High-pressure: Area of above average atmospheric pressure

Inter-Tropical Convergence Zone (ITCZ): Zones over the tropical regions where lower troposheric winds converge.

Isentrophic: Normally refers to a coordinate system with the vertical coordinate defined as the potential temperature.

Isobar: Line of equal pressure. Generally refers to lines to delineate pressure systems and gradients along the earth's surface.

Isohyet: As above but refers to equal rainfall depth measured in millimetre.

La Nina: Reversal of the El-Nino. Above normal rains frequently occur over central southern Africa.

Lapse rate: Rate at which the atmospheric temperature decreases with height. Expressed in Kelvin per metre (or 100 K/ 1000 metre).

Line-storms: Convective storms (thunderstorms) arranged in a more or less unbroken line of up to several hundred kilometre.

Maritime systems: Refers to weather systems prevailing or originating over the ocean.

MC: Divergence of the gradient vector of the meridional vapour flux. $MC = \overline{\nabla} \bullet \overline{\nabla}(qv)$.

Meridional flow: Atmospheric winds parallel nearly parallel to the earth's meridians (north/south flow).

Mesoscale: Weather systems with horizontal length scale in order of 100 km.

Meso-alpha scale: Weather systems with horizontal length scale greater than 250 km.

Mid-latitude westerly circulation: Southern hemisphere mid-latitude belt dominated by westerly winds

MITS: Model for the identification of tropical weather systems.

Mixing ratio: Mass of water vapour per unit mass of dry air.

MRL-5 radar: A dual-wavelength radar that operates on both the S- and X-bands.

NCEP data: National Centre for Environmental Processes computer generated meteorological data fields.

Numerical models: Computer models of the atmospheric flow fields based on the equations of motion and incorporating atmospheric physics and thermodynamics.

NWP: Numerical weather prediction.

Omega (ω): Vertical motion in the pressure coordinate system ($\omega = \frac{dp}{dt}$).

PCGRADS: Personal Computer Graphics and Display System.

Persistence forecasting: Generally understood to mean predicting today's weather for tomorrow.

POD: The probability of detection.

Potential Temperature: The temperature a parcel of air would attain if it is moved adiabatically to the 1000 hPa level (def. Chapter 4).

Precipitable Water (W): Maximum depth of rain produced if all the water vapour in a vertical column of air condenses and precipitates out. Defined chapter 2 pp 16.

Pressure gradient force: Measured across the isobars (contours). Normally expressed as force per unit mass. PGF = $\rho^{-1}\nabla p$ (ρ, density, p, surface pressure).

QPF: A quantitative precipitation forecast.

Quasi-geostrophic theory: Dynamical analysis of the atmospheric flow fields, on the synoptic scale, by assuming that the horizontal wind can be approximated by the geostrophic approximation and that vertical accelerations are small.

Radiosonde: An instrument attached to a hydrogen filled balloon which measures and transmits atmospheric pressure, temperature and relative humidity as it ascends.

Relative humidity: Degree of saturation by water vapour of the air. Defined as ratio of the observed vapour pressure divided by the saturation vapour pressure at the same temperature. See also chapter 2, pp 15.

Relative vorticity (ζ): Vertical component of the vorticity. $\zeta = \mathbf{k} \bullet \nabla \times \mathbf{V}$. Normally computed on a pressure surface and is a measure of the rotation of the wind at a point.

Ridging Atlantic Ocean High (AOH): High pressure system located over the southern Atlantic Ocean extending (moving) eastward and normally south of South Africa.

Runoff: Amount of water collected by the river.

Saturated adiabatic lapse rate (SALR): As the DALR but for a parcel of air saturated with water vapour. The SALR ≈ 0.6 K/100m near the earth's surface.

Saturation: Refers to the state when an equal number of water molecules evaporate from an open water body into the atmosphere as the number entering of molecules returning to the water body from the atmosphere. This number of molecules is the maximum the air can contain at that temperature. This number increases with the temperature of the air.

SEC: Divergence of the gradient vector of the southeastern vapour flux component.

$$SEC = \overline{\nabla} \bullet \overline{\nabla}(qV_{SE})$$

Scale (large, small, synoptic): Refers to the horizontal scale of the atmospheric motion.

Specific Humidity (q): Mass of water vapour per unit mass of moist air. Defined chapter 2, pp 16.

Southern Oscillation Index (SOI): An index computed by taking the difference between monthly average surface pressure at Tahiti and Darwin. The SOI is normally less than zero during El-Nino years.

Streamline analysis: Lines drawn on a weather map tangent to the wind direction in order to determine areas of divergence and convergence. Suitable for latitudes where the geostrophic assumption no longer applies.

Synoptic scale: Refers to motions with horizontal scale in order of 1000 km and a time scale of days.

THERIS: Tropical heavy rainfall identification system.

Thermal wind: The thermal wind represents the vertical geostrophic wind shear and can be expressed by $\overline{V}_T = \overline{V}_g(p_1) - \overline{V}_g(p_0)$. Where $\overline{V}_T$ is the thermal wind and $\overline{V}_g$ the geostrophic wind at pressure levels p_1 and p_0 ($p_1 < p_0$).

Total Static Energy (TSE): Total thermodynamic and geopotential energy of the air. Defined Chapter 2 pp 17.

Tropical cyclones: Also referred to as Hurricanes or Typhoons. Very intense tropical low pressure systems accompanied by destructive wind and rain.

Tropical temperate trough (TTT): A low pressure zone (trough) extending southwards from tropical low- to mid-latitude low pressure system.

Tropopause: Boundary between the troposphere and the stratosphere and located where the temperature decrease with height (in the troposphere) is reversed or terminates.

TSS: The Hansen-Kuiper Score.

Vapour flux: Product of the specific humidity (q) and the wind velocity **V**. Components of the vapour flux referred to is the meridional vapour flux component (qv) and the southeast wind component of the vapour flux (qv_{SE}). Defined chapter2 pp 18.

Vapour pressure: Partial pressure exerted by the water molecules contained in the air.

Vorticity: Three dimensional vector quantity describing the rotation of a fluid at a point. $\varpi = \nabla \times \mathbf{V}$.

WAR (Wetted area ratio): The ratio between the radar pixels indicating rainfall (> 2.5 mm) and the total number of pixels.

Water vapour: Water molecules (H_2O) (gaseous state of water) in the mixture of atmospheric gases.

Weighted mean: Average of several rainfall station within a grid box taking the distances from each other into consideration.

CHAPTER 1
INTRODUCTION

1.1 Climate and topography of South Africa.

South Africa is situated on the southern tip of Africa with its northern boundary at approximately 22°S and the southern most point, Cape Agulhas, at approximately 35°S. Namibia, Botswana and Zimbabwe border South Africa to the north with Mozambique and Swaziland to the east. Over the southeastern interior of South Africa the Mountain Kingdom of Lesotho is completely surrounded by South Africa. Following the definition provided by Taljaard (1994), the southern subcontinent or southern Africa refers to Africa south of 17° S. The Atlantic Ocean to the west and the Indian Ocean to the south and southeast flank southern Africa. In the east the Mozambique Channel lies between Mozambique and Madagascar supplying warm water to the strong Agulhas Current, which runs parallel to the southeast coast. The cooler Benguela Current runs northward off the west coast.

Taljaard (1994) provided a detailed description of the topography of southern Africa. The subcontinent is characterised by a moderately elevated plateau, for the greater part rising to over 1000 m above sea level and to more than 1500 m over extensive areas. The terrain rises steeply in most areas over the first 200-300 km from the coast. In the east the main escarpment rises to 1500 m or more. It runs southward from the Zoutpansberg, in the north, becoming the Drakensberg of Kwazulu-Natal and the northeastern interior of the Eastern Cape Province. The Maluti Mountains in Lesotho rise to over 3000 m in places.

The geographical distribution of rainfall over southern Africa is highly variable and is, to a large extent, controlled by the topography. Over the western interior the annual average rainfall varies between 100 and 200 mm. Over the remainder of the interior the annual average rainfall fluctuates between 200 to 700 mm with only the elevated mountain areas receiving more than 1000 mm of rain annually (Taljaard, 1996). Schulze (1965) stated that 85% of South Africa receives more than half of its rainfall in summer (October to March). Taljaard (1986) showed that the area of maximum summer rainfall in southern Africa follows a roughly anti-cyclonic circular track. Starting along the East Coast in September, through the four northern provinces of South Africa (Gauteng, Mpumalanga, Limpopo and Northwest) by October and November reaching the

Northern Cape Province by March. Zimbabwe, the northern parts of Botswana and Namibia also receive most of their rainfall from November to January.

The weather over the southern subcontinent of Africa is dominated by a high-pressure belt, which is, except for a few winter months, split in two by the continent. The Atlantic Ocean High (AOH) lies to the west and the Indian Ocean High (IOH) to the east (Fig.1.1). Variations in position and intensity of the two high pressure systems play an important role in the rainfall distribution over South Africa (Shulze, 1965). The mid-latitude westerly circulation, extending northward to these high pressure systems, controls the weather of South Africa to a large extent. Weather changes are largely influenced by perturbations in the Southern Hemisphere westerly circulation (De Coning, 1997). During the summer months, the influence of the westerly circulation becomes somewhat diminished as the high pressure systems migrate southward. In the summer the Inter-Tropical Convergence Zone (ITCZ) moves southward to approximately 17°S (Taljaard, 1994). Van Heerden and Taljaard contributing to Karoly and Vincent (1998) explained that it is during this time of the year that tropical weather systems invade southern Africa from the east in the form of tropical cyclones or easterly waves.

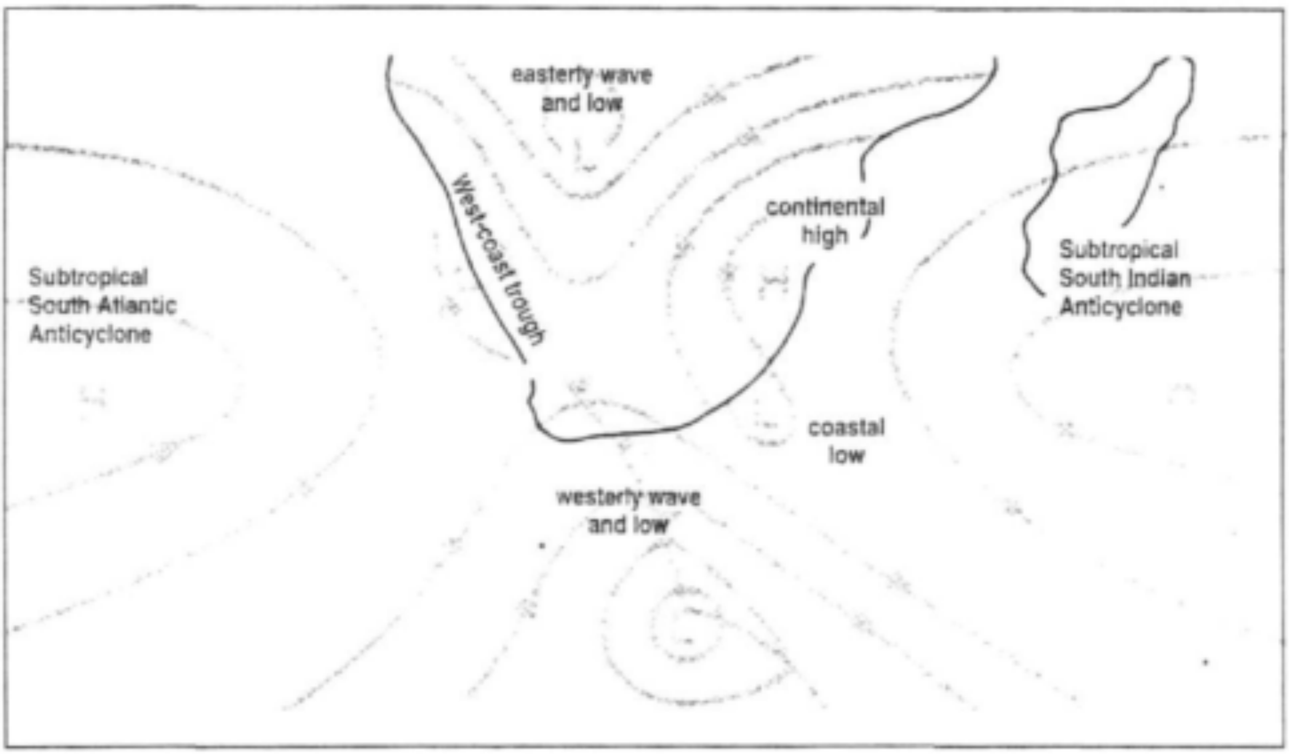

Figure 1.1 Important features of surface synoptic circulation over southern Africa. Adapted from Tyson and Preston-Whyte (2000).

1.2 Heavy rainfall over Southern Africa.

Rainfall over southern Africa varies considerably from year to year (Schulze, 1965). Below normal rainfall and droughts occur frequently. From time to time heavy rainfall and floods occur over southern Africa and are often associated with large financial losses, damage to infrastructure and loss of life. Viljoen, cited in Alexander and van Heerden (1991), lists 184 noteworthy flood events during the years from 1911 to 1988. Close to 30% of these flood events occurred over Kwazulu-Natal and 42% over the four northern provinces and the central interior of South Africa.

Alexander and van Heerden (1991) identified 6 flood classes with the lower end of the scale (class 0) defining heavy rain events, which could lead to significant river flow but only localised flooding. The top end of the scale comprises truly significant flood events with disastrous results such as the Kwazulu-Natal floods of 1987 (class 5) and the Free State floods of 1988 (class 4). Considering the six flood classes together Alexander and van Heerden (1991) found that the month with the highest frequency of floods is February and 67% of these flood events occur during the summer rainfall season (October to March). They also established that the eastern and southeastern coastal regions of South Africa had the most class 5 floods during the study period. They discussed how the return period of a serious flood event along the coast from Port Elizabeth to Maputu is approximately 20 years. Moreover they found an appreciable increase of serious floods from 1970 to 1990 and postulated that the possibility of getting serious flood events more frequently must be accepted.

1.3 Weather systems associated with heavy rainfall over southern Africa

The weather systems causing heavy rainfall over southern Africa are: tropical low pressure systems, tropical cyclones, the cut-off low (COL), the ridging Atlantic Ocean High (AOH) behind the cold front and the tropical temperate trough (TTT) (Alexander and van Heerden, 1991, Preston-White and Tyson, 1993, Taljaard, 1985, Triegaardt el al., 1991 and van Heerden and Hurry, 1987).

1.3.1 Tropical low pressure systems

Figure 1.3.1 depicts the circulation of a typical tropical low pressure systems also referred to as easterly lows (Tyson and Preston-White, 2000). Tropical low pressure systems were responsible for extremely heavy rainfall over southern Africa in the past two decades. Triegaardt et al. (1991) described the tropical characteristics of the weather system responsible for the heavy rainfall event over the central interior of South Africa during February of 1988. During February of 1996 the interaction between a tropical low pressure system and a COL was responsible for extreme rainfall over the central and northern interior (De Coning, 1997 and De Coning et al., 1998). Dyson and Van Heerden (2001) described how a tropical low pressure system caused widespread and heavy rainfall over the four northern provinces of South Africa during 5 to 10 February 2000. The dynamical characteristics of this continental tropical weather system are detailed in chapter 3.

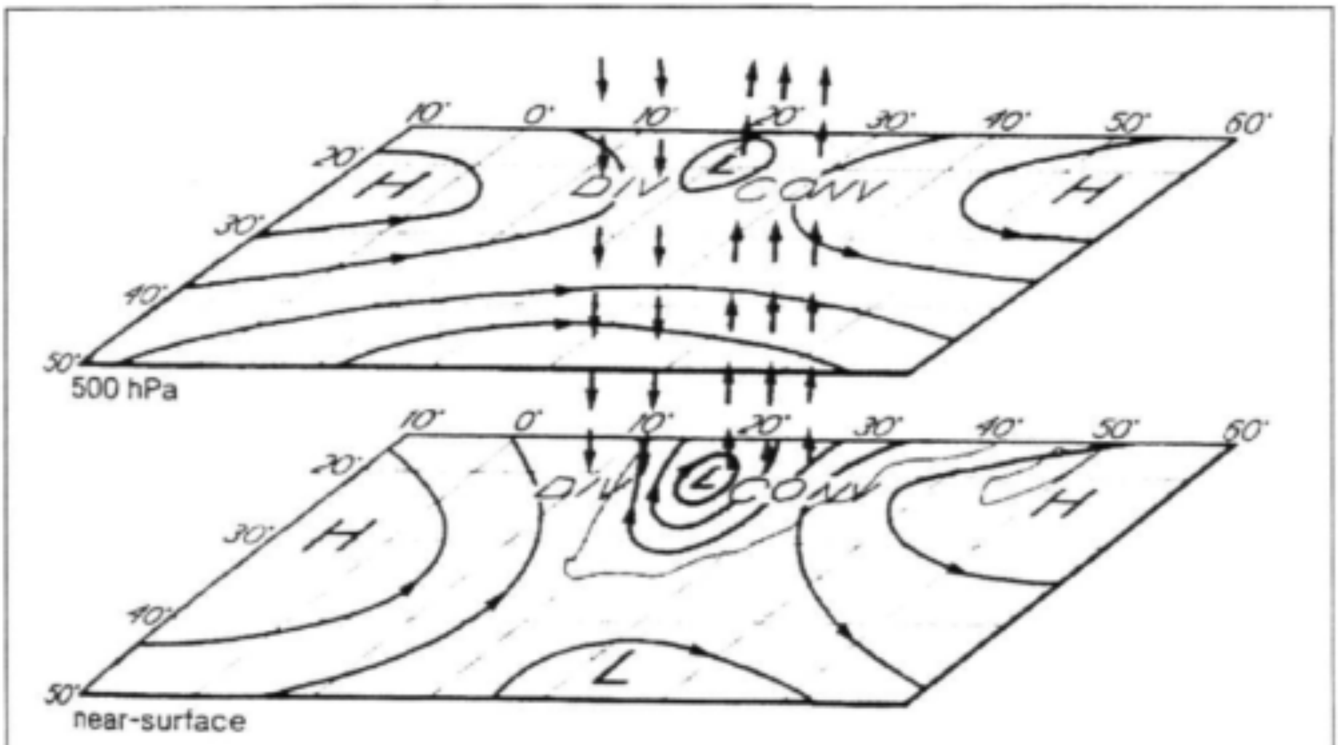

Figure 1.3.1: The surface and 500 hPa circulation associated with an easterly low. Adapted from Tyson and Preston-White (2002).

1.3.2 Tropical cyclones

On average 10 – 11 tropical cyclones occur over the Southwest Indian Ocean in a summer season. Only a small fraction of these cyclones occur in the Mozambique Channel (Kovacs et al., 1985). Between 1950 and 1988 only 10 tropical cyclones invaded southern Africa and had a significant effect on South Africa's rainfall (Alexander and van Heerden, 1991). A tropical cyclone making landfall in southern Africa is a rare event; however, when it does happen, extreme rainfall and flooding results (Poolman and Terblanche, 1984 and Dyson and van Heerden, 2001). Figure 1.3.2 depicts one such a cyclone, named Eline, which was responsible for wide spread heavy rainfall in Mozambique.

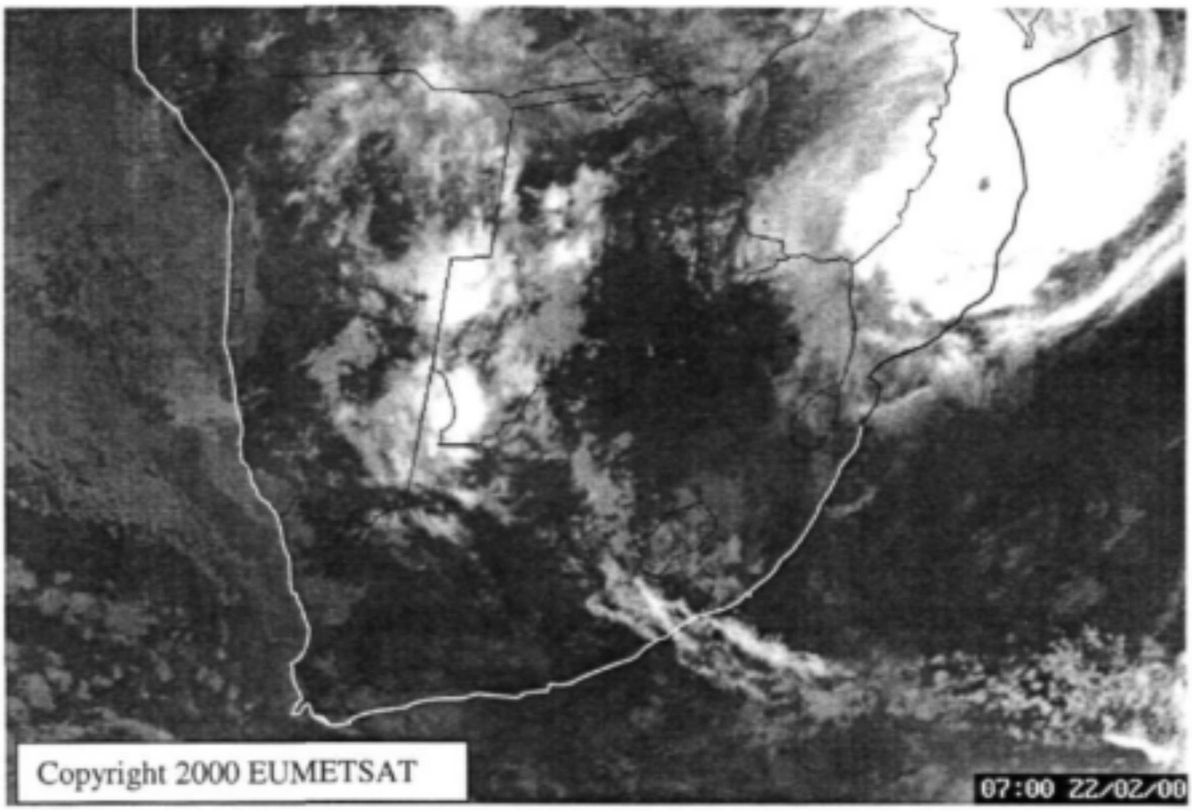

Figure 1.3.2 Geostationary satellite Meteosat infrared channel imagery at 0700 UT on 22 February 2000. The eye of tropical cyclone Eline is clearly visible over Mozambique.

1.3.3 Cut-off lows

Many flood events over South Africa are caused by cut-off low (COL) pressure systems (Alexander and van Heerden, 1991). Taljaard (1985) list at least 10 such events between 1974 and 1981, amongst them the Laingsburg flood of January 1981 also described by Estie (1981). Treigaardt et al. (1988) showed that a COL accompanied by a strong surface on-shore flow caused the extreme rainfall over Kwazulu-Natal during September 1987. When a COL occurs in winter widespread and heavy snowfall can occur. This happened during July 1996 (Strydom and Nel, 1996). Taljaard (1985) stated that considerable confusion exists, even amongst meteorologists, in distinguishing between a COL and a low pressure system in the tropical easterlies. To identify the COL he proposed the following definition: the low (COL) must be located equatorward of the 40° latitude and have a closed circulation in the upper troposphere, extending downward to the land surface and have a cold core of upper tropospheric temperatures. Taljaard (1985) makes provision for four classes of COL's but defines them in accordance with the rainfall they produce and not the circulation intensity they possess. COL's are generally predicted well by numerical models because they are large scale disruptions of the synoptic scale flow associated with significant meridional flow. In a modelling study performed by Tennant and van Heerden (1994) they found that COL's may develop and intensify significantly over the South African interior because of the presence of the steep escarpment and high topography. Compared to maritime COL's these systems also move slower and generally move in a southeasterly direction. However all COL's are associated with large curvature of the upper contours, resulting in strong vertical motion to the east of the COL. Figure 1.3.3 is an infrared satellite image depicting a COL over the western interior of South Africa. The cyclonic curvature is clearly evident in the cloud band spiraling around the cloud free area in the Northern Cape.

For significant rain from a COL the following conditions must apply:

- A surface high pressure system should be south or southeast of the country and maintain significant pressure gradients near the land.
- Moist cool maritime air, pushed by this high, must invade the land rapidly.

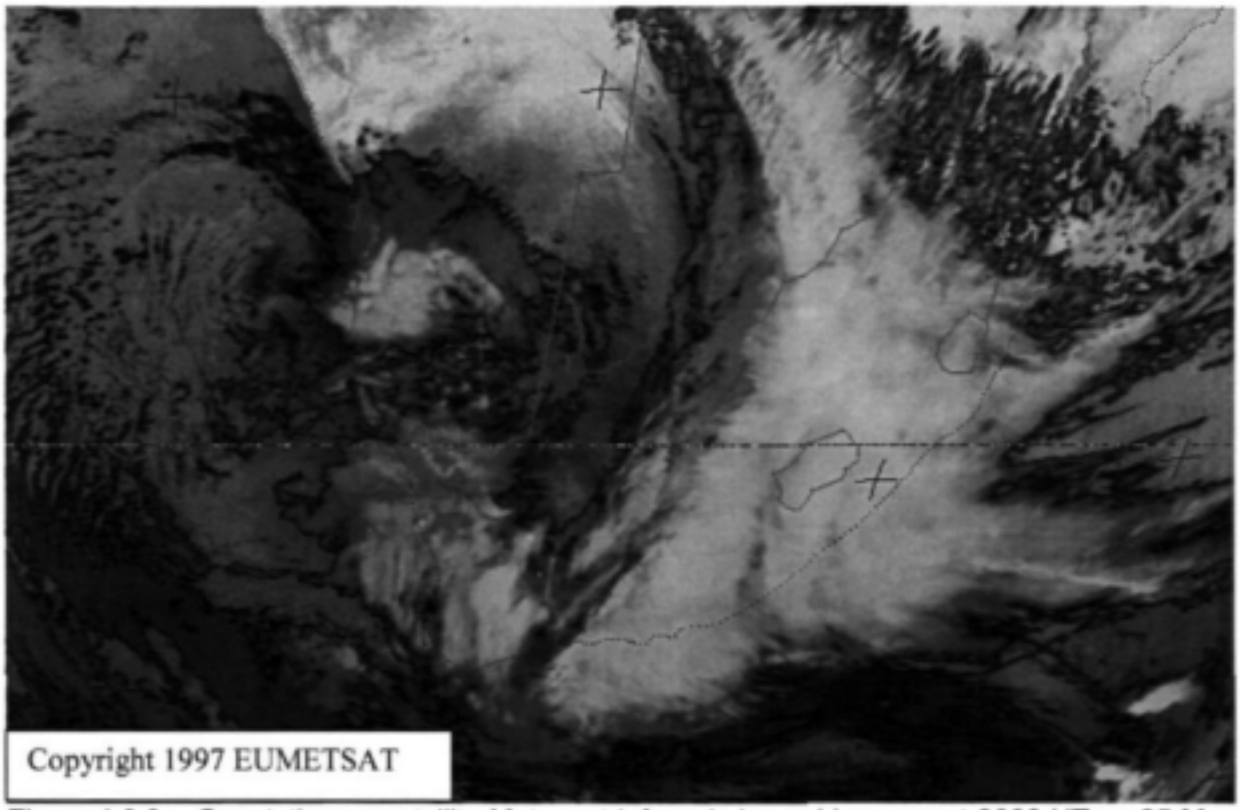

Figure 1.3.3 Geostationary satellite Meteosat infrared channel imagery at 0600 UT on 25 May 1997.

1.3.4 The advancing and sharp upper air trough

Upper air troughs linked to the mid-latitude westerly perturbations regularly move over the country. Upper troughs producing significant rainfall often have very sharp cyclonic curvature at the trough line. Provided that abundant water vapour is advected to the east of the trough significant rainfall can be generated in the line-storms developing ahead of the upper trough. These storms often develop just east of the surface trough or dry line. The dry line separates warm moist continental air, normally propagating southward, from the dry descending air invading the country from the west or southwest. The dry line tends to rotate anticlockwise over the central and southern interior of South Africa in conjunction with the coastal low as it moves up the southeast and east coasts of the country. The continental surface circulation is normally dominated by a high pressure system centred over the northeastern interior which causes modified sub-tropical air to rotate anticyclonically southward over the interior (Tyson and Preston-Whyte, 2000). Figure 1.3.4 depicts the circulation associated with an upper air trough over Southern Africa. The upper air trough lies west of the surface trough with a large area of upward motion to the east of the upper trough.

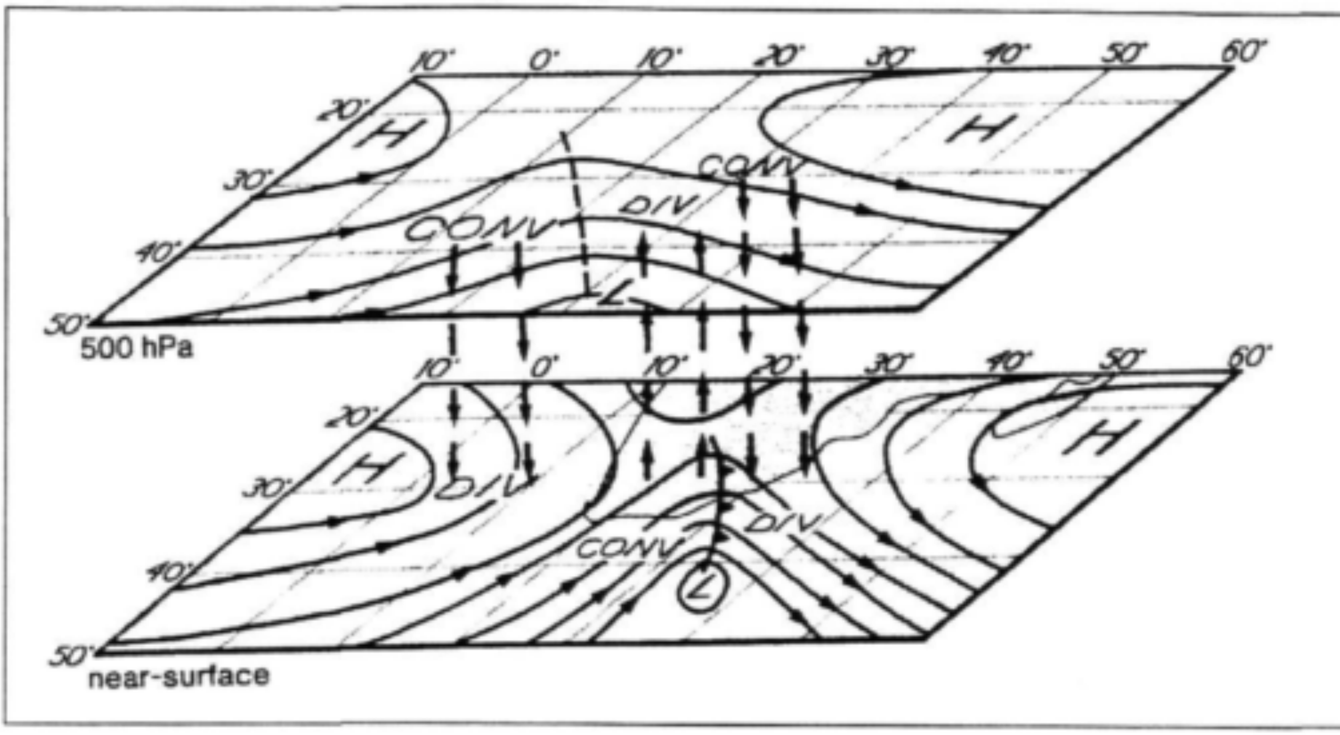

Figure 1.3.4: The surface and 500 hPa circulation associated with an upper air trough. (Adapted from Tyson and Preston-White (2002))

1.3.5 The ridging Atlantic Ocean High

The Western Cape Province as well as the coastal zone stretching eastward to Kwazulu-Natal often receive heavy rainfall during the passage of intense mid-latitude weather systems associated with a potent cold front followed by a strong ridge of the AOH. Over the Cape Peninsula and surrounds significant rainfall generally occurs in the northwesterly flow ahead of the cold front. The southern and southeastern coastal areas may experience heavy rainfall after the passage of the cold front when an intense ridge of the AOH causes a strong southerly to southwesterly on-shore flow (Alexander and Van Heerden, 1991 and Van Heerden and Hurry, 1987). The escarpment, which rises to approximately 1500 m within 200 – 300 km from the coast, plays a significant role in the production of the heavy rainfall (De Villiers, 1992, Dyson and Van Heerden, 2001, Tennant and van Heerden, 1994 and Triegaardt et al., 1988). De Villiers (1992) identified 195 heavy rainfall events between 1980 and 1989 over Kwazulu-Natal. Triegaardt et al. (1988) showed that the heavy rainfall over Kwazulu-Natal is predominantly due to a strong surface on-shore flow. The combined effect of the COL and a strong southeasterly on-shore flow in producing heavy rainfall along the coastal plains of South Africa is detailed in Chapter 4.

An example of an AOH responsible for heavy rainfall is depicted in figure 1.3.5. The arrows indicate the circulation around the high-pressure system. A strong on-shore flow was evident over KwaZulu-Natal and heavy rainfall occurred. (De Villiers, 2000).

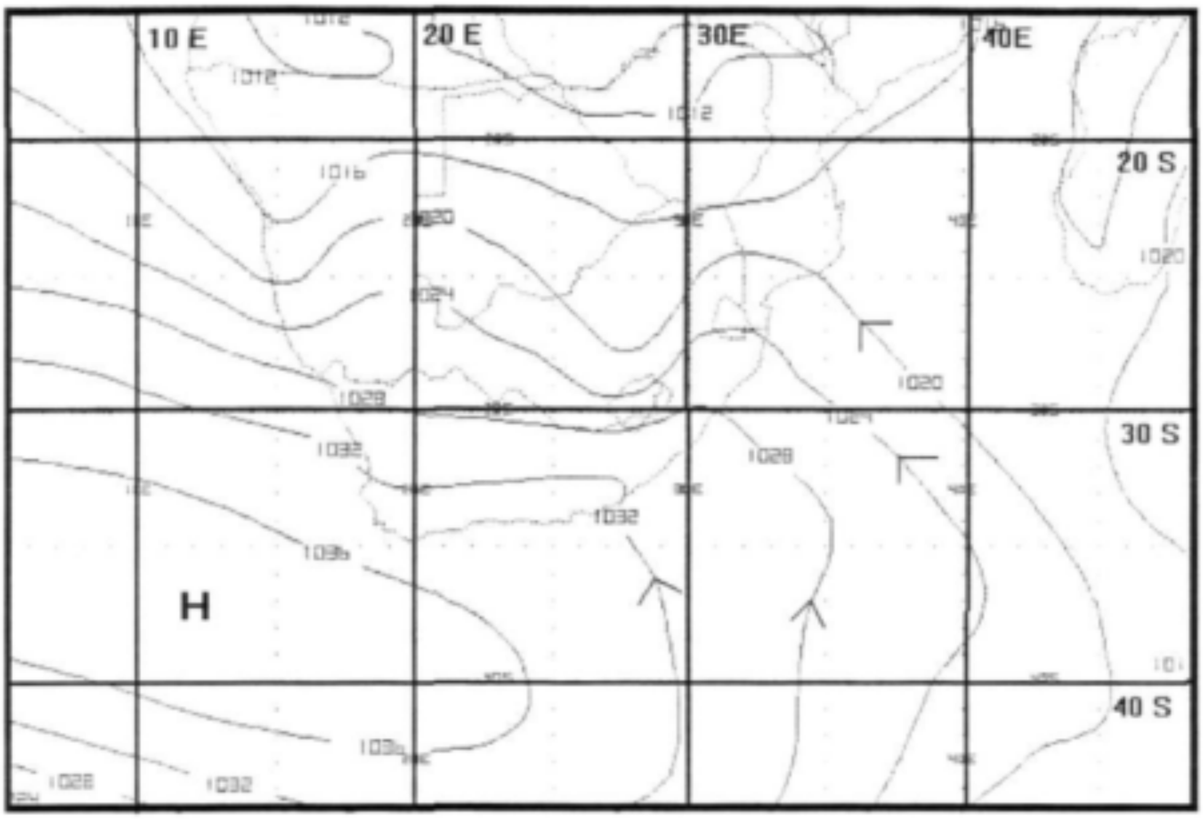

Figure 1.3.5: Sea level pressure in hPa at 1200 UT on 18 September 2000. The arrows indicate the circulation around the Atlantic Ocean High. (Adapted from De Villiers (2000)).

During the summer months the AOH may also be responsible for significant rainfall over the eastern interior if a process referred to as undercutting takes place. Undercutting is a term in general use by South African forecasters. It describes the vertical uplift of moist sub-tropical continental air over the central plateau of South Africa when cool maritime air advances over the Drakensberg. This happens when a cell of the AOH moves rapidly eastward south of the country and surface pressures build over Kwazulu-Natal (De Villiers, 1992). A large east west surface pressure gradient develops across the eastern escarpment causing the flow over the eastern highveld to become ageostrophic. This cross isobar (geopotential contour) flow arrives as a surge of cool maritime air on the eastern Highveld. The vertical ascent (similar to frontal uplift) experienced by modified continental subtropical air due to the westward surge is considered responsible for heavy rainfall. This phenomena may also explain the westward development of thunderstorms against the westerly upper air flow and even after the upper trough and storms had passed eastward. De Coning (1997) described the westward surge of convergence and vertical motion in a case study using isentrophic analysis.

However, significant and widespread rain only develops if the undercutting takes place underneath a wide area of vertical ascent and generally under a well established convective cloud system.

1.3.6 The tropical temperate trough

Crimp et al. (1997) and Harrison (1986) provided a thorough explanation of the importance of the tropical-temperate trough (TTT) in producing rainfall over South Africa. They estimated that approximately 39% of the mean annual rainfall could be attributed to the TTT. The TTT is easily identified on satellite imagery as long cloud bands linking tropical convective systems to the mid-latitude (temperate) frontal systems. Lindesay and Jury (1991) explained that a TTT is characterised by a trough linking an area of convection over tropical or sub-tropical Africa with a mid-latitude depression to the south of the subcontinent (Fig. 1.3.6). Heavy rainfall over the central interior of South Africa during February 1988 described by Jury et. al. (1993), Lindesay and Jury (1991) as well as the extreme rainfall during February of 1996 dealt with by de Coning et. al. (1998) are two examples of heavy rain producing TTT's. Features common to the TTT and the development of heavy rainfall are:

- A mature mid-latitude cyclone moving eastwards in the mid-latitudes, south of the land and often accompanied by a well defined cold front extending to the southern parts of South Africa.
- Strong onshore flow over the southern and southeastern coastal regions.
- An extensive high/ ridge at 200-300 hPa to the east or northeast of the subtropical convective cloud systems.

- Advection of water vapour (of sub-tropical origin) below and generally tangent to the cloud band.

Rainfall develops in the sub-tropical convective systems and also in the south due to the frontal system and strong onshore flow. Over the continental parts of South Africa rainfall occurs below the cloud band. It should be noted that the cloud band itself tends to swing anti-clockwise as the mid-latitude systems advance faster than the convective systems.

The TTT should be viewed as a combination of tropical, sub-tropical and mid-latitude weather systems and may possess some characteristics of all the weather systems described in this section.

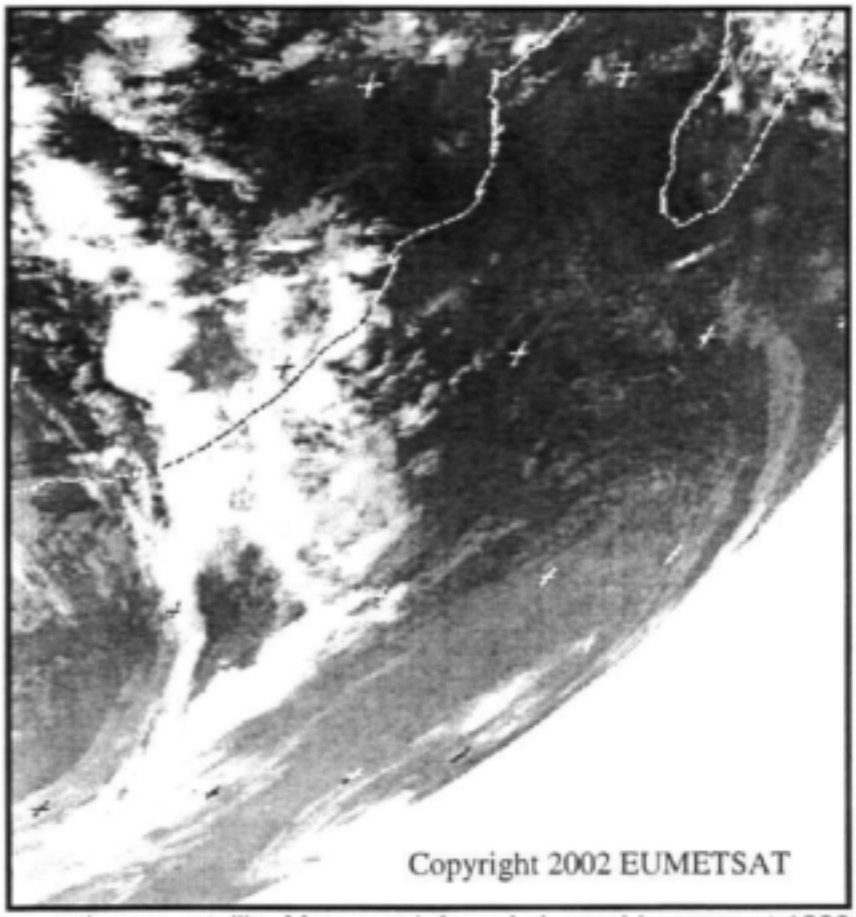

Figure 1.3.3 Geostationary satellite Meteosat infrared channel imagery at 1830 UT on 10 April 2002.

1.4 Aims of the Research

The main aim of this research project is to make available a Quantitative Precipitation Forecast (QPF) for input into the River Flow Project. This is to be achieved by improving forecasting techniques and developing a new forecasting system for the period 6 to 48 hours ahead.

To achieve this aim research can be subdivided into the following steps detailed per chapter in the report.

Chapter 2 describes the data used in this research and details the meteorological variables.

A synoptic climatology of heavy rainfall over South Africa was compiled and the results are detailed in chapter 3.

Chapter 4 deals with heavy rainfall from tropical weather systems. First a classification scheme to identify tropical weather systems over southern Africa was developed and is referred to as the model for the identification of tropical weather systems (MITS). This was followed by the development of the tropical heavy rainfall identification system (THERIS).

Chapter 5 describes the forcing mechanisms for heavy rainfall developing in baroclinic weather systems. A coastal zone heavy rainfall identification system (BARCOZ) was developed and tested.

Three verification techniques are described in chapter 6. First historic rainfall distribution forecasts were verified over the Vaal Dam catchment. In addition two methods were developed to verify the precipitation forecast of Numerical Weather Prediction (NWP) models.

The technology emanating from this project is dealt with in chapter 7.

Chapter 8 deals with conclusions and further research as well as practical applications proposed for the heavy rainfall identification systems.

CHAPTER 2
NUMERICAL WEATHER PREDICTION AND RAINFALL DATA

2.1 National Center for Environmental Prediction (NCEP) Data

The National Center for Environmental Prediction (NCEP) re-analysis data are used in conducting the case studies in Chapters 4 and 5. NCEP data are generally considered by meteorologists to be of a high quality. In all the case studies detailed in Chapters 4 and 5, the 1200 UTC analysis of the NCEP data is used. The NCEP data used in this report have a horizontal resolution of 2.5 degrees and have 17 levels in the vertical. Of the 17 vertical levels only 10 levels are utilized here, namely the standard pressure levels of 1000, 925, 850, 700, 600, 500, 400, 300, 250 and 200 hPa. The 850 hPa geopotential heights are assumed to represent the surface level in the investigation into the continental tropical systems detailed in chapter 4. The horizontal and vertical resolution of the NCEP data are suitable for researching weather systems on the synoptic scale. Small or mesoscale features will not be adequately resolved by this data set. The NCEP data proved quite adequate for identifying synoptic scale tropical and baroclinic weather systems as well as the widespread heavy rainfall they produce.

2.2 Eta Model Data

Mesinger et al. (1988) gives a thorough description of the Eta limited area model (LAM) while the physical parameterizations are described by Janjic (1984,1990). The Eta model is unique in that the step-mountain or eta vertical coordinate as defined by Mesinger (1984) is used in the model. The model topography is constructed as discrete steps, with tops located at model interfaces. This makes the Eta model especially useful in locations with complex topography such as South Africa, where the plateau in most areas rises steeply over the first 200-300 km inland from the coast.

The Eta model has been undergoing testing and development at the National Meteorological Center (NMC) in the USA since the late 1980's in preparation for operational use by the National Weather Service (Dunn and Horel, 1994). The SAWS obtained a copy of the model in 1993 after which it was tested and finally implemented. The current Eta model domain covers Southern Africa and surrounding oceans from approximately 9° S to 48° S and 13° W to 53° E. The model has a horizontal resolution of half a degree (48 km) with 38 layers in the vertical and is run twice daily, with initial conditions at 12 UTC and 00 UTC. Both grid scale (Zhao and Carr, 1997) and convective precipitation (Betts and Miller, 1986; Janjic, 1994) are produced. Subgrid-scale convection processes play a major role in the ability of the model to accurately forecast rainfall. In the SAWS Eta model, the Betts-Miller convective parameterization scheme is used in which moisture or upward vertical motion is not required explicitly to produce precipitation (Betts 1986; Betts and Miller 1986).

In order to make the research results emanating from this project available to the operational meteorologist it is important that the heavy rainfall identification systems are tested and operated on the Eta model prognostic fields and this was in fact done for the heavy rainfall over northeastern South Africa during February 2000. The accuracy of the Eta model precipitation is verified in chapter 6.

2.3 Rainfall Data

All the rainfall data used in this project were obtained from the South African Weather Service (SAWS). The number of SAWS rainfall stations varied considerably over the 1900's increasing to a maximum number of approximately 2500 rainfall stations by the middle 1970's. Since then the number of reporting rainfall stations has steadily decreased to approximately 1500 by the 1990's. Rainfall data were used in two ways:

Firstly daily rainfall charts, indicating the geographical distribution of the rainfall are generated using the interpolation scheme of Rautenbach (1996). This interpolation scheme has some disadvantages in that if rainfall occurs at a single rainfall station, geographical distant from other rainfall stations the isolated rainfall is not adequately captured by this interpolation scheme. Furthermore, if rainfall at a single station is significantly greater than rainfall at other nearby stations the interpolation scheme tends to smooth the rainfall field. Information on isolated heavy rainfall events is lost in this way. Another problem with the interpolation scheme is the fact that in the generation of the rainfall chart the 0-mm isohyet is not indicated and the first plotted isohyet is the same as the contour interval of the isohyets. If for instance the contour interval is 50 mm the first isohyet indicated on the figure is 50 mm, all rainfall less than 50 mm is not shown. In this research the focus point is widespread heavy rainfall and despite the disadvantages of the interpolation scheme, the authors are nevertheless convinced that the interpolation scheme captures most widespread heavy rainfall events adequately. The rainfall maps are used only as a graphical presentation of rainfall and the evaluation of THERIS and BARCOZ is performed by the methods described below.

The second application of the rainfall data is to evaluate the heavy rainfall identification systems. The average rainfall in the areas isolated by THERIS and BARCOZ as well as the percentage of rainfall stations reporting more than 0 mm, 10 mm, 20 mm and 50 mm of rain is determined. Because the rainfall stations have an irregular geographical distribution the weighted average method designed by Tennant (1999) is used to calculate the statistics. Tennant's method is used operationally by the SAWS. An adequate description is provided by Marx et al. (2002). The weighted average rainfall and weighted percentages were computed by taking the geographical position of each station relative to the other stations into consideration. When rainfall stations are distributed evenly over an area Tennant's method renders results very close to the mathematical average. However, the weighting method is more reliable when the rainfall stations are distributed unevenly over an area. A rainfall station, which is geographically distant (close) to other stations will have a larger (smaller) weight factor and will therefore contribute more (less) in the computation of the average and percentages.

2.4 Calculating the meteorological parameters used in the research.

A number of parameters generated by or derived from Numerical Weather Prediction models (NWP) are used by the heavy rainfall identification systems. The following meteorological parameters, not available as a model output in the NCEP and Eta data, are detailed here.

2.4.1 Specific Humidity (q)

Specific humidity, the ratio of the mass of water vapour to the total mass, per unit volume, (Gordon et al., 1998), is not available in the NCEP data set. Specific humidity is required for the calculation of many of the moisture and instability parameters used in Chapters 4 and 5. Gordon et al. (1998) provides the following expression for the computation of specific humidity.

$$q = \frac{r}{1+r} \qquad (1)$$

where r is the mixing ratio defined as the ratio of the mass of water vapour to the mass of dry air per unit volume (Huscke, 1959). Relative humidity (RH) is one of the variables available in the NCEP and Eta data sets and is used to calculate specific humidity. Relative humidity is defined as the ratio of the actual vapour pressure of air to the saturation vapour pressure, at the same temperature, and the following expression from Wallace and Hobbs (1977) is used to compute the RH.

$$RH = \frac{r}{r_s}$$

$$\therefore \qquad r = RH\ r_s$$

Where r_s is the saturation mixing ratio.

Substituting this relationship into equation (1):

$$q = \frac{r_s\ RH}{1 + r_s\ RH} \qquad (2)$$

The next step in the calculation of specific humidity is to find an expression for the saturation mixing ratio. Wallace and Hobbs (1977) provide the following expression.

$$r_s = 0{,}622\frac{e_s}{p} \qquad (3)$$

where e_s is the saturation vapour pressure and p pressure. It is accepted here that $p \rangle\rangle e_s$ for the range of atmospheric temperatures. The Clausius-Clapeyron equation from Wallace and Hobbs (1977) shows that the saturation vapour pressure is a function of temperature (T) alone, which in turn is available in the model fields.

$$e_s = 611\ \exp\left(\frac{L}{R_v}\left(\frac{1}{273.16} - \frac{1}{T}\right)\right) \qquad (4)$$

Where $L = 2464759\ \ J\,kg^{-1}$

$R_v = 461.48\ \ J\,kg^{-1}\,k^{-1}$

T= temperature in ° Kelvin.

Substituting equations (3) and (4) into equation (2) provides the means of calculating specific humidity at a pressure level.

2.4.2 Precipitable Water (W)

Huschke (1959) defines precipitable water (W) as the total mass of water contained in a vertical atmospheric column if all the water vapour in the column were to condense out. Although this definition is applicable in the study of continental tropical systems and precipitable water is one of the variables provided by NWP models, precipitable water was, however, calculated for the vertical column bounded by the 850 hPa to 300 hPa levels using:

$$W = \frac{1}{g}\int_{p_1}^{p_2} q\,dp$$

where $g = 9.8ms^{-2}$, p_1 = 300 hPa, p_2 =850 hPa.

In Chapter 4 MITS and THERIS are tested on the prognostic fields of the Eta model. Huschke (1959) states that the specific humidity (q) may be approximated by the mixing ratio (r) because both are very small quantities and can be considered the same for all practical purposes. The mixing ratio is one of the variables available in the Eta model data and W is computed by replacing the specific humidity by the mixing ratio.

2.4.3 Total Static Energy (TSE)

The total static energy (TSE) is the total energy within an atmospheric parcel of air without taking the small kinetic energy (due to macroscopic motion) into account (Triegaardt et al., 1991). Mathematically TSE is expressed by:

$$TSE = C_pT + gz + Lq$$

Where $C_p = 1004.64 J\,K^{-1}\,kg^{-1}$ and z is the geopotential height and the term gz is the geopotential energy accepting that g remains constant in the vertical column. The other two right hand terms represent the enthalpy and latent energy of the parcel. The average TSE in the troposphere is calculated between the 850 hPa and 300 hPa levels.

The vertical profile of TSE is used to determine whether the atmosphere is conditionally unstable. In the case studies described in chapter 3 the surface value of TSE is taken as the 850 hPa value. To calculate the level of conditional instability (LCI) the following formula is used: $LCI = TSE_{850} - TSE_i$ where i varies between 700 hPa and 400 hPa. For the atmosphere to be conditionally unstable up to 400 hPa (a requirement of MITS) the LCI must be positive for i = 700 hPa to 400 hPa. In THERIS it is required that the LCI must be positive up to at least 300 hPa.

2.4.4 Divergence of the average upper tropospheric winds

Using scaling arguments for synoptic scale flow Holton (1992) showed that the scale value of wind divergence is in the order 10^{-6} s^{-1}. Wind divergence is very sensitive to small changes in wind direction and strength. To remove small spurious wind perturbations in the wind field the average wind of the 200 hPa to 300 hPa layer is used in the computation of the average wind divergence.

2.4.5 Divergence of the gradient vector of the meridional vapour flux component

The horizontal wind can be expressed by $\overline{V} = u\bar{i} + v\bar{j}$ where *u* is the east west wind component of the wind and *v* the meridional component. The moisture flux is given by the product $q\overline{V}$ and the gradient of the meridional vapour flux component is: $\overline{\nabla}(qv)$. To calculate the divergence of the gradient vector of the meridional vapour flux (MC) the following expression is applied: $MC = \overline{\nabla} \bullet \overline{\nabla}(qv)$

2.4.6 Divergence of the gradient vector of the southeastern vapour flux component

The southeastern component of the wind (V_{SE}) is calculated by $V_{SE} = \frac{v-u}{\sqrt{2}}$. Following the same arguments given above the divergence of the gradient vector of the southeastern vapour flux component (SEC) can be expressed by $SEC = \overline{\nabla} \bullet \overline{\nabla}(qV_{SE})$

2.5 The PCGRADS based Analysis System.

The PCGRADS (Personal Computer Graphics and Display System) is a powerful system used by meteorologists to manipulate large meteorological data fields. This system is especially useful for manipulating large fields of atmospheric variables emanating from NWP and analysis models. During the development phase of the analysis system for tropical systems the principal researcher developed an analysis system, using PCGRADS features, to compute and display the atmospheric dynamics and other variables. The main features researched with this system are:

- Synoptic features at 8 pressure levels (1000 to 200 hPa) inclusive of: geopotential height fields, wind fields and relative humidity
- Temperature advection at the pressure levels as well as vertically averaged temperature advection in the lower troposphere.
- Relative vorticity and relative vorticity advection at the pressure levels.
- Moisture fields at pressure levels inclusive of: moisture flux, precipitable water, mixing ratio, water vapour flux by the meridional- and SE component of the wind, moisture flux gradients and their divergence (MC and SEC).
- Wind divergence at pressure levels and vertical profiles.
- Vertical motion at pressure levels and vertical profiles.
- Instability indices and total static energy.

Masks: These are single field masks, isolating an area where a selection of parameters contributing to heavy rainfall all coincide.

CHAPTER 3

HEAVY RAINFALL EVENTS OVER SOUTH AFRICA:

A STATISTICAL CLIMATOLOGY, 1940 – 1999.

Contribution by E Poolman

3.1 Introduction

Chapter 1 contains an introduction to floods which have occurred in southern Africa. The heavy rainfall leading to flooding is, however, difficult to predict accurately despite phenomenal improvements in numerical weather prediction during the 1980's and 1990's (Hammon, et al 1993). This happens because precipitation is parameterised in numerical weather prediction models and not derived directly from the independent atmospheric variables. Weather forecasters must acquire experience and knowledge to adjust the numerical precipitation forecasts in order to issue better rainfall forecasts. To achieve this goal requires a sound understanding of the weather systems producing rainfall, especially those that cause heavy rainfall.

In this chapter a two-pronged approach is taken: first, an identification scheme for past heavy rainfall events is developed, using their daily rainfall footprints; second, the climatological characteristics of these heavy rain events are studied.

A full record of all daily heavy rainfall was extracted from the SAWS rainfall archive for the years 1940 to 1999. Prior to 1940 rainfall station distribution over large parts of South Africa was too irregular (sparse) for this record. The trends and statistics of heavy rain events in South Africa, which this record reveals, are described in this chapter. This record should also be useful for the evaluation of conceptual models describing the heavy rainfall weather systems.

3.2 Processing methodology

3.2.1 Definitions

Houze, et al (1990) define a major rain event as one in which more than 25 mm rain falls over an area greater than 12 500 km^2 in 24 hours. Bradley and Smith (1993) define extreme rainstorm as a major rain event when the adopted daily rainfall accumulation is at least 125 mm at one or more rainfall station.

In this report, which applies to South Africa, a larger area than used by Houze in defining a heavy rainfall event is adopted so as to capture meso-alpha scale (length scale more than 250 km) rainfall events. Therefore a heavy rain event is defined as a region with more than 25 mm rainfall, in 24 hours and covering an area of least 20 000 km^2. This definition ensures that heavy rain events caused by meso-alpha scale, or larger, weather systems are captured.

3.2.2 Methodology

The rainfall station data are interpolated to a regular grid where each square represents an area of half a degree by half a degree (approximately 50 km by 50 km). The first step is to calculate a representative daily rainfall figure for each small square, taking into account the rainfall at different stations in the square. The next step is to mark all squares with representative rainfall values exceeding 25 mm. Areas where eight or more marked squares are adjacent identify a heavy rain event for that day. Separate heavy rain events sometimes occur on the same day.

Several techniques were tested in order to find the best representative rainfall value for each one of the 2 500 km^2 areas. These techniques include computing the median, mean, a weighted mean and an adapted Cressman interpolation. The last three techniques produce figures consistently close to one another. The median rainfall is often very unrealistic. In the end the weighted mean, developed by Tennant (1999) is applied. It produces realistic values and is used widely in this report (chapters 4, 5 and 6).

The number of heavy rainfall events for each day is identified as well as the region where each event occurs. Landman (1997) defines five homogeneous rainfall regions by applying principal component analysis on historical rainfall data. Landman's definition is applied here and the regions are listed in table 3.1:

Table 3.1: Five homogeneous rainfall regions over South Africa

Region	Acronym	Description
1	SW	Predominantly the winter rainfall area, the western half of the Western Cape Province
2	WI	The eastern half of Western Cape- and Northern Cape Province
3	SE	Eastern half of Eastern Cape- and Kwazulu Natal Province
4	CI	Free State- and North-west Province
5	NE	Gauteng-, Mpumalanga- and Limpopo Province

A rough estimate of the water yield from each heavy rain event is computed using the mean rainfall for the event multiplied by the area covered. A statistical analysis on the heavy rainfall data reveals trends in the variability and distribution of these events during the years between 1940 and 1999.

3.2.3 Storm Tracking

A weather system producing heavy rain may last several days causing widespread heavy rain over several regions. To detect these multi-day events an analysis is performed to identify heavy rain events lasting longer than one day. A simple tracking technique is used where it is hypothesised that a heavy rain event, which overlaps the previous day's area by at least 10%, is considered a continuous event. This provides for a record of long duration (or multi-day) heavy rain events (1940-1999). Statistical analysis on this record reveals the trends, variability and the geographical distribution of multi-day heavy rain events.

3.3 Heavy rainfall events statistics

3.3.1 Heavy rain days

The 60-year heavy rain event data set includes the spatial distribution of each event and allows the classification of the weather systems associated with these events. They are the COL, TTT and TC as described elsewhere in this report. This dataset is checked against some past weather systems which produced heavy rain. All of them are captured satisfactorily.

In his 'Climate of South Africa', Schulze (1965), states that almost four times more rain days occur during the summer months than during winter months. Figure 3.1 illustrates the monthly distribution of heavy rainfall days (1940-1999) for each of the homogeneous areas referred to by Landman (1997). Clearly these results support the early statistics produced by Schulze almost 40 years ago. Most of the heavy rainfall days also occur over the eastern- and north-eastern parts of South Africa (figure 3.1).

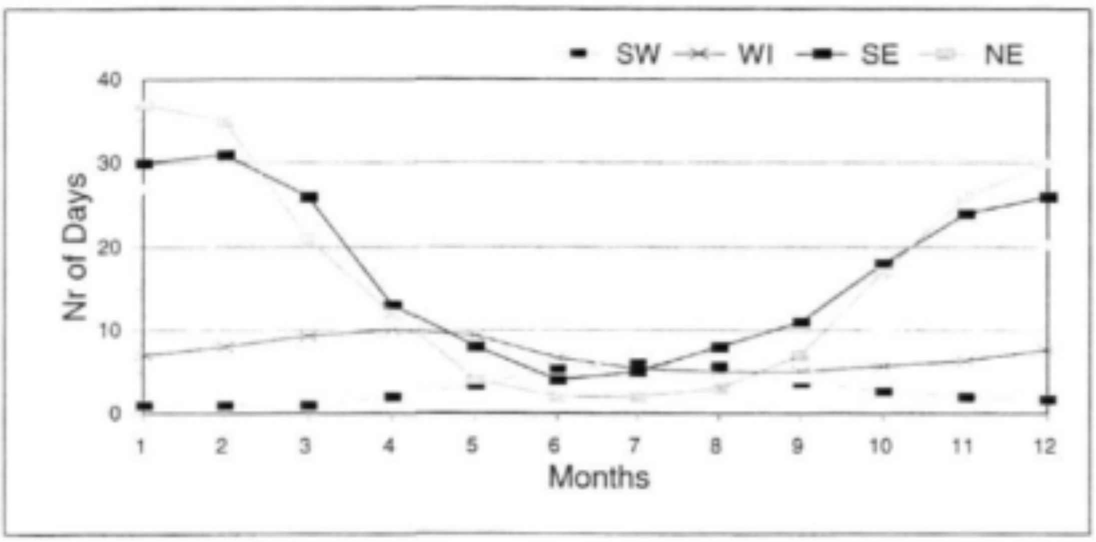

Figure 3.1 Year average heavy rain days

Figure 3.2 depicts the average monthly water yield, per Landman's area, produced during heavy rainfall days. Heavy rain days in January yield on average approximately 148 billion tons of water countrywide compared to about 26 billion tons in July (figure 3.2). Therefore the contribution of summer heavy rainfall days and the weather systems which cause them is far more important for South African hydrology than winter heavy rain days and the weather systems which cause them. In chapter 4 and elsewhere in this report the summer tropical weather systems over southern Africa and their interaction with baroclinic systems are discussed. These atmospheric circulation systems and their interdependence must be understood if precipitation forecasting, especially of heavy rainfall, is to be improved.

Figure 3.3 displays the number of heavy rain days per summer-year (running from July to June) for the years 1940 to 1999. The variability of the number of heavy rain days between years is striking. Taljaard (1996) states that except for 1972 the years 1970 to 1978 had the highest rainfall, on record, over South Africa. Figure 3.3 indicates that well above average number of heavy rain days also occurred in this period. This figure shows an all time low number of heavy rainfall days during 1991/92, considered one of the driest periods on record (Taljaard, 1996).

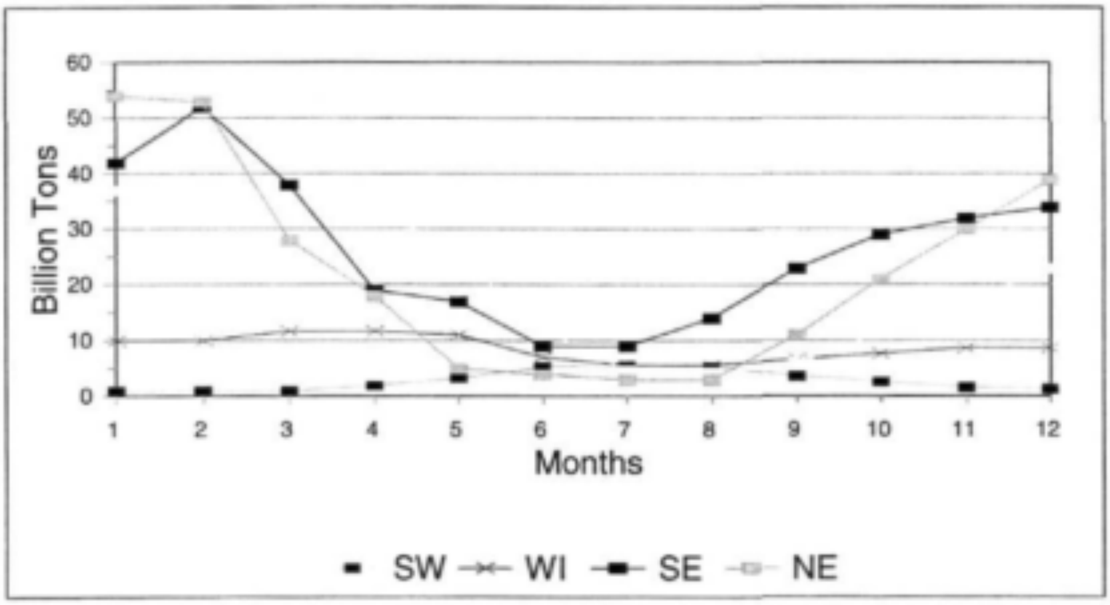

Figure 3.2 Year average water amount

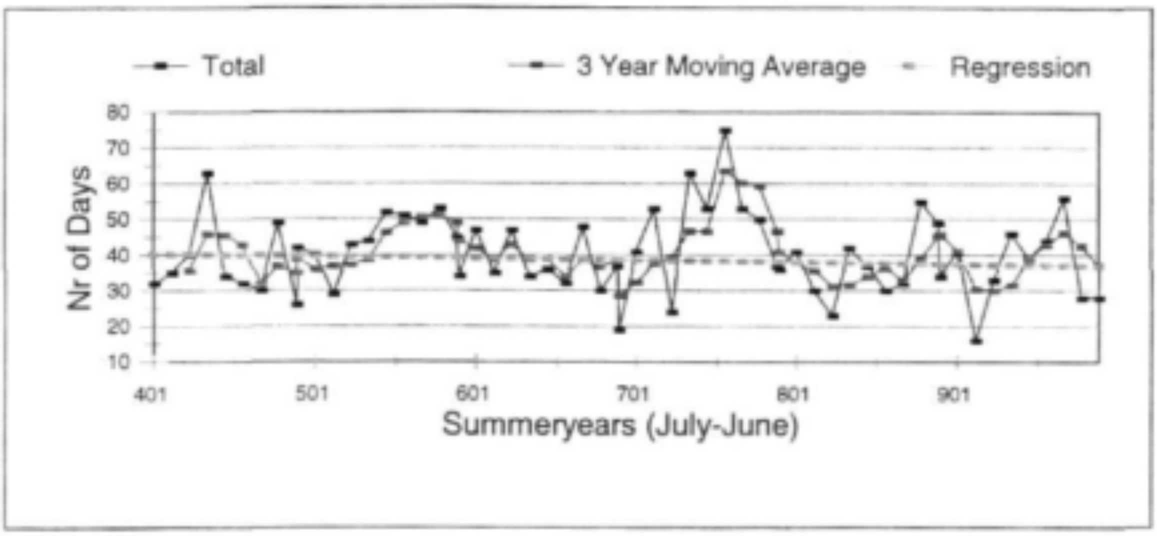

Figure 3.3 Summer year (July to June) number of heavy rain days. 401 represents 1940/41, 501 represents 1950/51 etc.

Schulze (1989) lists a large number of South African researchers who described the relationship between South African continental rainfall and the El Nino Southern Oscillation (ENSO) phenomenon. They all found that during La Nina years above normal rainfall generally occurs over South Africa and the opposite during El Nino years. Van Heerden et al (1988) indicated that the Southern Oscillation Index (SOI) and South African monthly rainfall is significantly correlated over the central interior of the country, coinciding roughly with Landman's CI region. It is therefore expected that more heavy rain days should occur here during La Nina years and less in El Nino years. Unexpectedly the correlation coefficient between the SOI and number of heavy rain days for the CI region is only 0.27, indicating that they are uncorrelated.

Careful inspection of Figures 3.3 and 3.6 reveals that variation in the number of heavy rainfall days and events indicates an increase in the inter-annual amplitude after approximately 1969/70. A decrease in the period is also probable. This means that an increase in the inter-annual variability of the number of heavy rainfall events happened. If this trend continues it points towards an increasing number of heavy rain days during a year with above normal rainfall and a decrease in the number of heavy rain days during a year with below normal rainfall. In other words, this may be evidence of increasing intensity of heavy rainfall events. But the regression line in Figure 3.3 shows a slight decline in the total number of heavy rain days. The high incidence of successive years with fairly high number of heavy rain events in the 1950's and the number of years with few rainfall events in the 1980's probably forced this decline.

3.3.2 Multi-day (long lasting) heavy rainfall events

Multi-day heavy rainfall events were identified using the storm tracking process. Generally the pattern in the number of multi-day heavy rain events per region during the year (figure 3.4) is similar to the pattern for single-day events depicted in Figure 3.1. Most of the multi-day events occur during the summer months and over the eastern regions of South Africa. In February, for the SE region and to a lesser extent the NE region, a significant decrease in the number of multi-day heavy rain events in comparison with December and January occur. This is also at odds with the number of single-day events as depicted by Figure 3.1, which shows a high number of single-heavy rain days during February. A possible explanation could be that multi-day heavy rain events during February last longer than those of either December or January. This may be because of the high incidence of slower moving tropical rain systems during February, over the eastern parts of the country. This supposition is supported by Figure 3.5 which shows a slight decrease in the number of single-day heavy rain events (January to February), but a slight increase in the number of multi-day events for February. Figure 3.5 also shows that single-day heavy rain events are predominantly summer features. They represent two-thirds or more of all heavy rain events throughout the year.

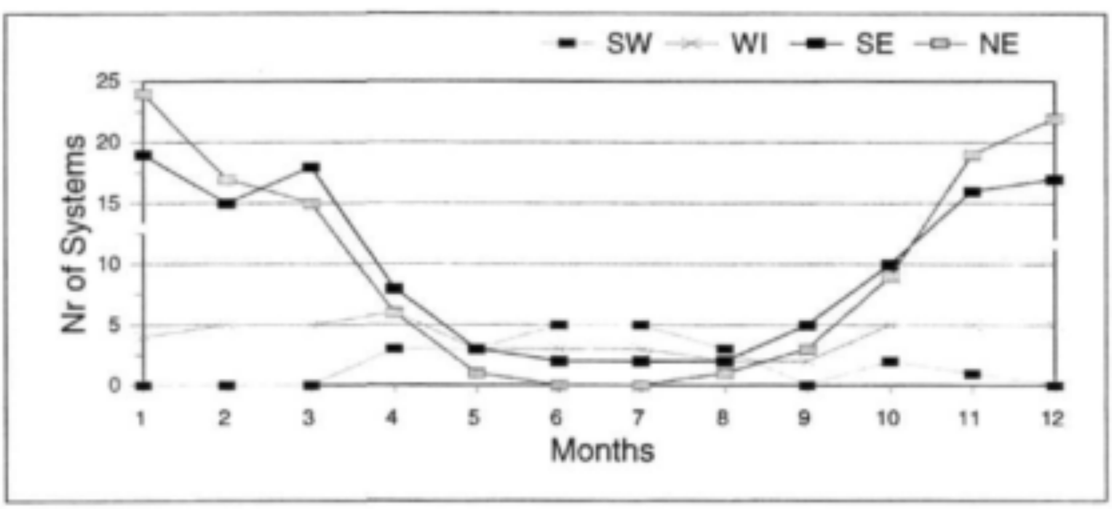

Figure 3.4 Year average number of heavy rain systems per region.

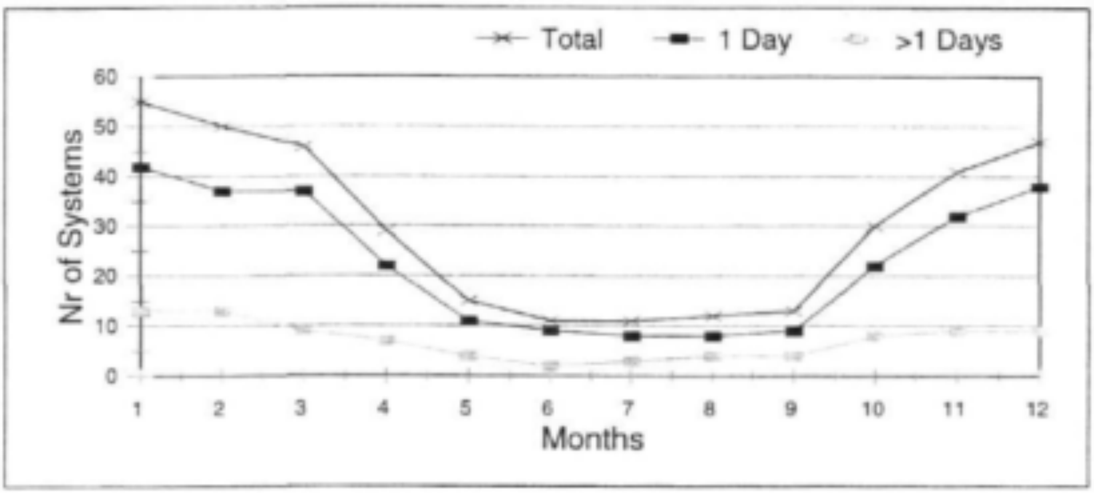

Figure 3.5 Year average number of one-day or longer heavy rain days.

Figure 3.6 depicts the annual variability of the total number, number of single and number of multi-day heavy rainfall events (systems). These are also referred to here as systems to differentiate from the number of heavy rainfall days which include days forming part of multi day events. The Southern Oscillation Index is also shown in this figure. Figure 3.6 shows lower annual variability than is evident in Figure 3.3 which includes days forming part of multi-day events.

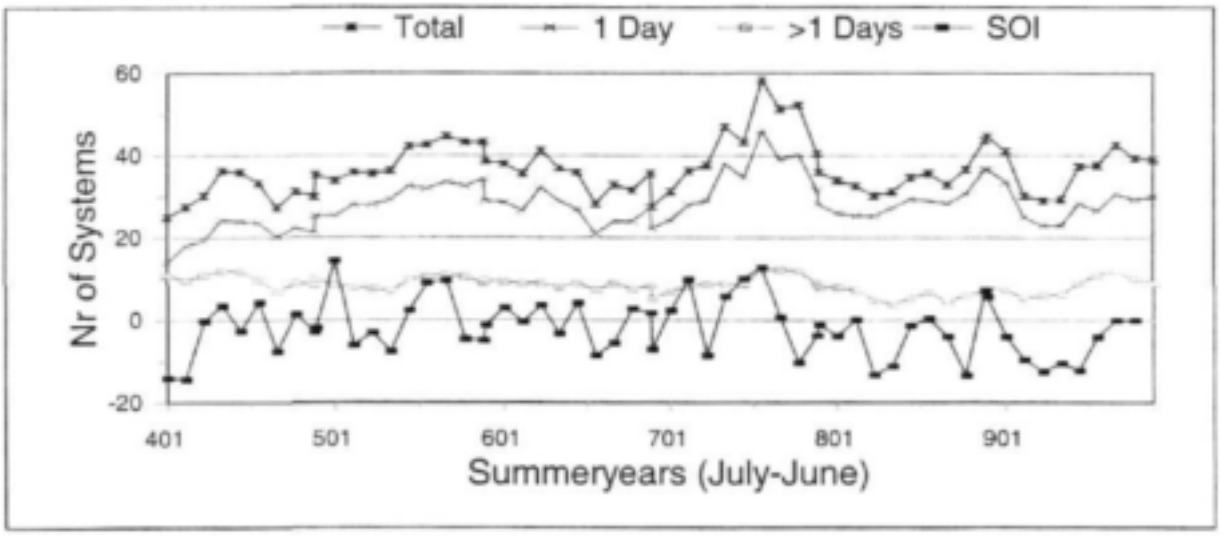

Figure 3.6 Summer year (July to June) number of heavy rain systems. 401 represents 1940/41, 501 represents 1950/51 etc.

Generally the same conclusions can be made regarding the period and amplitude of heavy rain events (systems), as can be made for heavy rain days. Once again the correlation with SOI is insignificant, even more so for the multi-day events (systems). Figure 3.7 portrays the three-year running mean for the data depicted by Figure 3.6. The steady increase in the total number as well as the number of single day events (systems) is clear. But at the same time, the steady decrease of multi-day events (systems), since 1940, stands out. The regression lines shown in Figure 3.8 even better illustrate these tendencies. The validity of the trends hypothesised by figure 3.8 survives a Monte Carlo test at the 90% confidence level.

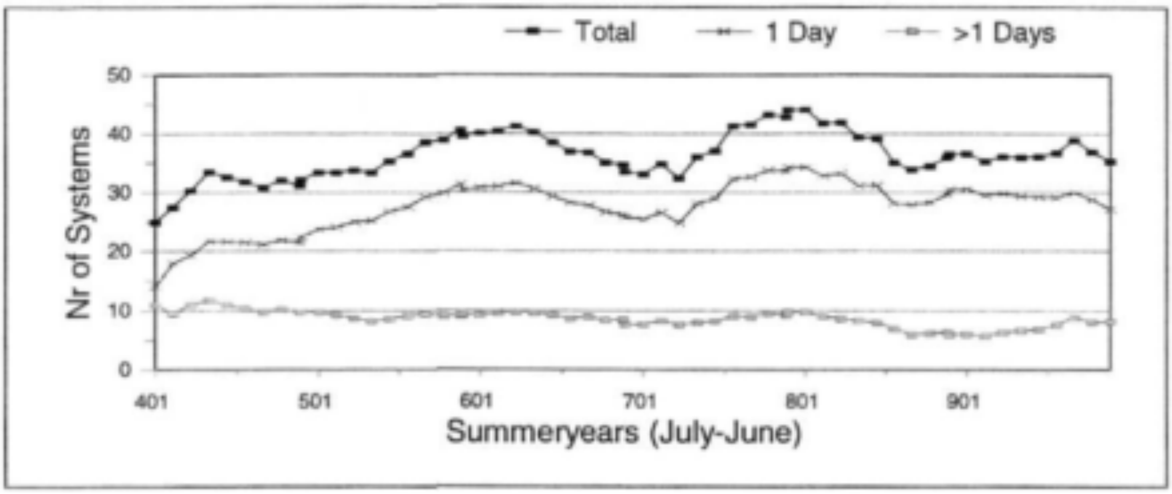

Figure 3.7. Three year running mean of summer year heavy rain systems. 401 represents 1940/41, 501 represents 1950/51 etc.

The data as depicted by Figures 3.1-8 suggests that between 1940 and 1999 there was a small but significant increase in the number of heavy rain events (systems) lasting one day, and a small but significant decrease in the number of multi-day events (systems). These results may be very significant in terms of the weather systems causing the rainfall but unfortunately a meteorological reason for this tendency is not yet available.

A complete record of heavy rain days and multi-day heavy rain events (systems), over South Africa, is available spanning the period 1940 to 1999. Analysis of this dataset leads to the following conclusions:

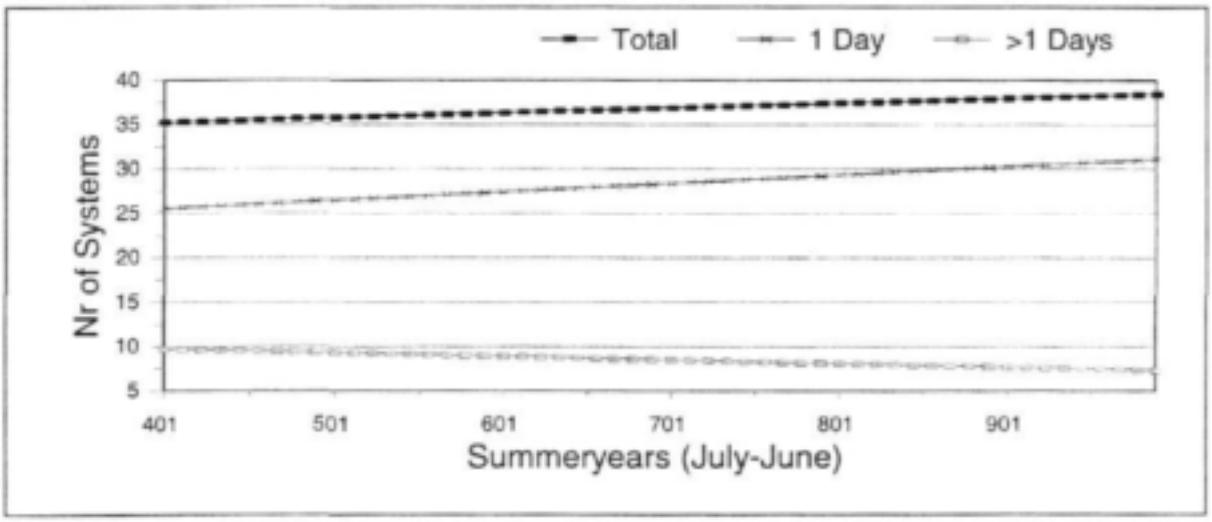

Figure 3.8 Trend of summer year heavy rain systems from 1940 to 1999. 401 represents the year 1940/41, 501 represents the year 1950/51, etc.

Most of the heavy rain events occurred in the eastern- and north-eastern parts of the country and during the summer months.

It is postulated that tropical weather systems play an important role in the development of heavy rain weather events over South Africa. Unfortunately, without a weather system classification valid for each heavy rainfall event (day) this assumption remains speculative.

A change in amplitude and period of the annual number of heavy rain days occurred during the 1970's. Similar results were found for the number of heavy rain events (systems). For both, the amplitude increased and the period became longer after the 1970's.

The occurrence of heavy rain events is uncorrelated with the SOI.

A statistically significant increase (to the 90% confidence level) exists in the number of single day heavy rain events during the years 1940-1999. But a similar decrease in the number of multi-day heavy rainfall events (systems) also exists in the data.

CHAPTER 4
TROPICAL WEATHER SYSTEMS

4.1 Continental tropical weather systems over Southern Africa.

Van Heerden and Taljaard, contributing to Karoly and Vincent (1998) discussed circulation systems over tropical and subtropical southern Africa. They identified three types of low pressure systems (tropical cyclones, tropical lows and heat lows) which are common over the low latitudes of continental sub Saharan Africa. They explained how a tropical low over the interior of southern Africa can be identified on loops of half-hourly geostationary satellite images by considering the low-level cyclonic circulation and anti-cyclonic upper tropospheric circulation depicted by the cloud motion. These systems generally move from east to west over the subcontinent but very rarely reach the African west coast. The third type of low, which frequents the lower latitudes, is the so-called heat low. These are shallow low pressure systems and form because of the intense heating of the lower few hundred metres of air in contact with the hot land surface.

In discussing the COL, Taljaard (1985) provided a brief description of the tropical easterly low over southern Africa by explaining how the low is cold cored below 700 hPa and warm cored in the middle and upper troposphere. Preston-White and Tyson (1993) proposed that an easterly wave can be distinguished from an easterly low by considering the level of maximum wind divergence. In the latter case wind divergence should occur at higher levels in the troposphere.

4.2 Forecasting techniques for tropical weather systems

Numerous research results exist which describe heavy rainfall from tropical weather systems over Southern Africa. Examples are the results of Alexander and Van Heerden (1991), Dyson and Van Heerden (2001), Lindesay and Jury (1991) and Treigaardt et al. (1988). Unfortunately research on forecasting techniques best suited for tropical weather systems have largely been neglected in South Africa. At the onset of this research project in 1999, disappointingly few recent research results were available on forecasting techniques in Southern Africa. One exception was De Coning (1997) who described how isentropic analysis could be used as a forecasting tool in South Africa. Isentropic analysis was applied with some success in identifying heavy rainfall areas for the heavy rainfall event during February 1996.

The years 1940 to 1970 were dubbed the golden period of African tropical meteorology. Meteorologists of the British school in East Africa, the Rhodesias (now Zimbabwe and Zambia) as well as the French school in equatorial western Africa all researched the circulation systems favouring rainfall in the region (Van Heerden and Taljaard contributing to Karoly and Vincent, 1998). Forsdyke (1949) considered that forecasting in the tropics requires different techniques from those employed in temperate latitudes. The quasi-geostrophic theory (Holton, 1992) is less amenable because the geostrophic wind relationship no longer holds and the flow generally occurs across the isobars. Furthermore, Forsdyke also suggested that streamline analysis be used to research tropical circulation and be employed to prepare forecasts. Thompson (1957) and Riehl (1979) supported this approach. At present streamline analysis is used in many countries where tropical weather systems are common such as the Northern Territories in Australia. Streamline analysis is however not in common use by forecasters in South Africa. Riehl (1979) found that upper air winds, surface pressure anomalies, 12 and 24-hour pressure changes, 24-hour changes in the height of upper isobaric surfaces and a plot of temperature and specific humidity are essential parameters for tropical weather forecasting. Forsdyke (1949) and Thompson (1957) found upper air ascents to be fundamental in tropical forecasting. They found that when the environmental lapse rate is greater than the saturated adiabatic lapse rate and high levels of humidity exist up to the freezing level, widespread or general precipitation is likely. Riehl (1979) explained how a vertical profile of total static energy could be used to identify an unstable atmosphere.

During most of the year atmospheric circulation over South Africa, especially the central and southern regions, is dominated by extra tropical weather systems such as cut-off lows, cold fronts and the ridging Atlantic Ocean High. Weather forecasters in South Africa are experienced in forecasting rainfall from these systems. During late summer weather systems from the tropics invade the northern regions of South Africa. Because tropical weather systems only appear during three or four months of the year weather forecasters often lack the experience to identify them timeously. Invading tropical weather systems are often associated with heavy rainfall and flooding (February 1988, February 1996, February 2000). In addition the highest frequency of heavy rainfall events occur over the eastern and northern parts of South Africa and then during the late summer months. It is therefore very important that South African forecasters identify these tropical systems and apply appropriate forecasting techniques. In order to predict heavy rainfall from tropical weather systems it becomes imperative that the forecaster must first be able to identify a tropical weather system.

4.3 A model for the identification of tropical weather systems (MITS)

The model for the identification of tropical weather systems (MITS) is a conceptual model with which tropical characteristics of the atmosphere can be illustrated. An important motivation for the development of MITS was to provide operational meteorologists with a tool, which they can use in an operational environment to promptly identify tropical circulation patterns. MITS can also be used as an aid to issue timely and accurate rainfall forecasts by identifying areas where tropical convection is possible. MITS is based on atmospheric dynamics and if used, would free the forecaster from having to be concerned with the complex dynamics. However, it is important that the theoretical detail be available to the operational meteorologist to serve as background information and as a basis for possible criticism and refinement. MITS, together with its theoretical basis, could also be used in the training of forecasters, which could ensure that young operational meteorologist will be well versed in the basic principles governing tropical circulation.

Southern Africa is characterised by a moderately elevated plateau, for the greater part rising to over 1000 m above sea level and to more than 1500 m over extensive areas (Taljaard, 1994). The geopotential height of the 850 hPa pressure level is close to 1500 m above sea level and it is common practise in the forecasting offices in South Africa to use the geopotential heights of the 850 hPa level as the surface level. It therefore made sense to develop MITS specifically for the interior of South Africa, much of which lies close to the 850 hPa level.

MITS consists of five procedures. Firstly the vertical displacement of low and high-pressure systems with height is investigated. Then the relationships between upper tropospheric temperatures and large-scale synoptic systems are detailed. The third component is to search for a moist diverging high in the upper troposphere. The fourth factor to consider is the average value of total static energy (TSE) throughout the troposphere. The fifth component is the conditional instability of the atmosphere as determined from the vertical distribution of TSE. Upward motion in the lower and middle troposphere is of paramount importance for the production of widespread rainfall and areas where this upward motion exists are located by MITS. The final and most important product of MITS is to provide the operational meteorologist with a single field, which indicates where rainfall in a tropical atmosphere is likely to occur.

4.3.1 Dynamical characteristics of MITS

4.3.1.1 Vertical integrity of low and high-pressure systems.

The low must be upright from 850 to 400 hPa and should be overlain by a ridge of high pressure at 200 hPa.

Holton (1992) defines a barotropic atmosphere as one in which the density is a function of pressure alone. This means that isobaric surfaces are also surfaces of constant temperature so that $\overline{\nabla}_p T = 0$. Where $\overline{\nabla}_p = \bar{i}\frac{\partial}{\partial x} + \bar{j}\frac{\partial}{\partial y}$ and T is temperature. In the absence of a temperature gradient on a specific pressure level the thermal wind will be zero. The thermal wind represents the vertical geostrophic wind shear and can be expressed by $\overline{V}_T = \overline{V}_g(p_1) - \overline{V}_g(p_0)$. Where $\overline{V}_T$ is the thermal wind and $\overline{V}_g$ the geostrophic wind at pressure levels p_1 and p_0 ($p_1 < p_0$). When the thermal wind is equal to zero the geostrophic wind will not change with height. Therefore in such a theoretical barotropic atmosphere the gradient of geopotential energy remains constant with height. Synoptic scale high and low pressure systems will in this ideal situation "stand upright" with height.

Holton (1992) further states that barotrophy provides very strong constraints on the motions in a rotating fluid and is in fact never achieved in the atmosphere. Nevertheless in a tropical atmosphere the circulation will tend towards this situation. The first component of MITS is therefore to look for a low-pressure system, which stands approximately upright with height from the surface (850 hPa) up to 400 hPa.

In the real tropical atmosphere strong surface and middle tropospheric convergence occurs in association with the "upright" low-pressure system. As will be dealt with later, this convergence in turn results in upward motion and if adequate water vapour is available convective cloud or so-called "hot towers" will develop. Riehl (1979) explains the process by which the hot towers act as energy tubes through which energy from the lower troposphere is transported to the upper troposphere where it is distributed horizontally by the upper air divergence. The condensation releases a large amount of latent heat, which is in turn responsible for above normal upper tropospheric temperatures (Triegaardt et al., 1991). The latent heat release therefore, quickly results in a warm core developing above the lower level low (Taljaard, 1985). Holton (1992) shows that the geopotential thickness of a layer is directly proportional to the average column temperature with the result that an upper tropospheric high-pressure system forms above the surface low.

4.3.1.2 Average column temperatures in the 500-300 hPa layer

A core of high average column temperatures should be present in the 500-300 hPa layer.

Paragraph 4.3.1.1 details how the upper tropospheric high develops because of the above normal temperatures in the upper troposphere, which in turn come in to existence because of the release of latent heat. The average column temperatures in the 500-300 hPa layer are therefore used as the second component of MITS. The warm core in the column underneath the 200 hPa high (component 1 of MITS) is fundamental to the identification of tropical weather systems.

The horizontal temperature gradient of the column temperatures can also be used to determine the baroclinicity of the atmosphere. The absence of such a temperature gradient is indicative of a barotropic atmosphere. Although this theoretical situation is never achieved in the real atmosphere, a weak temperature gradient can nevertheless be used to identify a 'tropical atmosphere'.

4.3.1.3 Moist diverging high in the upper troposphere

Precipitable water values in the troposphere should exceed 20 kg m^{-2} and be in the same geographical position as the 200 hPa ridge of high-pressure and upper tropospheric wind divergence.

It is common practice in the forecasting offices of the SAWS to use relative humidity to identify areas of high water vapour content. However relative humidity in itself does not specify the mass of water vapour present in the atmosphere. Huschke (1959) defines precipitable water (W) as the total water vapour contained in a vertical column extending between two specified levels. To build an upper tropospheric high-pressure system requires the release of latent heat through condensation. High values of precipitable water in the column directly below the 200 hPa high-pressure system show that this process is indeed taking place.

The developing upper tropospheric high causes horizontal wind divergence. This divergence removes air horizontally in the upper troposphere. It is because of this wind divergence that the vertical integrity of the tropical system can be maintained. Without the upper tropospheric divergence the system would fill up because of the lower level convergence and latent heat release.

4.3.1.4 Average total static energy (TSE).

*Average TSE in the 850-300 hPa layer should exceed 330 * 10^3 J kg^{-1}. Tight horizontal gradients of TSE identify a zone of air mass change.*

It is common practice for forecasters to use the equivalent potential temperature to pinpoint areas where the properties of an air mass are changing by searching for tight gradients of equivalent potential temperatures. Holton (1992) states that an alternative to the equivalent potential temperatures is TSE (also referred to as moist static energy). This is particularly applicable when convection is studied. TSE is the total energy within an atmospheric parcel of air but neglecting the small kinetic energy value (Triegaardt et al., 1991) and is computed by: $TSE = C_pT + gz + Lq$, where C_p is the specific heat of dry air, z is the geopotential height, L the latent heat of condensation and q the specific humidity. The first term on the right hand side of the equation represents the enthalpy, the second term the geopotential energy and the third term the latent energy. In an atmosphere where above normal upper tropospheric temperatures occur, as is the case in a tropical atmosphere, the contribution of the enthalpy will be to increase the TSE values. The high geopotential heights in the upper troposphere in a tropical weather system will in turn increase the geopotential. The contribution of the latent energy in a tropical atmosphere will also be to increase the TSE because of the high moisture content of the air. In MITS the average TSE is computed in the 850-300 hPa layer. This is done in order to capture the contribution of the water vapour in the lower troposphere, as well as the contribution of the above normal temperatures and geopotential heights in the upper troposphere. Dyson and Van Heerden (2002) have shown that TSE values greater than 330 * 10^3 J kg^{-1} are indicative of tropical circulation over southern Africa.

4.3.1.5 Deep cumulus convection and vertical motion.

Upward motion ought to be present from 700 to 400 hPa, the atmosphere should be conditionally unstable up to 400 hPa and precipitable water values exceed 20 kg m^{-2}.

The continuity equation (Holton, 1992) $\frac{\partial\omega}{\partial p} = -\overline{\nabla}_p \bullet \overline{V}$ expresses the relationship between horizontal wind divergence and change of omega ($\omega = \frac{dp}{dt}$) with pressure. If $\overline{\nabla}_p \bullet \overline{V} < 0$ (convergence) then $\frac{\partial\omega}{\partial p} > 0$ which means that ω decreases (increases) with height (pressure). Above areas where convergence occurs in the lower and middle troposphere ω should decrease with height, which means, because of the negative relationship, upward motion must increase with height. Above the 400 hPa level ω increases with height in association with the upper tropospheric divergence. An important component of MITS is to isolate those areas where upward motion exists from 700 hPa to 400 hPa. The interior of South Africa is approximately 1500 m above sea level, which means that the 700 hPa level is approximately 1500 m above the surface and is still representative of the lower troposphere. The 700 hPa level is also close to the summer convective cloud base level.

The vertical distribution of TSE is used to investigate the conditional instability of the atmosphere. Harrison (1988) explained that a conditional unstable atmosphere is required for deep cumulus convection. A typical vertical profile of TSE indicating conditional instability is depicted by Figure 4.3. TSE decreases from the surface up to approximately 500 hPa and then increases steadily with height. The dashed line in Figure 4.3 is the surface value of TSE and is reached again only as high as at the 200 hPa level. This means that the atmosphere is conditionally unstable and deep cumulus convection is possible up to 200 hPa. In MITS it is required that deep convective development should be possible up to at least 400 hPa and that the surface value of TSE is the value at 850 hPa.

When the atmosphere is conditionally unstable up to 400 hPa and upward motion occurs in the 700-400 hPa layer, atmospheric conditions are favourable for the development of extensive convective precipitation. Experimental results obtained in this research indicate that if the other two parameters, discussed in this paragraph (vertical motion and conditional instability), are favourable rainfall is probable from tropical weather systems when precipitable water in the 850-300 hPa layer also exceeds 20 kg m^{-2}. Therefore when the three variables mentioned here occur simultaneously convective rainfall is likely.

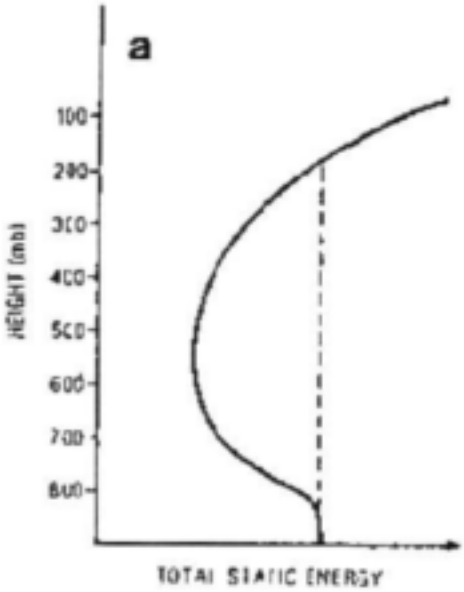

Figure 4.3: A typical vertical profile of total static energy associated with deep convection. The dashed line is the upward projection of the surface energy value (after Harrison, 1988).

4.4 MITS in February 1988

During February of 1988 extreme rainfall occurred over large areas of Southern Africa. Widespread flooding occurred and Bloemfontein was isolated from the outside world, except by air, as connecting routes were washed away or flooded (Jury et al., 1993, Lindesay and Jury,1991 and Triegaardt et al., 1991). Almost the entire summer rainfall area of South Africa received well above the average February rainfall. Over the central interior rainfall was exceptionally heavy with the recorded monthly rainfall between 4 and 6 times the mean February rainfall. Bloemfontein Airport received 530 mm of rain during February 1988. Over the southern Free State, De Wetsdorp reported 442 mm, Trompsburg 417 mm, Jamestown 461 mm, Buffelsfontein 409 mm and Danielskuil 512 mm. Unprecedented heavy rain also fell over the

Northwest (Stella 448 mm) and the Northern Cape Provinces. The flood producing rainfall occurred in a relatively short period from 19 to 22 February 1988 (Triegaardt et al., 1991).

The synoptic circulation on 21 February 1988 is considered representative of the atmospheric circulation during this heavy rainfall event and is used here to illustrate the tropical nature of the atmospheric dynamics.

4.4.1 Rainfall on 21 February 1988

Table 4.4 lists 24-hour rainfall totals on 21 February 1988 at a few rainfall stations. Two of them in Bloemfontein had rainfall in excess of 300 mm. The other 7 stations all had more than 200 mm and are close to Bloemfontein. The central interior received widespread rainfall with 24-hour rainfall totals in excess of 50 mm mainly over the western Free State and surrounding areas.

Table 4.4: 24-hour rainfall exceeding 200 mm for 21 February 1988

Latitude (° S)	Longitude (° E)	Rainfall (mm)	Place
29.1	26.2	311	Bloemfontein Hamilton
29.1	26.2	310	Bloemfontein Zoo
28.7	25.8	284	Dealesville
29.0	26.1	283	Bainsvlei
30.4	26.8	266	Rouxville
29.5	26.6	259	Baden
27.8	24.7	246	Pampierstad
30.2	26.5	237	Smithfield
27.7	25.4	210	Holfontein

4.4.2 MITS on 21 February 1988.

The 1200 UTC analysis of the NCEP data is used here.

Figure 4.4.1 depicts the low, middle and upper air circulation pattern on 21 February. The main feature is the closed low centred over Botswana at the 850 hPa level (Fig. 4.2.1a). Figure 4.4.1b shows that the closed low is maintained at 700 hPa although it is displaced slightly southward. At 500 hPa (Fig. 4.4.1c) and 400 hPa (Fig. 4.4.1d) the low becomes a sharp trough and continues its southwestward displacement as it becomes entrained in the westerly flow extending northwards from the mid-latitudes. However, at the 500 hPa and 400 hPa pressure levels a secondary trough extends northeastward over Botswana and at approximately the same position as the closed low at 850 hPa. Figure 4.4.1e shows that the 200 hPa upper air trough is west of South Africa while a strong ridge over central Botswana displaces the closed low at 850 hPa. The first component of MITS is met over Botswana.

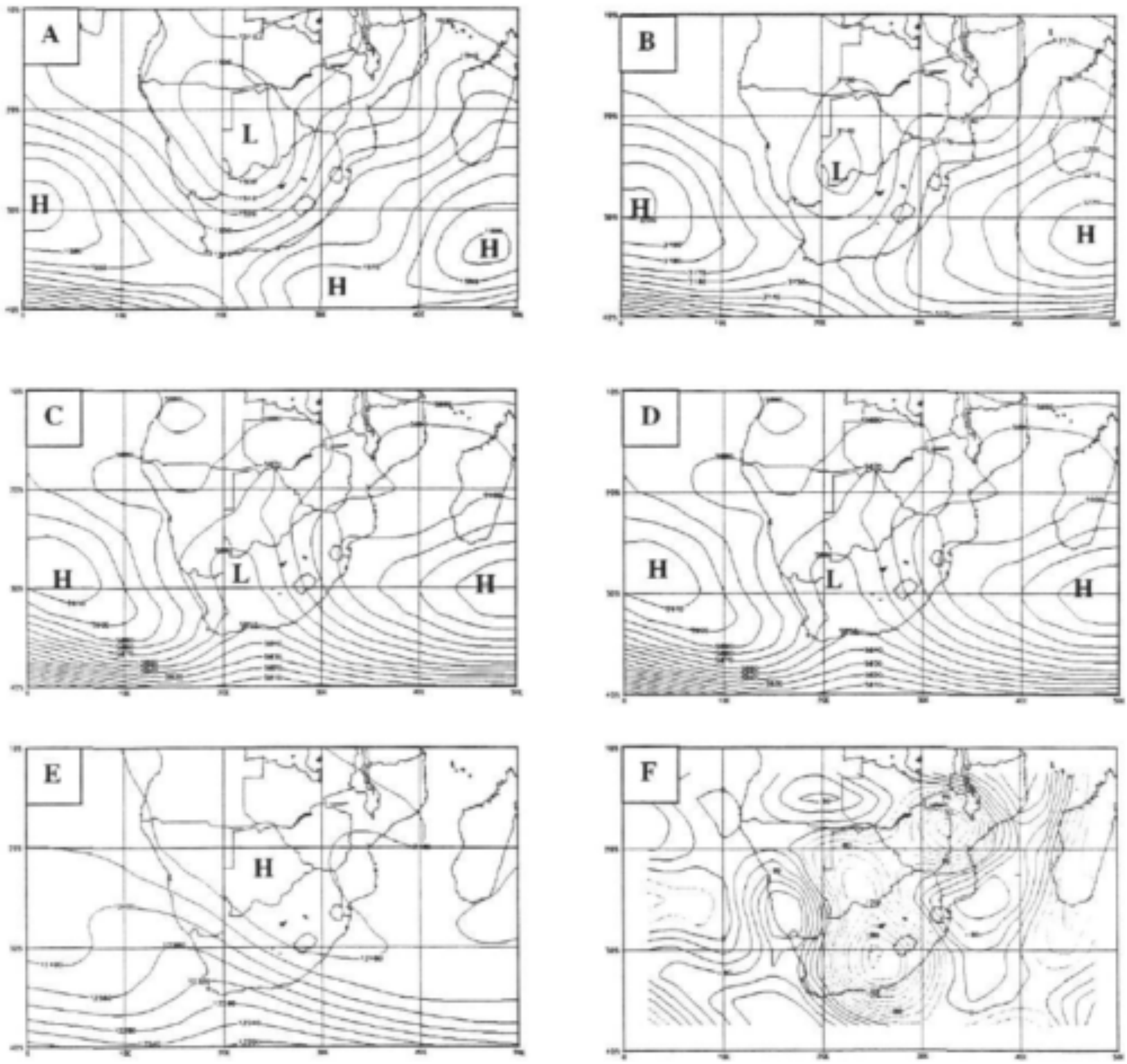

Figure 4.4.1: The 850, 700, 500, 400 and 200 hPa geopotential heights for 21 February 1988, shown in A, B, C, D and E respectively. Figure F displays the wind convergence (solid lines) and divergence (dashed lines) at the 200 hPa pressure surface, units multiplied by 10 $^{-6}$ per second.

The highest 500-300 hPa average column temperatures (greater than –16° C) (Fig. 4.4.2), as expected, occurred in the vicinity of the 200 hPa upper air ridge. A tight gradient of column average temperature exists between the warm core over Botswana and the cold core over the southwestern Cape. On the other hand the average column temperature gradient eastward between the warm core over Botswana and the Mozambican regions is weak. Although the atmosphere must in the strictest sense still be classified as baroclinic over this area it is clear from the weak average column temperature gradient distribution that the atmosphere is becoming less baroclinic. The second component of MITS is met and is clearly illustrated by Figure 4.4.2

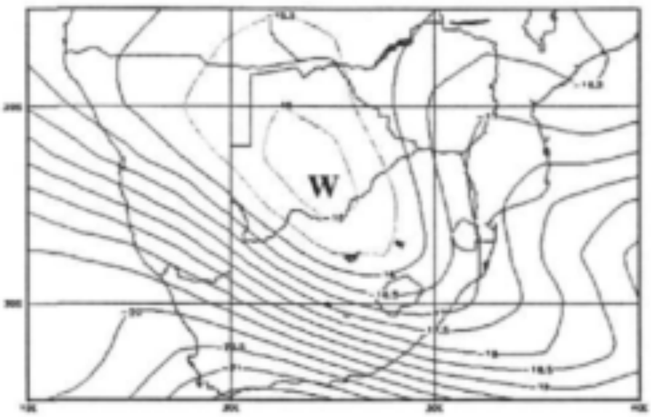

Figure 4.4.2: Average 500-300 hPa column temperatures on 21 February 1988. Temperatures are in degrees Centigrade. Dashed lines indicate temperatures greater than -16 degrees Centigrade.

The precipitable water (in units of kg m $^{-2}$) in the layer bounded by 850 hPa and 300 hPa is shown in Figure 4.4.3. Values greater than 20 kg m $^{-2}$ (indicated by dotted lines) show a remarkable correspondence to the positive wind divergence at 200 hPa (Fig. 4.4.1f). The maximum values of precipitable water occur in a band over the central interior of South Africa extending a tongue into southern Botswana. Considering the position of the ridge of high pressure at 200 hPa (Fig 4.4.1e) in association with the positive wind divergence (Fig 4.4.1f), and the high values of precipitable water, it is clear that this warm thermal high can also be classed as a moist diverging high. The third component of MITS is also satisfied.

The average total static energy (TSE) of the 850-300 hPa layer is shown in Figure 4.4.4 Values larger than 335 $*10^3$ J kg^{-1} (dotted lines) occur over the central interior of South Africa, Botswana and Zimbabwe. The high values of average TSE on 21 February 1988 are due to a combination of the presence of the moist air in circulation (potential of latent heat release), anomalously high temperatures in the upper troposphere (enthalpy) and the upper tropospheric ridge of high pressure (geopotential). The fourth MITS component stating that the average TSE values in the troposphere should exceed 330 * 10^3 J kg^{-1} is therefore also met.

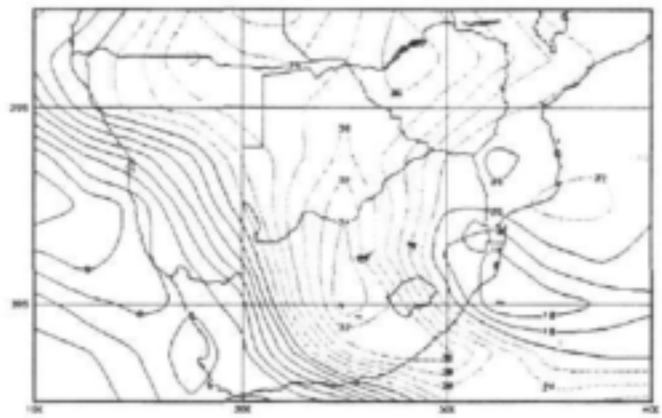

Figure 4.4.3: Precipitable water in the 850-300 hPa layer on 21 February 1988 in units of kg m^{-2}. Dashed lines indicate precipitable water values greater than 20 kg m^{-2}.

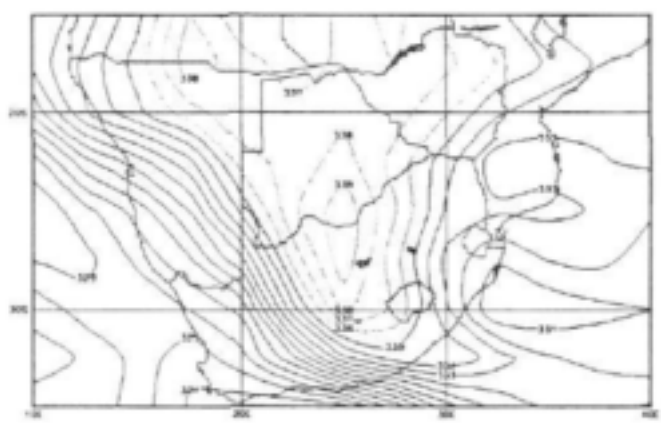

Figure 4.4.4: Average total static energy of the 850-300 hPa layer on 21 February 1988, in units of 10^3 J kg $^{-1}$. Dashed lines indicate values greater than 335 * 10^3 J kg^{-1}.

Figure 4.4.5 portrays the vertical distribution of TSE at Bloemfontein (more than 300 mm rain in 24-hours). This vertical distribution of TSE is a typical example of a conditionally unstable atmosphere (Triegaardt et al., 1991). The TSE decreases with height up to 500 hPa although there is an insignificant increase in TSE values between 700 and 600 hPa. From 500 to 300 hPa there is a steady increase in TSE but the value at 850 hPa remains greater than the 300 hPa value. This means that the layer of deep convection is higher than the 300 hPa level and is indicative of atmospheric conditions favourable for the development of convective cloud.

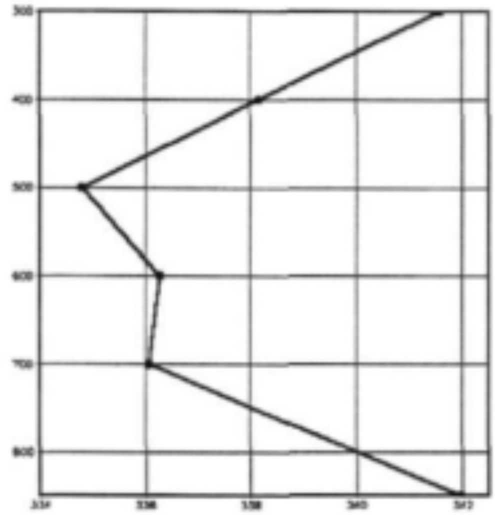

Figure 4.4.5: Vertical distribution of total static energy (10^3 J kg^{-1}) on 21 February 1988 at 29° S 26° E (near Bloemfontein).

The vertical distribution of omega, near Bloemfontein, as illustrated by Figure 4.4.6, is a further indication of favourable atmospheric conditions for the development of rain producing cloud structures. The air is ascending throughout the troposphere with values close to zero at the surface (850 hPa) as well as at 100 hPa. Maximum uplift occurs at 400 hPa with a value approximately –0.4 Pa s^{-1}. An investigation of Figures 4.4.3, 4.4.5 and 4.4.6 show that the 5th requirement of MITS is met. Convective development did indeed take place in the area close to Bloemfontein, as was indicated by MITS.

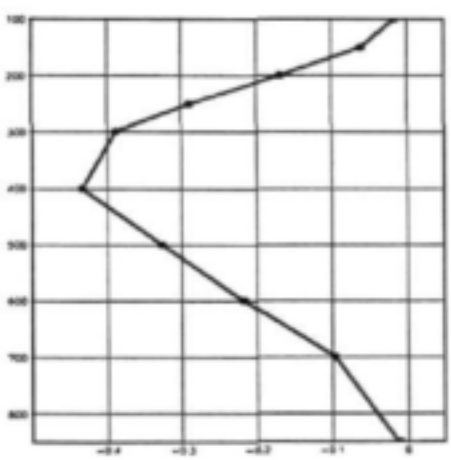

Figure 4.4.6: Vertical distribution of omega values (Pa s^{-1}) on 21 February 1988 at 29° S 26° E (near Bloemfontein).

4.5 MITS in February 2000

The NCEP data used for February 1988 analyses are generally accepted to be of a high quality and showed that the tropical characteristics of the atmosphere were well simulated. Unfortunately these data are of little use in a forecasting environment where prognostic fields from numerical weather prediction must be analysed in order to create a forecast. It was therefore decided to test MITS on the prognostic fields of the limited area model Eta that is currently operational in the SAWS.

Dyson (2000) and Dyson and Van Heerden (2002) provided a detailed description of the performance of MITS during February 2000. Due to the large number of diagrams needed to demonstrate MITS only 1 day, 8 February 2000, was selected to discuss here.

4.5.1 Synoptic conditions and rainfall during February 2000

February 2000 will be remembered for the devastating floods, which occurred over the Northern Province of South Africa and central Mozambique. Hundreds of people lost their lives and floodwaters displaced tens of thousands of people. Most of the rainfall occurred during two periods namely 5-10 February and 22-25 February 2000. During both periods the severe rainfall was caused by a tropical weather system moving from east to west over the southern sub-continent (Dyson and Van Heerden, 2001).

4.5.2 MITS on 8 February 2000

All the fields discussed here were obtained from the 12h prognosis of the 0000 UTC Eta model run on 8 February 2000 and all the MITS results detailed here are therefore valid for 1200 UTC on the 8^{th}.

On 8 February 2000 the surface tropical low pressure system was situated over the Namibia Botswana border, with a secondary low over the central interior of South Africa. The high-pressure system prevailing over the northeastern interior of South Africa maintained an inflow of moist tropical air from the Mozambique Channel over the central and eastern interior of the country. Widespread and heavy rainfall occurred over Gauteng-, eastern parts of the Northwest- and western part of the Northern Provinces (shaded area in Figure 4.5.6). On this day Germiston in Gauteng had 144 mm, Stockpoort in the Northern Province 145 mm and Marico in the Northwest Province 155 mm.

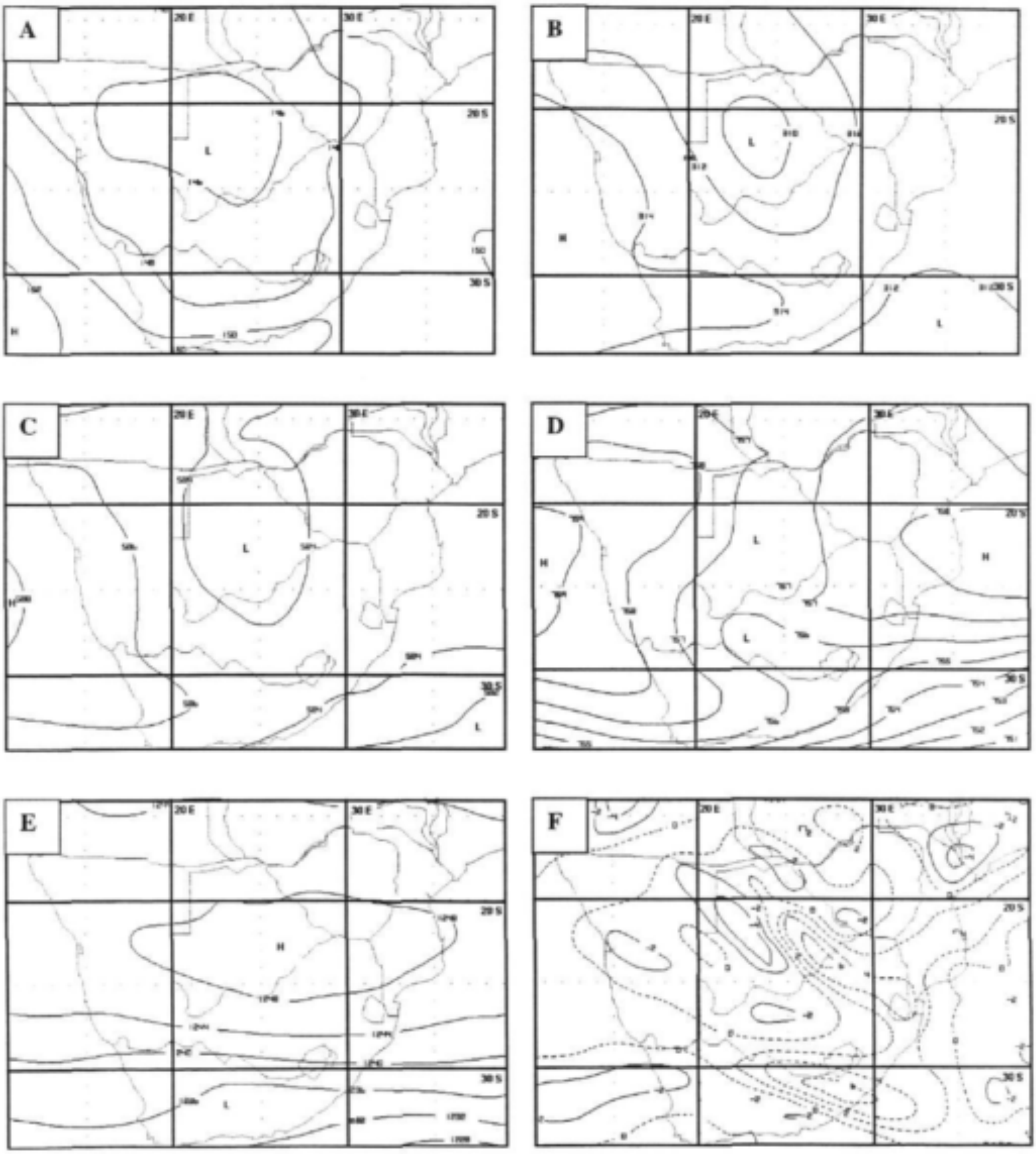

Figure 4.5.1: The topography of the 850, 700, 500, 400 and 200 hPa pressure surfaces for 8 February 2000, shown in A, B, C, D and E respectively. The contours are labelled in geopotential decametre. Figure F displays the average 200 to 300 hPa wind convergence (solid lines) and divergence (dashed lines).

Figure 4.5.1 represents the 850 hPa, 700 hPa, 500 hPa, 400 hPa and 200 hPa geopotential height fields. The fact that the low is "standing upright" is clearly evident. Near the centre of the low over Botswana the 850-, 700- and 500 hPa contours are nearly parallel. Fig. 4.5.1d (4.5.1e) depicts the 400 hPa (200 hPa) geopotential heights. A broad weak trough is present at 400 hPa in the same geographical position as the low illustrated in Figure 4.5.1(a-c). However, at 200 hPa a closed high-pressure system lies right above the low on the lower levels, which is typical of tropical circulation systems. Figures 4.5.1 clearly illustrate that the first component of MITS is satisfied.

Figure 4.5.2 depicts the average column temperatures in the 500-300 hPa layer. The highest temperatures (-14.5 °C) occur over central Botswana. A comparison with Figure 4.5.1e shows that this core of high temperatures lies in the same geographical position as the 200 hPa high. Comparing the temperature gradient over the Northern Cape Province with the temperature gradient over the Northern Province and Mozambique it is clear that the air in circulation over the eastern parts of the subcontinent is typical of a tropical circulation system.

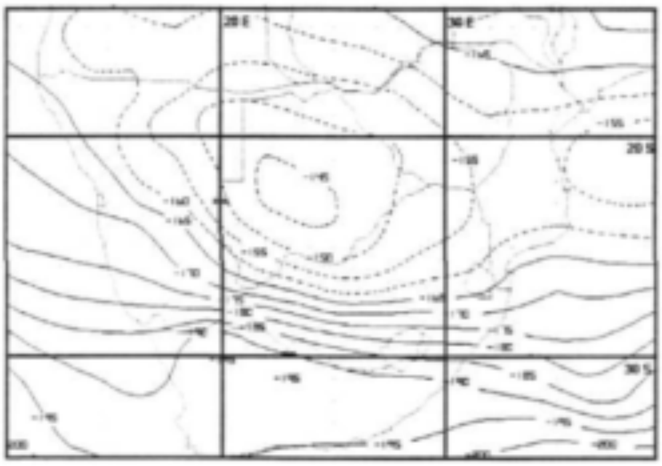

Figure 4.5.2: Average 500-300 hPa column temperatures on 8 February 2000. Temperatures are in degrees Centigrade. Dashed lines indicate temperatures greater than -16 degrees Centigrade.

Figure 4.5.3 shows the precipitable water in the 800-300 hPa layer with the dashed contours indicating values greater than 20 kg m^{-2}. Comparing Figures 4.5.1e, 4.5.2 and 4.5.3 it is clear that the high values of precipitable water overlap the position of the 200 hPa high pressure. Wind divergence occurs over the central and eastern parts of the 200 hPa high coincident with the high values of precipitable water. Both the second and third MITS components are clearly satisfied.

The average total static energy (TSE) is depicted in Figure 4.5.4. Over most of the country TSE values are greater than 330 * 10^3 J kg^{-1}. The dashed lines indicate values higher than 335 * 10^3 J kg^{-1} with maximum values of 337 * 10^3 J kg^{-1} over Gauteng and the Northwest Provinces. The tight gradient of TSE over the central interior is a clear indication of the change of the properties of the air mass towards to the south and west. The high TSE values roughly coincide with heavy rainfall on this day satisfying the fourth MITS component.

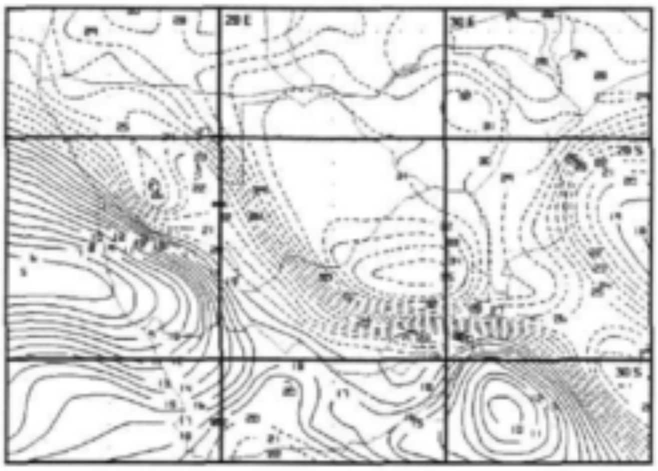

Figure 4.5.3: Precipitable water in the 850-300 hPa layer on 8 February 2000 in units of kg m^{-2}. Dashed lines indicate precipitable water values greater than 20 kg m^{-2}.

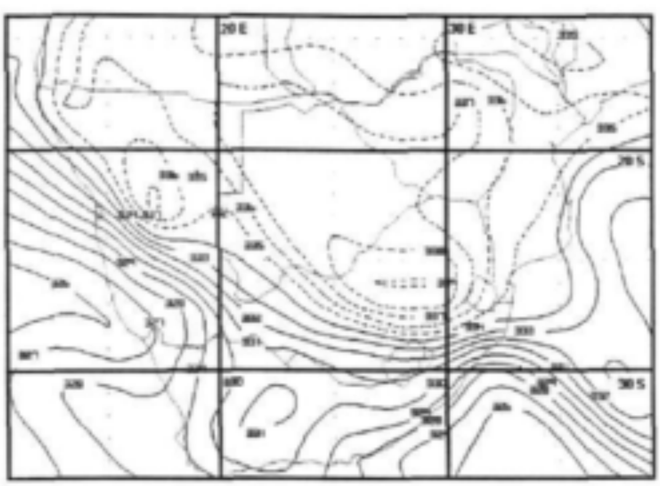

Figure 4.5.4: Average total static energy of the 850-300 hPa layer on 8 February 2000, in units of 10^3 J kg $^{-1}$. Dashed lines indicate values greater than 335 * 10^3 J kg^{-1}.

The arrows in Figure 4.5.5 indicate areas where the atmosphere is conditionally unstable up to 400 hPa encouraging deep cumulus convection. However conditional instability also occurs in baroclinic circulation systems and this factor alone cannot be used to determine the tropical nature of a weather system. The dashed contours on Figure 4.5.5 indicate those areas where upward motion exists in the column bounded by the 700 hPa and 400 hPa levels. Where the upward motion field overlaps the arrows (conditionally unstable atmosphere) conditions are conducive for deep cumulus convection. In Figure 4.5.3 the precipitable water values greater than 20 kg m^{-2} are indicated and serve as a reminder that although atmospheric conditions are favourable for deep cumulus convection, no thundershowers will develop in the absence of sufficient water vapour.

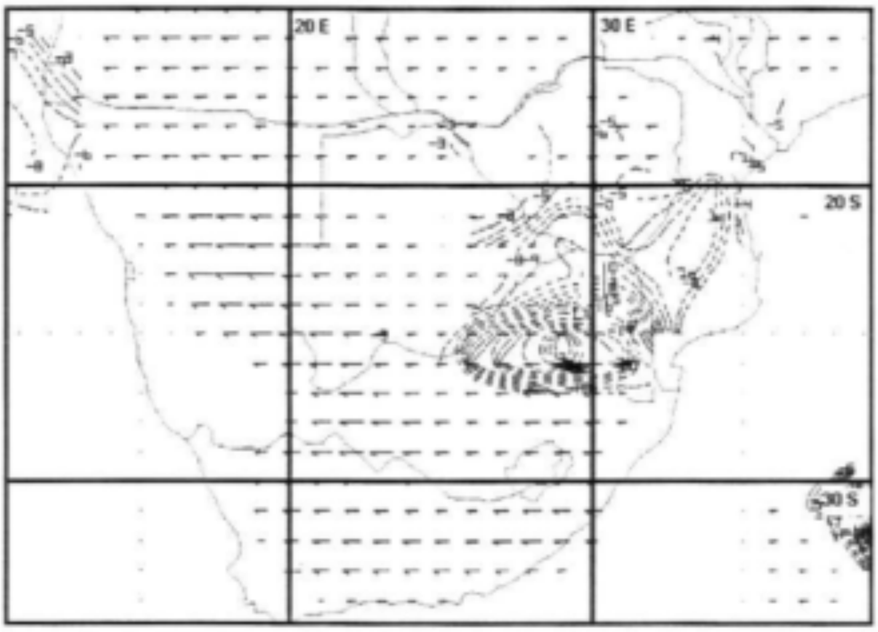

Figure 4.5.5: Areas of conditional instability (arrows) and upward motion from 700 to 400 hPa (dashed lines).

4.5.3 MITS results and actual rainfall

The blocked areas in Figure 4.5.6 portray the areas where MITS criteria for precipitable water, conditional instability and vertical motion overlap while the geographical distribution of the actual recorded rainfall on 8 February 2000 is displayed by the shaded area. The rainfall was recorded over 24 hours (0600 UTC on the 8th to 0600 UTC on the 9th) while the prognostic field is valid only for 1200 UTC on the 8th. This diagram does not serve as a verification of the MITS forecast but gives some graphical representation of the accuracy of the predicted convective rainfall areas. Two areas were isolated by MITS. First is an extensive area over the north-eastern interior of South Africa extending to eastern and southern Botswana as well as into western Zimbabwe. The second area isolated by MITS is a small area over eastern Namibia. Within South Africa some rainfall occurred over the entire area isolated by MITS. Heavy rainfall, however, was confined to Gauteng-, the eastern parts of the Northwest- as well as the western parts of the Northern Province.

Additional investigations into the accuracy of the convective rainfall areas isolated by MITS in February 2000 as well as experimental use by the operational forecasters in the Central Forecasting Office have revealed that this field often overestimates the rainfall areas. In the following section of this chapter the tropical heavy rainfall identification system (THERIS) will be detailed. In THERIS additional constraints are placed on the atmospheric dynamics.

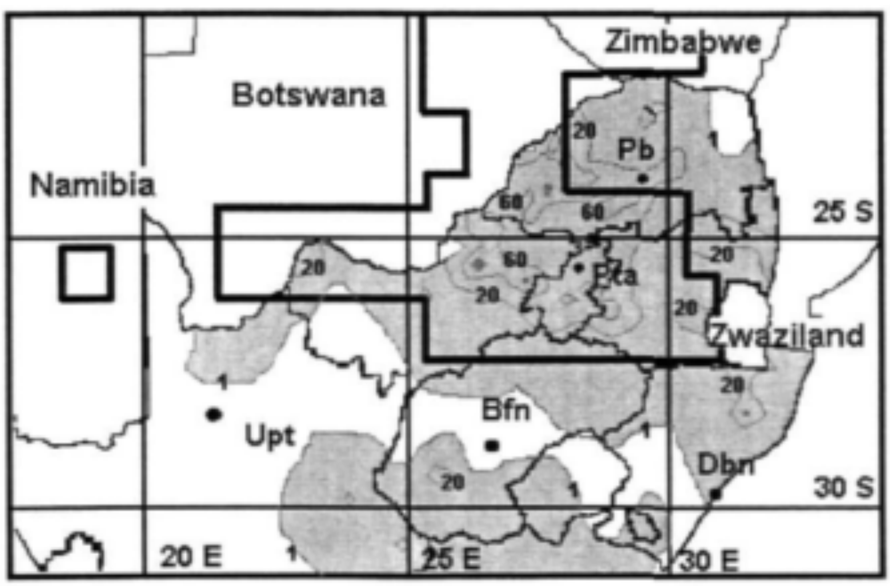

Figure 4.5.6 MITS results for 8 February 2000. The blocks indicate the areas where convective development is predicted. The shaded areas are observed rainfall.

4.5.4 MITS conclusions

A great deal of interaction exists between the five components of MITS. It may seem like duplication to use all of them. There are two reasons why this is done. Firstly one has to make sure that the dynamical properties of a tropical atmosphere are illustrated in a manner which is easy to understand. A 200 hPa high probably exists somewhere over southern Africa each day (and will necessarily be associated with above normal column temperatures). However only a few of the upper tropospheric highs are tropical and develop because of latent heat release. It is illustrated to the forecasters, by various means, that if this high is associated with high water vapour, high values of TSE and conditional instability, tropical circulation dominates. The second reason for the inclusion of all five components in MITS is to lead the forecaster step by step to the final component where a single field is generated which indicates areas where convective rainfall is probable. In the tropical heavy rainfall identification system (THERIS), discussed in the next section of this chapter, a similar approach is followed. It is important that the forecasters are made aware of the principles underlying the design of THERIS so that it can be used with confidence.

4.6 A tropical heavy rainfall identification system (THERIS)

For the duration of a severe weather event, tremendous pressure is placed on the operational meteorologist in the central forecasting office (CFO) in Pretoria. During the occurrence of severe weather events there is a tremendous increase in the number of telephonic enquiries and requests for special weather forecasts to aid in disaster mitigation efforts. As a result a great deal of the operational meteorologists' time is taken up by these additional duties leaving a very small amount of time for the careful analysis of model products and weather maps in order to prepare forecasts. During the heavy rainfall of February 2000 forecasters in CFO also had to issue aviation forecasts for the rescue efforts conducted in Mozambique by the international community (Scholz, 2000).

The tropical heavy rainfall identification system (THERIS) was designed to give the operational meteorologist immediate access to a single field where areas of forecast tropical heavy rainfall are depicted. THERIS, to a large extent, makes use of the same principles used in the design of MITS but placing additional constraints on the atmospheric dynamics to isolate those areas where heavy rainfall from tropical weather systems is likely to occur.

4.6.1 Dynamical characteristics and criteria of THERIS

4.6.1.1 Precipitable water values in the troposphere should exceed 20 kg m^{-2}.

Precipitable water was dealt with in MITS. The critical value of 20 kg m^{-2} was determined by experiments conducted during research by Dyson (2000). It should be kept in mind that this variable alone does not identify heavy rainfall areas.

4.6.1.2 Average wind divergence in the 300-200 hPa layer.

As was the case in MITS the average wind in the 300-200 hPa layer is computed before the wind divergence is calculated. A large volume of average wind divergence is responsible for maintenance of the vertical integrity of a tropical weather system. In THERIS the average wind divergence in the upper troposphere points to the probability of tropical circulation but is also a mechanism for maintaining and enhancing the upward motion in the lower and middle troposphere.

*4.6.1.3 Average TSE values in the troposphere should exceed 335 * 10^3 J kg^{-1}.*

In MITS it was stipulated that an average TSE value exceeding 330 * 10^3 J kg^{-1} is indicative of tropical circulation. In THERIS the average value of TSE is set somewhat higher and should exceed 335*10^3 J kg^{-1}. This additional condition on the average TSE value in the troposphere is stipulated to isolate those areas where the combination of the entropy, geopotential and latent energy peaks. Experimental results obtained by Dyson (2000) show that the critical value of 335 * 10^3 J kg^{-1} could be applied to assist in identifying areas of heavy rainfall.

4.6.1.4 The atmosphere must be conditionally unstable up to at least 300 hPa.

As was the case in MITS the vertical profile of TSE can be used to identify a conditionally unstable atmosphere. In THERIS it is expected that the atmosphere is conditionally unstable up to at least the 300 hPa level, this is 100 hPa higher than the level stipulated in MITS. If the atmosphere is conditionally unstable up to 300 hPa then deep cumulus convection is possible up to the upper troposphere and convective cloud developing under these conditions will probably extend vertically to the tropopause. This is exactly what needs to be achieved for the development of heavy rainfall from a tropical system. Rodgers and Yau (1989) stated that the likelihood of precipitation in cumulus clouds increases with cloud thickness. Also, Triegaardt et al., (1991) found that in the areas of heavy rainfall in February of 1988 the atmosphere was conditionally unstable up to the 100 hPa level.

4.6.1.5 Upward motion should exist from 700 to 300 hPa.

As in the case with conditional instability in THERIS it is required that upward motion should exist up the 300 hPa level. To sustain the upper tropospheric high pressure in the 200-300 hPa layer it is important that heat is transported in the vertical by Riehl's (1979) 'energy tubes'. Experimental results by Dyson (2000) indicate that convective showers are still possible even if upward motion stops between 400 hPa and 300 hPa. These clouds can still produce significant rain but the heavy rainfall generally occurs in isolated pockets.

In order to provide an environment favourable for the development and sustenance of hot towers extending up to the near tropopause, it is required that synoptic scale upward motion exists up to and above the 300 hPa level. An example of the vertical distribution of omega depicted by Figure 4.4.6 shows a deep mid–tropospheric layer with negative values of ω or small values of $\frac{\partial \omega}{\partial p}$. From the continuity equation small values of $\frac{\partial \omega}{\partial p}$ means that small values of the horizontal wind divergence exists in this layer. However the figure shows negative omega values extending to beyond the 200 hPa level. More importantly the figure depicts how the values of $\frac{\partial \omega}{\partial p}$ are minimised (rapid decrease of upward motion with height) to well above the 300 hPa level. This requires that horizontal wind divergence starts from the 400 hPa level and reaches maximum values at levels above the 300 hPa level. The hot towers provide the sensible heat sustaining the upper tropospheric high while the horizontal wind divergence, at these levels, provide the mechanism to maintain the systems' vertical integrity and the upward motion required for copious rainfall.

4.6.1.6 Maximum uplift should occur below the 300 hPa level.

Following the arguments presented in the previous paragraph it can be reasoned that in order to have a deep upper tropospheric diverging layer requires large negative values of $\frac{\partial \omega}{\partial p}$ in this layer. It therefore follows that the minimum value of ω should occur below the 300 hPa level in order to satisfy the requirement $\frac{\partial \omega}{\partial p} << 0$ above 300 hPa. However if the minimum ω values occur above the 300 hPa level the depth of the upper tropospheric diverging layer will decrease. If this happens it is argued that the horizontal wind divergence may be insufficient to remove enough heat and mass from the upper troposphere. This will result in the lower tropospheric low filling up and a rapid decrease of upward motion followed by the collapse of the tropical system.

4.6.2 THERIS Results

THERIS was initially developed on historical heavy rainfall events using the 1200 UTC analysis of the NCEP data set. The THERIS results were then compared to the SAWS rainfall which occurred in the geographical area isolated by THERIS. These results are discussed in paragraph 4.6.2.1.

As was the case with MITS it is important that THERIS should also be tested on the prognostic fields of a numerical weather prediction model. The Eta model is used operationally in the SAWS and THERIS was tested on the prognostic fields of this model. THERIS can be applied to the prognostic fields of any NWP model.

The heavy rainfall, which occurred during February 2000, served to test THERIS in the real forecasting environment. A THERIS field is created at 6-hourly intervals starting with the 6-hour prognoses of the 0000 UTC Eta run and ending with the 30-hour prognoses. A single field is compiled which includes all the possible heavy rainfall areas for a 24-hour period ending at 0600Z. This 24-hour period is the same as the 24-hour period, which the SAWS uses for daily rainfall. The measured rainfall is statistically compared with the areas of predicted heavy rainfall to verify THERIS. The results of this verification are provided in paragraph 4.6.2.2

In discussing the THERIS results applicable to the NCEP and Eta data, one should consider that the data sets differ significantly. The NCEP data have a horizontal resolution of 2.5 degrees while Eta's horizontal resolution is 0.5 degrees. NCEP has data for 17 vertical levels while Eta has 38 vertical levels. In both data sets only 8 of the vertical levels were utilized by THERIS they are: the 850-, 700-, 600-, 500-, 400-, 300-, 250- and 200 hPa levels. In NCEP the analysis at 12 UTC are utilized while in Eta the prognostic fields for a 24h period are used.

To evaluate THERIS results the average rainfall in the areas isolated by THERIS as well as the percentage of rainfall stations reporting more than 0 mm, 10 mm, 20 mm and 50 mm of rain were used. Since rainfall stations have an irregular geographical distribution the weighted average method designed by Tennant (1999) is used to calculate the statistics. Tennant's method is used operationally at the SAWS and a full description of this method is provided by Marx et al. (2002).

4.6.2.1 THERIS results for NCEP case studies.

NCEP data were obtained for 11 historical heavy rainfall days over South Africa. They are: 24-26 January 1981, 19-22 February 1988, 8-10 March 1988 and 12-13 February 1996. During 24-26 January of 1981 a well established COL was present over the west coast of South Africa but with a tropical sector over the eastern interior (Dyson, 2000). The heavy rainfall along the coast on 24 and 25 January 1981 was captured by BARCOZ and is described in chapter 5. From 19-21 February 1988 a continental tropical system was present over the central interior of South Africa and was responsible for wide spread and heavy rainfall (Triegaardt et al, 1991). Jury et al (1993) described the COL which was present over South Africa during March 1988. As was the case in January 1981 a tropical sector was identified over the central interior. In February 1996 a continental tropical system was present over Botswana while a COL moved over the country from the west (De Coning, 1997).

Table 4.6.1 depicts the THERIS results for the 11 days. The average rainfall in the areas identified by THERIS varied between 2 and 50mm. On 9 of the 11 days the average rainfall in the THERIS area was more than 10mm while for more than half of the days (6) the average rainfall was more than 20mm. On 2 days during February 1988 the average rainfall was more than 30mm and an average of 50mm rain occurred on 20 February 1988.

The geographical distribution of rainfall as well as the areas isolated by THERIS is depicted in Figure 4.6.1. On 24 January 1981 (Fig. 4.6.1a) THERIS identified an area of heavy rainfall from the Northwest Province to the interior of Kwazulu-Natal. The average rainfall over this area was 26 mm with some rain at 89% of the stations. On 26 January (Fig. 4.6.1b) THERIS identified areas of heavy rainfall over the central interior of South Africa. The average rainfall for this area was 18 mm with more than 90% of the stations receiving some rainfall.

On 19 February 1988 an extensive area of potential heavy rainfall is identified over the central interior of South Africa (Fig. 4.6.1c). The average rainfall in the THERIS area was 28mm with 19% of the station receiving more than 50mm. On 20 February the predicted heavy rainfall area shifted slightly eastwards (Fig. 4.6.1d). Extensive and heavy rainfall occurred in the THERIS area. The average rainfall in the area was 50 mm with close to 90% of the stations getting some rain. On 21 February 1988 THERIS identified a heavy rainfall area over the central interior of South Africa (Fig. 4.6.1e). The average rainfall in this area was 34mm while more than 50mm of rain occurred at 24% of the stations.

Table 4.6.1: Average rainfall (mm) and percentages for the areas identified by THERIS for the NCEP data. (% gt 0 = percentage of rainfall stations reporting more than 0mm of rain, % gt 10= more than 10mm of rain, % gt 20= more than 20mm of rain, % gt 50=more than 50mm of rain)

Date	**Average**	**% gt 0**	**% gt 10**	**% gt 20**	**% gt 50**
24 January 1981	26	89	72	48	13
26 January 1981	18	94	68	33	4
19 February 1988	28	72	57	51	19
20 February 1988	50	88	73	64	40
21 February 1988	34	84	64	50	24
8 March 1988	2	13	7	0	0
9 March 1988	15	63	33	23	9
10 March 1988	10	66	35	11	0
11 March 1988	12	76	36	15	6
12 February 1996	24	85	72	46	8
13 February 1996	22	73	59	43	12
	22	**73**	**52**	**35**	**12**

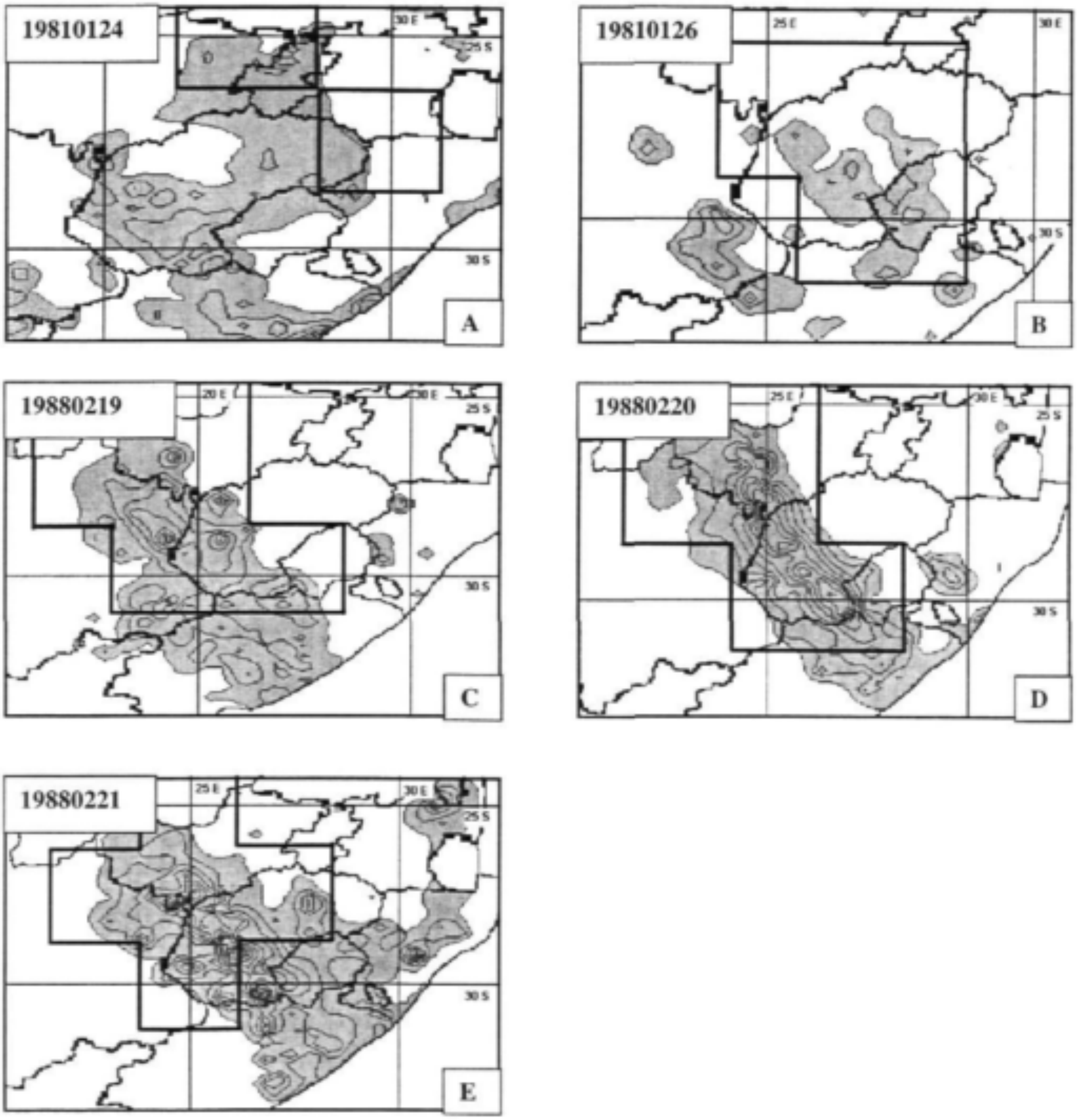

Figure 4.6.1 THERIS results for the NCEP data. The blocks indicate the areas where heavy precipitation are predicted. The shaded areas are observed rainfall with the first isohyet at 20 mm. Up to 20 mm rain is possible outside the 20 mm isohyet.

4.6.2.2 THERIS results for Eta case studies

THERIS was tested for both heavy rainfall periods in February 2000. They were 5-10 February and 22-25 February 2000 (Dyson and Van Heerden, 2001). The 0000 UTC runs of the Eta model were utilised in this investigation. The evaluation of the Eta model shows that on 6 February 2000 the 12 and 24-hour prognoses of the geopotential height fields misplaced the position of the tropical low over the northeastern parts of southern Africa. Due to the inaccuracy of the Eta model on 6 February, the data will not be discussed here. Furthermore, THERIS did not predict any heavy rainfall over South Africa on 5, 23, 24 or 25 February 2000. Only those days for which heavy rainfall was predicted are discussed here.

The THERIS results on 6 days in February 2000 are depicted in Figure 4.6.2. Shaded areas on this figure show the distribution of actual rainfall depths greater than 20 mm. On 7 February 2000 THERIS predicted two areas of heavy rainfall (Fig. 4.6.2a). The first one (indicated by 1) is bounded by 24°S to 25°S latitude and 28°E to 29°E longitude and lies somewhat to the northeast of the recorded (heavy) rainfall area. Table 4.6.2 shows that the average rainfall in this area was 51mm with 94% of the stations receiving some rainfall while 50mm of rain was measured at 28% of the stations. Area 2 (indicated by 2) lies south of the area of heavy rainfall. The weighted average rainfall in area 2 was only 2 mm. Actual rainfall depths over the eastern parts of the Northwest Province varied between 30 and 50 mm. THERIS predicted the area of heavy rainfall approximately 200 km southwest of where it actually happened. It is noteworthy that areas 1 and 2 lie on both sides of the band of heavy rain stretching southeastward from Botswana. It should also be noted that this band of rain lies roughly adjacent to the main watershed dividing the western Highveld from the lower lying Bankeveld and the Bushveld. The terrain slopes southward and rises some 300 to 400m from the Bushveld to the Highveld regions of the Northwest Province. It could well be that this gentle escarpment played a significant role in anchoring the rainfall near the slope. THERIS operating on model output, which does not adequately model the effect of the topography on the atmospheric dynamics, probably misplaced the heavy rainfall areas because of this.

On 8 February widespread and heavy rainfall occurred over the western parts of the Limpopo Province, Gauteng and the eastern extremities of the Northwest Province (Fig. 4.6.2b). Comparing area 1 with the shaded rainfall areas on Figure 4.6.2, shows that THERIS placed the heavy rainfall too far westward. However THERIS fared quite well in isolating the heavy rainfall area. The average rainfall over the area was 30 mm with close to 80% of all the rainfall stations in the area receiving some rain.

Table 4.6.2: Average rainfall (mm) and percentages for the areas identified by THERIS for the Eta data. (% gt 0 = percentage of rainfall stations reporting more than 0mm of rain, % gt 10= more than 10mm of rain, % gt 20= more than 20mm of rain, % gt 50=more than 50mm of rain)

Date	Average (mm)	% gt 0	% gt 10	% gt 20	% gt 50
7 February 2000 (Area 1)	51	94	72	66	28
27 February 2000 (Area 2)	2	34	3	0	0
8 February 2000	30	79	62	47	22
9 February 2000	17	47	41	24	7
10 February 2000	26	77	60	48	19
22 February 2000	0	0	0	0	0
	21	**55**	**40**	**31**	**13**

Figure 4.6.2c shows the geographical distribution of the rainfall on 9 February 2000. Rainfall totals exceeding 20 mm occurred over the northern parts of the Northwest Province as well as over Gauteng. Area 1 on the figure indicates the THERIS forecast heavy rainfall area. As was the case on 8 February, THERIS identified the heavy rainfall area to the south and west of where it actually happened. The weighted average rainfall for this day (Table 4.6.2) indicates that the average rainfall over area 1 was only 17 mm. Close to 50% of all the stations had rain with 41% of the stations getting more than 10 mm. Only 7% of the stations in area 1 had rainfall of more than 50 mm.

On 10 February 2000 THERIS isolated a large area of heavy rainfall over the eastern half of South Africa. Comparing area 1 to the geographical distribution of rainfall exceeding 20 mm (shaded areas on Figure 4.6.2d) shows that the heavy rain did indeed fall over a large part of area 1. THERIS was misleading only over small parts of the northern Free State as well as the southern parts of Kwazulu-Natal. Table 4.6.2 lists the weighted average and weighted percentages for area 1. The average rainfall was 26 mm with close to 80% of all the stations reporting rainfall. On 10 February 2000 the tropical low pressure system had moved to northern Namibia. A trough extended southward over the central interior of South Africa (figure not shown). In the upper troposphere a high pressure dominated the circulation over Botswana

Figure 4.6.2 THERIS results for the Eta data. The blocks indicate the areas where heavy precipitation is predicted. The shaded areas are observed rainfall with the first isohyet at 20 mm. Up to 20 mm rain is possible outside the 20 mm isohyet.

and Namibia with a weak westerly trough over the southwestern interior of the country (figure not shown). The significance of the results of THERIS on 10 February lies therein that in all probability the weather forecaster would not have predicted heavy rainfall so far to the east of the dominant tropical system over Namibia. THERIS indicated that the atmospheric circulation over Gauteng and as far south as Kwazulu-Natal was still meeting THERIS criteria and conducive to the development of heavy rainfall. THERIS is capable of isolating heavy rainfall areas even when the tropical atmospheric circulation was beginning to decay.

On 22 February the tropical cyclone Eline was near Beira. Heavy rainfall occurred over Mozambique (rainfall figures unavailable) as well as the northeastern region of the Northern Province (Fig. 4.6.2e). THERIS failed to isolate heavy rainfall over these areas. Analysis of the Eta model prognosis for this area reveals that most of the criteria stipulated for THERIS were not met. The precipitable water values did not exceed 20 mm, the average TSE was less than 335 $*10^3$ J kg^{-1}, deep cumulus convection was not predicted up to 300 hPa and uplift was not indicated throughout the middle and upper troposphere. Similar reasons proposed for 7, 8, and 9 February 2000 can be made for this day. The authors are convinced that the rainfall which occurred over the northeastern Limpopo Province can be linked to orographic uplift.
THERIS, however, identified an area (indicated by 1 in Figure 4.6.2e) of heavy rainfall over southern Gauteng and the northeastern Free State. Not one of the SAWS rainfall stations in area 1 had any rainfall at all. Area 1, isolated by THERIS, is small and reflects the conditions at a single model grid point. After analysis of the 0000 UTC Eta model prognoses it became apparent that atmospheric conditions over area 1 in fact only marginally met THERIS criteria. Furthermore positive wind divergence started to occur in the middle troposphere and this the authors consider detrimental to the development of heavy rainfall even if the circulation is classified as tropical. For operational use the meteorologist will be well advised to be cautious if THERIS, using model output, isolates heavy rainfall at a single grid point.

4.6.3 THERIS conclusions

The six components of THERIS were chosen to identify heavy rainfall in a tropical atmosphere. All the components should co-exist before an area of heavy rainfall is predicted. The constraints placed on the atmospheric dynamics by the six components are strict and because of these constraints not all of the areas where heavy rainfall occur are positively identified. Although this is not the ideal situation one of the aims of THERIS was to limit the number of false alarms of heavy rainfall.

This research indicated that the production of heavy rainfall in a tropical atmosphere is very sensitive to upward motion and wind divergence in the layer above 400 hPa. Evidence, not conclusive at this stage, suggests that decreasing upward motion and associated horizontal wind divergence is required to maintain the vertical integrity of the tropical system. The minimum value of omega should also be reached below the 300 hPa level.

THERIS has the capability to assimilate many model prognostic variables, apply strict conditions and identify areas where all are met. It is a tool, which therefore, provides the forecaster with a means of performing complex analysis, which would otherwise be beyond his/her capability in the short time available.

THERIS generally succeeded in identifying and pinpointing the geographical areas where heavy rain from tropical weather systems occurred. THERIS was tested on 5 days during February and generally succeeded in isolating areas of heavy rainfall. THERIS came close to achieving 100% success on 7 February 2000. Considering that THERIS used model prognostic fields, the results obtained on this day were very good. THERIS results for 10 February 2000 were the best prognosis of heavy rainfall from a tropical system ever made in South Africa.

THERIS is the first automated product available as input for Quantitative Precipitation Forecasts (QPF) in South Africa and in the long term could well be beneficial to water management in the southern subcontinent.

CHAPTER 5
BAROCLINIC WEATHER SYSTEMS

5.1 Significant Circulation features

Baroclinic weather systems producing heavy rainfall are truly significant features of the South African rain regime. Taljaard (1985), Triegaardt (1988), Preston-White and Tyson (1993) as well as Harrison (1983) described the baroclinic weather systems over South Africa. From the large number of studies, combined with the practical experience gained by the authors, as well as the many verbal reports received from SAWS operational forecasters, several significant circulation features common to baroclinic weather systems producing heavy rain are recognized:

Significant vertical wind shear as well as the westward extension of trough- and ridge axis with height must exist. The 200-300 hPa contour inflection point should lie above, or somewhat west of the 850 low / trough line.

Or expressed in terms of circulation parameters

Large values of relative vorticity advection in the 200-300 hPa layer must occur above the surface convergence.

This feature is important because with significant vertical wind shear the differential vorticity advection can be maintained or maximized as the upper system approaches the surface convergence. Holton (1992), using the quasi-geostrophic approximation of the equations of motion, expands on this process in considerable detail.

Upward motion should occur through most of the lower and middle troposphere and the maximum vertical motion should be in the 600- 400 hPa layer.

Significant upward motion, accompanied by adiabatic expansion and cooling, is required to produce copious amounts of rainfall. This is the only way in which the surface air, containing adequate water vapour, can be cooled for condensation and the resultant rainfall production. It must be understood that in this case we refer to synoptic scale upward motion, which is generally in the order of cm s^{-1}, and not the high vertical velocities found in convective clouds. It is accepted that synoptic scale vertical motion indicates an atmospheric environment that will promote convective development. These convective cloud systems may themselves be embedded within the synoptic scale layered cloud associated with widespread rain.

Sustained in phase lower tropospheric temperature advection. This means lower tropospheric cold air advection below the upper trough and warm moist air advection below and upstream of the upper ridge. This ensures the further development of the system.

Sustained in phase surface temperature advection is a fundamental requirement for the further development or maintenance of an active baroclinic system. Holton (1992) details how cold (warm) air advection below the upper trough (ridge) will maintain the deepening of the system. This will also help to maintain the vertical integrity of the system. Cyclogenesis over South Africa results in considerable increase in the curvature of the upper contours. Because of the direct relationship between relative vorticity (ξ) and curvature of the upper contours the net result is an increase in upper horizontal vorticity advection. This in turn enhances vertical motion (Holton 1992). In the many case studies, detailed in this chapter, it was often noted that the cold air advection over the southern and eastern regions of South Africa is considerably enhanced by adiabatic cooling of the surface air as it moves inland and over the mountains.

Significant convergence of water vapour must exist in the lower layers of the atmosphere.

Andrews (2000) using the Clausius-Clapeyron equation details the exponential relationship between saturated vapour pressure and temperature. The rapid decrease of water vapour content with decreasing temperature (atmospheric pressure) is also well illustrated on standard meteorological T-φ diagrams by the lines of saturated mixing ratio. The fact remains that the upper air (low temperatures/pressure) contains very little water vapour in comparison with the surface and near surface layers. To get significant rainfall therefore requires the atmosphere to move surface air with abundant water vapour upwards for condensation and rainfall production. In chapter 4 (Tropical Weather Systems) the precipitable water content of the vertical column is dealt with. Even over tropical regions the precipitable water seldom exceeds 40 mm. Rainfall amounts from active baroclinic systems, with considerably lower precipitable water content, can exceed this value by an order of magnitude (per day). The only way in which rainfall rates of these magnitudes can be maintained is if the surface circulation maintains large convergence of surface water vapour. Only then, provided the other factors detailed above co-exist, can high rainfall rates be maintained by baroclinic weather systems.

5.2 Two case studies of severe rainfall events

5.2.1 The September 1968 Port Elizabeth Flood

Many features mentioned in paragraph 5.1 were observed in the atmospheric circulation that prevailed on 1 September 1968 when the so-called Port Elizabeth flood occurred.

On the Sunday morning of 1 September 1968 serious floods developed over the city of Port Elizabeth (PE). More than 400 mm of rain fell in some 4 hours over the city. Floodwaters washed away homes, roads, bridges and factories. Fortunately it was a Sunday otherwise loss of life could have been large. Even so 9 people lost their lives. Damage to the infrastructure amounted to more than R 30 million (1968, R1 > \$1, R2 ≈£1) (Hayward and van den Berg, 1968). Hayward and Van den Berg (1968), using all the meteorological tools available at the time plus a combined experience of synoptic analysis exceeding 50 years, made a detailed analysis of this event. They determined that a cut-off low (COL) was responsible for the widespread rain over the Eastern Cape Province. In fact the 70 or so mm of rain which fell after 1000 UT, on this day, was typical of the heavy rains produced by a typical COL. The total rainfall for this event has certainly been exceeded in a few other cases. Best known of these are the Natal Floods of September 1987 when between 600 and 800 mm rain fell over large parts of Natal, but spread over 4 days.

Why the disastrous floods occurred only over a relatively small area (central PE) has never been explained satisfactorily. Hayward and van den Berg (1968) could only speculate on the reason for the severe localized floods over Port Elizabeth on the 1st.

The NCEP dataset contained analysis data for 1 and 2 September 1968. This provided the opportunity to again investigate the Port Elizabeth floods, this time using all the dynamical tools which were unavailable to Hayward and Van den Berg. It also provided the opportunity to search for the right combination of dynamical features and forcing mechanisms responsible for heavy rain and floods. We also need answers to the question: can we better predict these floods today?

5.2.1.1 The 1968 synoptic scale analysis

The highest rainfall total for the 24 hour period starting at 0600 on the 1st over the Port Elizabeth city centre was 552 mm (Hayward and Van den Berg (1968)). Some 470 mm fell during the 4 hours starting 0600 UT on this day. Figure 5.2.1 is an autographic rainfall gauge chart from the Port Elizabeth Weather Office. This instrument recorded the phenomenal rainfall rates over the city from 0600 to 1000 UT on the 1st. The rainfall rates recorded for the period after 1000 UT are the rates one normally associates with widespread heavy rain from a cut-off low-pressure system (Taljaard, 1988).

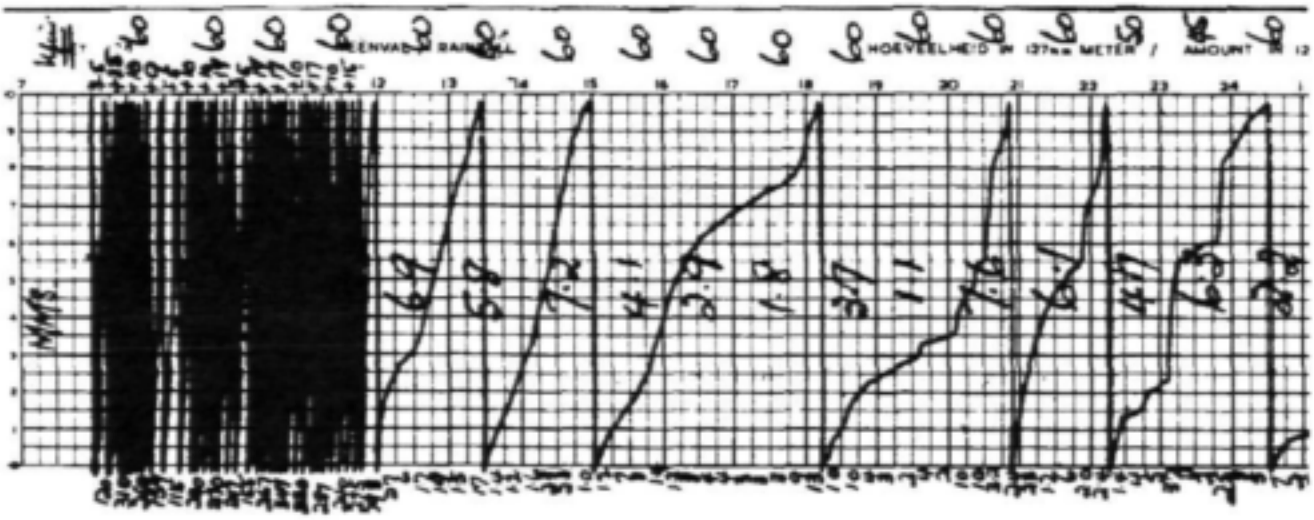

Figure 5.2.1: Autographic rain gauge record at Port Elizabeth for 1 September 1968. Vertical scale is 10 mm rain. Horizontal scale is in hours. Record started at 0600 UT on 1 September 1968. Adapted from Hayward and Van den Berg (1968).

Figure 5.2.2 displays the geographical extent and the rainfall totals from 1 to 3 September 1968. It should be noted that only two relatively small areas had totals exceeding 200 mm, the Port Elizabeth area as well as the area to the west of East-London.

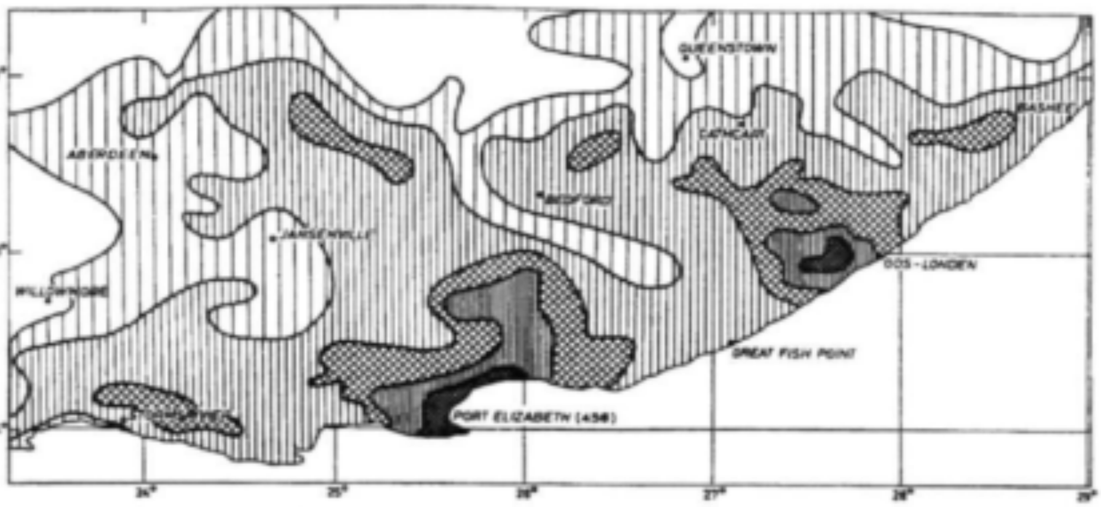

Figure 5.2.2: Rainfall totals for the period 1 to 3 September 1968. Isohyets are 25, 50, 100, 150 and 200mm. Adapted from Hayward and Van den Berg (1968).

Figure 5.2.3 illustrates the association between the rainfall totals and the topography of Port Elizabeth. The relationship between the isohyets over the city and the western end of Algoa Bay should be noted.

Figure 5.2.3: Rainfall over the Port Elizabeth metropolitan area on 1 September 1968. The isohyet spacing is 100 mm. Height contours are in feet. After Hayward and Van den Berg (1968).

Figure 5.2.4 is a composite surface pressure and 850-hPa geopotental height in meters (gpm) contour map. Hayward and Van den Berg (1968) used this map to indicate the flow of moist maritime air off the southern Indian Ocean over the bay area near Port Elizabeth. They also discussed the low pressure system at the 850 hPa level over the Eastern Cape Province and positioned the upper air cut-off low at 500 hPa midway between Port Elizabeth and Cape Town as did the NCEP analysis depicted by Figure 5.2.5. They and others, notably Taljaard (1985), Triegaardt et al. (1988) and Tennant and Van Heerden (1994) described the relationship between the movement of the cut-off low and heavy rainfall over the coastal regions of South Africa. Apart from the excellent distribution of radiosonde data and reliable vertical pressure and temperature profiles Hayward and Van den Berg had little else available which could be used to explain the floods. It should be remembered that in 1968 only a few computers existed in South Africa, and those were of feeble power compared to the average modern desktop PC. It was completely beyond the means of Hayward and Van den Berg to compute and use any of the circulation parameters available today.

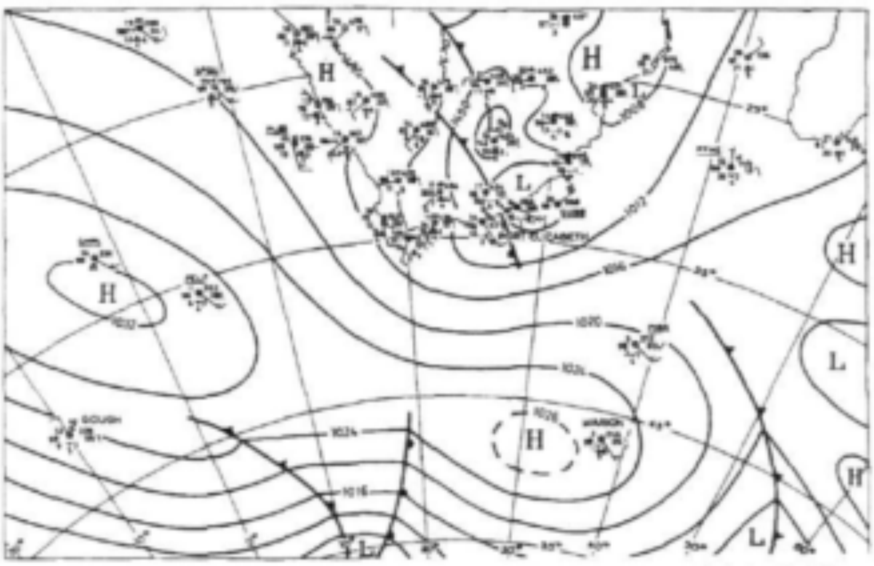

Figure 5.2.4 Composite surface pressure and 850 hPa geopotential height synoptic map at 1200UT on 1 September 1968. Adapted from Hayward and Van den Berg (1968).

However Hayward and Van den Berg (1968) did speculate that the local topography and the sub-geostrophic surface winds due to strong vertical ascent were responsible for the flood.

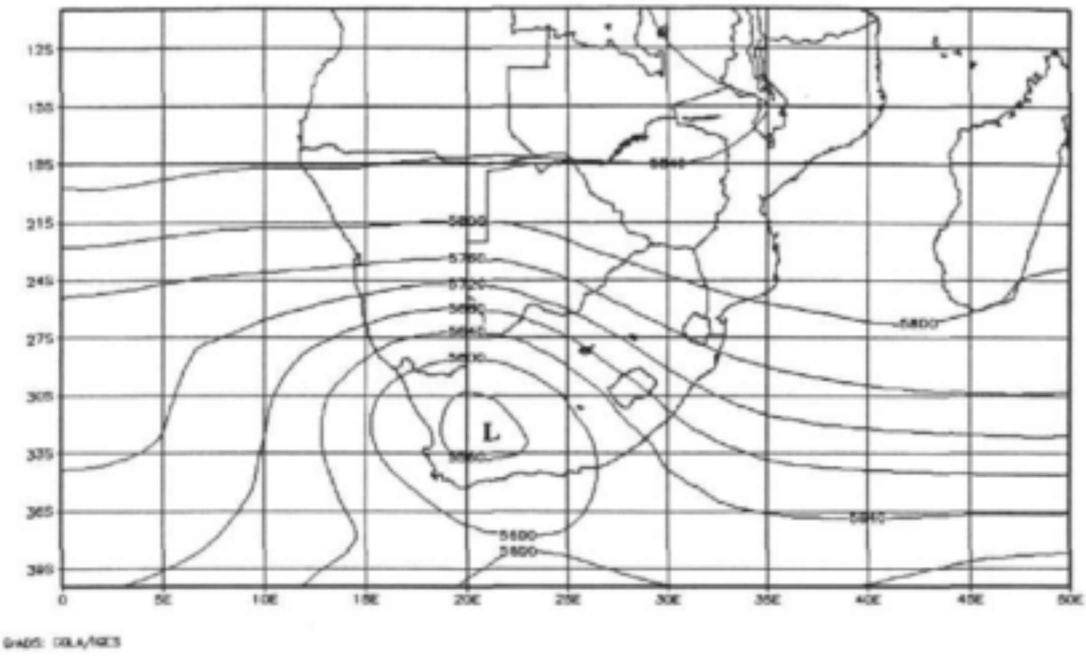

Figure 5.2.5: 500hPa geopotential heights at 1200 UT on 1 September 1968.

5.2.1.2 NCEP Data analysis

A full analysis was performed on the NCEP data for 1 September 1968. As far as the synoptic scale circulation is concerned the NCEP analysis and the 1968 hand analysis are for all practical purposes the same (maps not shown). The PCGRADS system was used to calculate and display a large number of circulation parameters. This was done in order to gain some insight into the movement and development of the cut-off low. The mid tropospheric relative vorticity advection as well as the near surface temperature advection were also investigated.

Figure 5.2.6 is a plot of the advection of relative vorticity (**V•∇ξ**) at 500 hPa. Quasi- geostrophic theory as expounded by Holton (1992) indicates that an upper low will tend to move along the line from minimum to maximum relative vorticity advection. Considering the position of these extremes as depicted by Figure 5.2.6, it means that the cut-off low should move eastward.

Figure 5.2.7 depicts the advection of temperature (V•∇T) along the 925 hPa level. Insignificant warm air advection is observed ahead of the cut-off low. If the effect of latent heat release is not considered these figures 5.2.6 and 5.2.7 indicate that the cut-off low will move eastward but will not deepen appreciably. Mid tropospheric latent heat release due to the condensation of water vapour will increase the column average temperatures. Because of the direct relationship between column average temperatures and geopotential thickness the upper ridge must grow causing the system to intensify. In fact Hayward and Van den Berg (1968) found that the low moved up the Transkei coast but did not intensify.

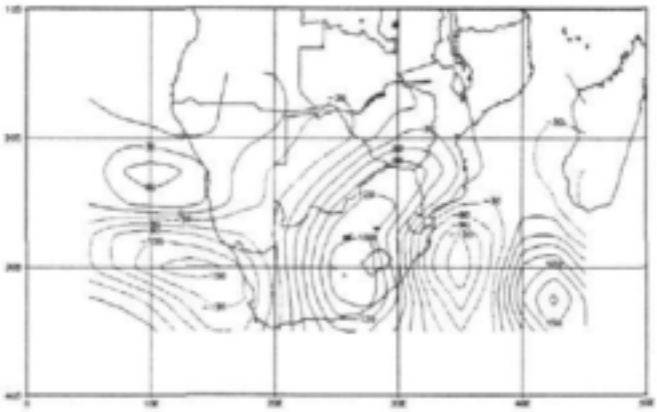

Figure 5.2.6: Horizontal relative vorticity advection at 500hPa on 1 September 1968. Units multiplied by 10^{-10}.

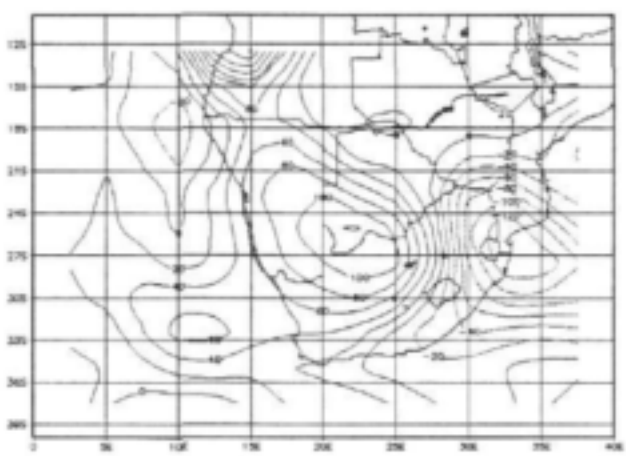

Figure 5.2.7: Advection of temperature at 925hPa on 1 September 1968. Units multiplied by 10^{-5}.

Widespread heavy rain develops when synoptic scale upward motion (w > 0) occurs and is maintained by the circulation. Figure 5.2.8 is a composite map indicating the 300-200 hPa horizontal wind divergence and the 500 hPa vertical motion, shown as negative values of ω. The maximum upper divergence and upward motion (ω < 0) lie near East-London where 50 to 100 mm rain fell on the 1st. The synoptic scale dynamics explain the widespread heavy rain (> 50 mm) but fail to provide answers for the Port Elizabeth flood.

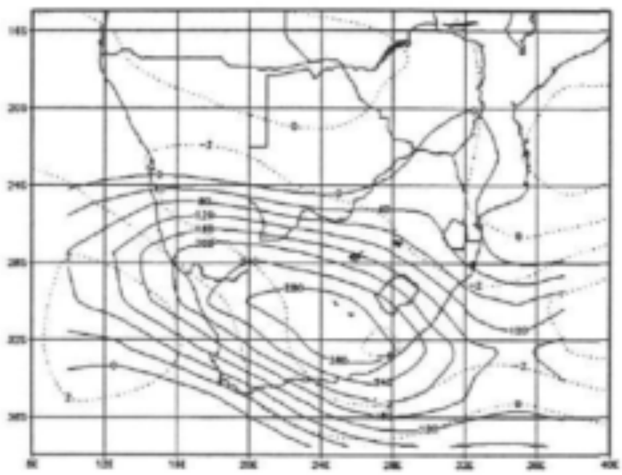

Figure 5.2.8: Average 300-200hPa wind divergence (solid lines) and the omega values (dotted lines). Divergence units multiplied by 10^{-6} and omega by 10^{-1}.

To have maintained the large rainfall rates over Port Elizabeth on 1st required that vast amounts of water vapour had to converge over and near the city. Figure 5.2.9 is a plot of the moisture flux convergence at the 1000-hPa level. The figure does not indicate large moisture convergence near Port Elizabeth.

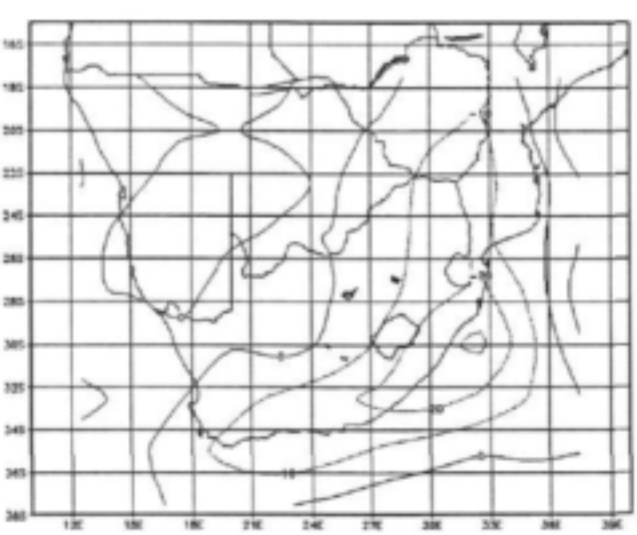

Figure 5.2.9: Moisture flux convergence at 1000hPa at 1200 UT on 1 September 1968. Units multiplied by $10^{-2}kgkg^{-1}\,s^{-1}$

Consider what happened in a $1 m^3$ hypothetical box over the Port Elizabeth city centre on the 1st.

- It rained some 400 mm in 4 hours into the box.
- This means 400 kg water collected in the 1 m^3 box in the 4 hours.
- This translates to a water accumulation rate of 0.03 kg m^{-3} s^{-1} in the box.
- To maintain this rain rate the atmosphere had to converge water at a rate exceeding 0.03 kg s^{-1} in the vertical column above the box.

However, Figure 5.2.9 depicts the convergence of water vapour over Port Elizabeth at 15 x 10^{-7} kg kg^{-1} s^{-1} at the 1000 hPa level. This implies the following:

- If in this case 1 kg of air has a volume of 1 m^3 then the rate of accumulation equals 15 x 10^{-7} kg m^{-3} s^{-1}.
- Assume that this rate is maintained for the lower 3000m (approximately to the 700 hPa level).
- Then the total accumulation of water vapour above Port Elizabeth is 45 x10^{-4} kg m^{-3} s^{-1}.
- In 4 hours this rate will accumulate 64.8 kg m^{-2} water vapour above Port Elizabeth.
- If all the water vapour were converted to rainfall it results in rainfall of only 65 mm.

The rainfall rate of 15 x 10^{-7} kg m^{-3} s^{-1} is a figure computed from the wind and water vapour mixing ratio fields of the NCEP analysis, which have a horizontal resolution of some 250 km. At this horizontal scale, it is unlikely that the water vapour accumulation rates required at Port Elizabeth could be resolved. However the arguments put forward here do indicate that heavy rainfall is only possible if the water vapour convergence is large.

5.2.2 Laingsburg: The retrograding low of 25 January 1981

Contribution by L Masimini

5.2.2.1 The Laingsburg flood

Heavy rainfall occurred in the SW-Cape on 25 January 1981. The floods that resulted claimed 103 lives and caused significant destruction to infrastructure. Dyson (2000) identified places in the southwestern Cape Province, which received rainfall in excess of 300mm on 25 January 1981. The highest rainfall occurred at Jonkersnek with 337mm, Disavlei 333mm, Dassieshoek 242mm and Witfontein 223mm. Heavy rainfall was concentrated in the Western Cape Province but significant rainfall also occurred over the central interior and the southeastern coastal regions of the country. Estie (1981) described how the heavy rainfall over the Southwestern Cape was responsible for the Buffels River to overflow, consequently washing away a large part of Laingsburg, a small town in the central Karoo.

Estie (1981) described how this heavy rainfall could be attributed to the so-called black southeaster. A black southeaster occurs when there is a strong high-pressure system south of the continent, which advect moist warm air into a low-pressure over the southern parts of South Africa. Estie (1981) identified the system, which was responsible for the heavy rainfall on 25 January 1981 as a COL. This COL is an example of a system retrograding to the west and this occurred from 24 to 25 January 1981 over the Western Cape Province.

The aim of this study is to describe the retrograde movement of the COL from 24 to 25 January 1981. The atmosphere conditions responsible for the heavy rainfall over the Southwestern Cape will be described briefly.

5.2.2.2 Circulation features on 24 and 25 January 1981

The National Center for Environmental Prediction (NCEP) reanalysis data were used to investigate the movement of the COL and also to describe the dynamical characteristics of the system.

Figures 5.2.10(a) and 5.2.10(b) depict the 500 hPa geopotential height field in geopotential metres (gpm) on 24 and 25 January 1981 respectively. The closed low leaned westward in the vertical from the surface to 500 hPa on both days. On the 24^{th} the low was situated at 33°S 20°E and on the 25^{th} at 30°S 17°E, showing a northwest movement of the 500 hPa low during this period.

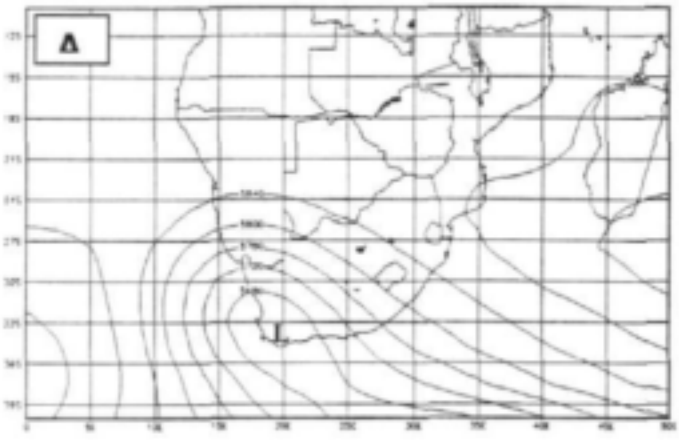

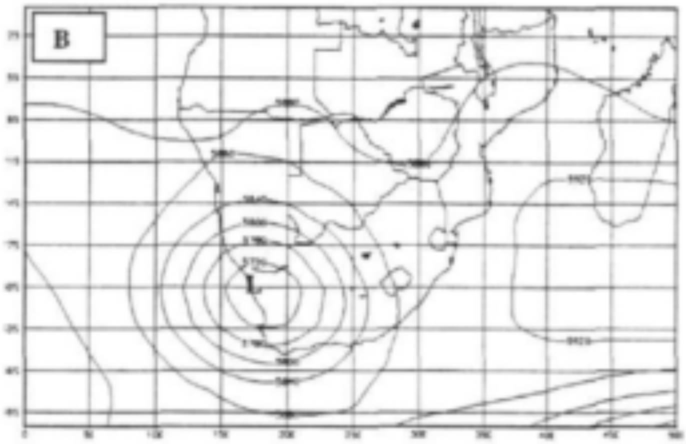

Figure 5.2.10: 500hPa geopotential heights on (A) 24 January 1981 and (B) 25 January 1981

Figure 5.2.11 portrays vorticity advection at 500hPa on 24 January 1981. Maximum values of positive vorticity advection (solid lines) occur at the geographical positions: 30°S 22°E and 28°S 16°E, northeast and northwest of the 500hPa low. Quasi-geostrophic theory (Holton,1992) predicts that the low is expected to move towards the area of maximum positive vorticity advection. Thus the low should move either to the east or slightly northeast. The COL in fact moved towards the northwest. In this case the low did not move to the maximum value of vorticity advection but to the secondary maximum at 28°S 16°E situated along the Namibian coast.

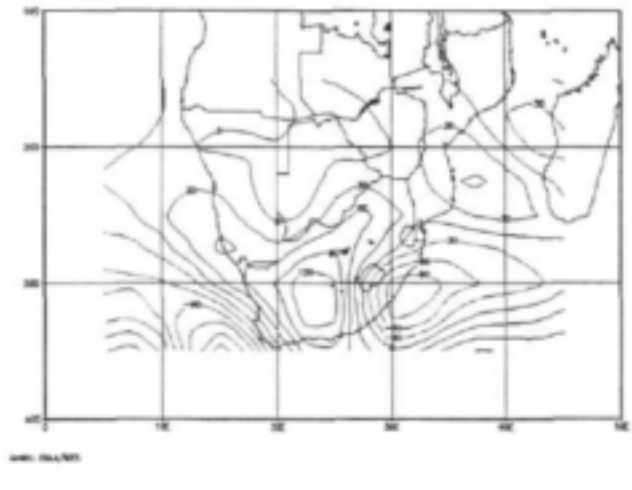

Figure 5.2.11 Horizontal relative vorticity advection at 500hPa on 24 January 1981. Units multiplied by 10^{-10}.

Figure 5.2.12 shows the average temperature advection of the 1000-700hPa layer on the 24 January 1981. Cold air advection (negative values) occurred north and northwest of the COL. The maximum value of cold air advection in fact occurred at 30°S 18°E, near the boundary between South Africa and Namibia. Holton (1992) states that cold air advection should deepen the COL. It is therefore a reasonable assumption that the 500hPa low will deepen and move towards northwest by the 25th. Considering figures 5.2.10a and b it is clear that this did indeed happen.

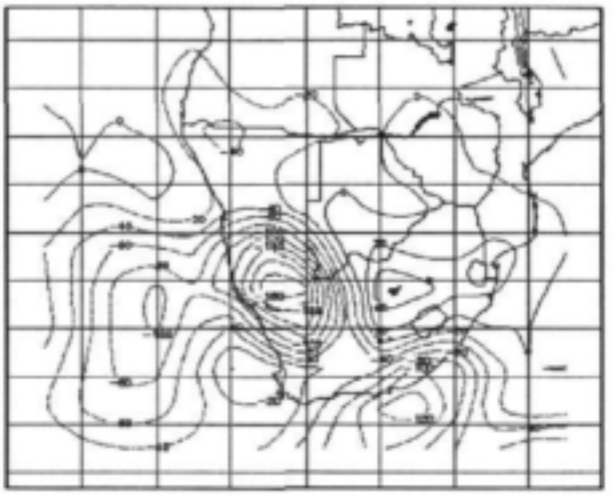

Figure 5.2.12: Average temperature advection in the 1000-700 hPa layer on 24 January 1981. Units multiplied by -10^{-5}

The large area of cold air advection to the north and northwest of the COL plus the positive vorticity advection at 500hPa ahead of the secondary trough was enough to cause the northwesterly movement of the COL in perfect agreement with the quasi-geostrophic theory.

5.2.2.3 Rainfall distribution on 25 January 1981: Dynamical aspects.

Two areas over the Western Cape Province were selected; one (34°S 19°E) received heavy rainfall in excess of 300 mm and the other (31°S 21°E) no rainfall.

Figure 5.2.13 depicts the omega (ω) field at 500hPa on 25 January 1981. The minimum values (dotted lines indicating upward motion) occurred at the geographical position 33°S 22°E, east of the area of maximum rainfall. At both of the selected areas Figure 5.2.13 shows significant upward motion ($\omega < -0.3$hPa s^{-1}) and both should have an equal chance of rainfall.

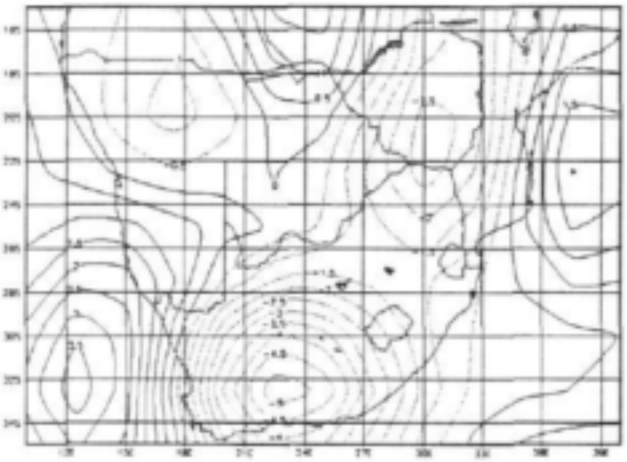

Figure 5.2.13: Vertical motion (omega) values at 500hPa on 25 January 1981. Units are multiplied by 10^{-1}.

However for rainfall to develop, the upward motion in the middle troposphere should be accompanied by lower level convergence and upper tropospheric wind divergence. It is important to take note that heavy rainfall did not develop over the area where maximum upward motion occurred. Clearly this indicates that other factors such as low-level temperature and water vapour advection also play vital roles in the development of heavy rainfall.

Investigation into the vertical profile of the vertical motion and horizontal wind divergence fields over the two selected areas (not shown) indicated that a significant difference existed between the area where heavy rainfall occurred and where no rainfall occurred. In the area of heavy rainfall, a minimum value of omega of -0.3 Pa s^{-1} occurred at 600hPa and was accompanied by significant surface convergence and maximum wind divergence at 300hPa. In the area where no rainfall occurred the minimum omega value of -0,25 Pa s^{-1} occurred at 500hPa. In the no rain area the upper troposphere wind divergence was present but the surface convergence not.

5.2.3 Review of the two case studies

Synoptic scale dynamical features fail to explain the incredible rainfall rates observed at Port Elizabeth. The weather forecaster using all the tools available on a system such as PCGRADS and a perfect synoptic scale prognosis would still have failed to predict the flood. Synoptic scale model or analysis output does not have the resolution to resolve events of this nature. Regional models of a much smaller resolution may be the way to go.

In the case of the Laingsburg flood the analysis further indicated heavy rainfall does not necessarily occur where vertical velocity, surface convergence and upper air divergence are maximized. In the area of heavy rainfall the minimum omega values occurred at approximately 600hPa and the vertical profile of the horizontal wind divergence had the classical profile. Large lower level convergence occurred below upper air wind divergence which maximized at the 300hPa level. The analysis also indicated the need for moisture flux for rainfall development.

Taken together the two case studies show that two simultaneous occurring features, even on the synoptic scale, could be useful to identify areas where heavy rainfall is probable. They are:

Large scale vertical motion
Surface or near surface convergence of water vapour

5.3 Dynamical Features Associated with Heavy Rainfall from Baroclinic Weather Systems

NCEP re-analysis data were obtained for 26 days with significant rain, somewhere, over South Africa. On 16 of the days, listed below, heavy rain was observed over large areas of the country.

1 September 1968	2 September 1968	25 August 1970	26 August 1970
27 August 1970	28 August 1970	20 August 1979	21 August 1979
25 January 1981	26 September 1987	27 September 1987	28 September 1987
29 September 1987	8 March 1988	9 March 1988	7 July 1996

On all of the 16 days, with heavy rainfall, the atmospheric circulation exhibited considerable vertical wind shear and could therefore be classified as baroclinic weather systems if the definition of baroclinicity of Holton (1992) is applied. Both MITS and THERIS were applied to these data fields (circulation fields) in order to check for the tropical features defined by Dyson (2000). On two of the days 8 March 1988 and 9 March 1988 the atmospheric circulation over the central interior could be considered tropical even with an upper low southwest of the country. They were therefore not used in the analysis described in this chapter but are briefly referred to in chapter 4. On the other 14 days analysis of the atmospheric circulation identified strong vertical wind shear and the presence of typical baroclinic weather systems such as described in Chapter 1.

Computer contoured rainfall fields, using 24 hour rainfall data from the SAWS, were used to identify areas where heavy rainfall occurred. The quality of the rainfall contours produced by this contouring package leaves much to be desired. However the rainfall maps it produced did serve the purpose of this research as it identified the area where heavy rainfall occurred with an acceptable degree of accuracy. Serious investigation of the actual rainfall depths and distribution is beyond the scope of this research project. It was considered sufficient to locate the area where heavy rainfall (more than 40 to 50 mm) occurred. Considering the spatial distribution of the rainfall taken together with the dynamics the following subdivision of rainfall types and or location was made:

- *Coastal zone rainfall refers to rainfall along the coast extending inland to the main escarpment.*
- *Inland rainfall refers to continental rainfall inland of the escarpment.*

The PCGRADS system allows for the display of weather maps as well as circulation features derived from the geopotential-, temperature-, wind- and moisture fields available for many vertical layers in the NCEP analysis. As a basic starting point the dynamical features, listed below, were all studied on the days on which heavy rainfall occurred:

- *The synoptic scale geopotential field on several pressure fields.*
- *The horizontal temperature advection occurring in the lower troposphere.*
- *Horizontal relative vorticity fields and horizontal relative vorticity advection in the upper troposphere.*
- *Horizontal wind divergence and vertical profile of the horizontal wind divergence.*
- *Mid troposheric vertical motion (ω) and vertical profile of the vertical motion.*
- *Moisture indices*

It became obvious that many of these circulation and dynamical features coincide with heavy rain, especially along the coastal zone. Quasi- geostrophic theory (Holton, 1992) predicts heavy rainfall where dynamical features such as the upper air divergence in association with strong synoptic scale upward motion (ω < -0.3 Pa s^{-1}), lower level convergence and in phase temperature advection coincide. In the case studies the area with heavy rainfall did not necessarily coincide with the area where these dynamical factors came together. The divergence and vertical motion fields often occurred east of where the heavy rainfall occurred. This could, in isolated cases, be due to the eastward motion of the systems. The influence of the topography and the interaction of land and sea surfaces certainly also play a significant role on the development of heavy precipitation along the coastal zone. Dyson (2000) and Dyson and Van Heerden (2001) indicated the seriousness of this problem. It was beyond the scope of this project to investigate these factors. The horizontal scale of the NCEP data fields (250 km) makes this impossible.

In order to develop an operational system to isolate heavy rainfall from these baroclinic systems the right combination of the dynamical factors needs be determined. This entailed locating the geographical position (area) of the primary forcing mechanism(s) of the heavy rainfall. The primary forcing mechanism(s) were generally found over a much wider area than where the heavy rainfall actually occurred. In the 14 case studies of heavy precipitation from baroclinic systems the cut-off low dominated followed by the ridging high. They have three main features in common:

- *Strong advection or convergence of water vapour exists over the south-, southeast- or east coast.*
- *Mid-tropospheric upward motion is present.*
- *Presence of significant upper level differential vorticity advection.*

The so-called tropical temperate trough was never isolated amongst the 14 case studies. The tropical temperate trough links (sub-) tropical- and baroclinic circulation systems. Heavy rainfall accredited to this system will probably be isolated when the THERIS and baroclinic heavy rainfall systems (BARCOZ) are combined.

5.3.1 Forcing mechanisms of heavy rain from baroclinic circulation systems

The large number of dynamical features available as well as a combination of them all displayed on maps with the PCGRADS system is very confusing and does not serve operational meteorologists well. Several procedures to view different dynamical features simultaneously (referred to as overlays) were developed in order to determine and extract the essential dynamics that force heavy and widespread rainfall.

5.3.1.1 Overlays

The following combination of circulation parameters survived extensive experimentation with the NCEP data and comparison with the rainfall fields. They are combined into the following three overlays. An overlay is simply a figure where two or more atmospheric variables are displayed together.

- *Moisture flux convergence at the 850-hPa level and the average 300-200 hPa wind divergence.*
- *500 hPa vertical motion (ω field) and the average 300-200 hPa wind divergence.*
- *Average 300-200 hPa wind divergence and $\omega < -0.2$ Pa s^{-1} at all levels from 700- to 400 hPa.*

During the analysis it became apparent that the area covered by heavy rains does not necessarily lie below areas with large vertical motion accompanied by upper air divergence but often near areas of large gradients of these fields. Table 5.3.1 summarizes the results when these overlays were applied to the days with heavy rain along the coastal region. The overlays failed to isolate a significant number of areas of heavy continental rainfall. The table indicates the degree of success achieved by each of the overlays to isolate areas of heavy coastal rain.
Investigation of Table 5.3.1 reveals that some of the overlays are close to defining the area with heavy coastal rainfall but without an acceptable level of consistency. Overlay 1 indicates that low level moisture convergence and upper wind divergence are important while Overlay 2 indicates that mid-tropospheric upward motion, sustained by strong upper wind divergence may be decisive. Considering the results obtained by using Overlays 1 and 2 suggests a combination between lower level water vapour convergence and significant mid-tropospheric upward motion, sustained by in phase upper wind divergence, is the way to go. Results with overlays using lower troposphere temperature advection in combination with other parameters (not shown) were disappointing.

Table 5.3.1: Evaluation of Overlays relevant for *Coastal Rain*. YY means that the overlay indicated an area of heavy rain. YN means that the area isolated is close to or covering only parts of the recorded heavy rain. Failure to isolate an area is indicated by FF and FD means heavy rainfall was isolated but the result is misleading.

Date	Overlay 1	Overlay 2	Overlay 3
1 September 1968	YY	YY	YN
2 September 1968	YN	YN	FF
25 August 1970	YY	YY	YY
26 August 1970	YN	YY	YY
27 August 1970	YN	YN	YN
28 August 1970	FF	FF	FD
20 August 1979	YY	YY	YN
21 August 1979	YN	YY	YN
25 January 1981	YY	YN	YN
7 July 1996	YY	YY	YY

5.3.2 The role of water vapour convergence at 1000- and 850 hPa levels

Generally the results from the many case studies indicate that heavy rainfall along the coastal zone may develop from systems where:

The synoptic scale circulation is baroclinic and vertical motion exists through a significant mid tropospheric layer. A flux of lower level water vapour must also be maintained beneath the region of upward motion.

However heavy rains happened along the coastal zone in the absence of strong vertical motion, notably so on 2 September 1968 and 28 August 1970. However, on all of the days with heavy rain, these two included, moisture convergence occurred in the lower layers (1000- and 850 hPa) beneath the zone of upward motion.

Holton (1992) observed that surface advection of cold (warm) air beneath the upper trough (ridge) results in the deformation of the system. This in turn results in enhanced vertical motion. It was also noted by Sutcliffe (1953), amongst others, that self-development is also dependent on the latent heat release of ascending saturated air. In all of the case studies researched most warm and cold air advection and water vapour flux were primarily by the meridional component of the wind. This develops if a strong 1000 hPa level high-pressure system is south or south-east of the land and at the same time a significant continental low pressure system at the 850 hPa level lies over the southern interior. Under these conditions the surface flow crossing the coast is strong and often comes from the southeasterly direction. The continental surface pressure distribution also maintains a southerly flow of moist continental air to the east and southeast of the continental low. The strong flow of maritime air from the southeastern sector over the south-, southeastern- and eastern coastal regions of South Africa during episodes of heavy rain was noted by several researchers, notably Triegaardt et. al. (1988), Taljaard (1985), Tennant and Van Heerden (1994) as well as De Villiers (1992). All concurred that this strong flux of moisture laden maritime air is one of the primary forcing mechanisms for heavy coastal zone rainfall.

It therefore made sense to compute the flux of water vapour by the1000- and 850 hPa level meridional (S/N) wind component as well as the flux of water vapour by the component of the 1000- and 850 hPa wind along the SE/NW azimuth. In most of the case studies strong gradients of moisture flux along the S/N and SE/NW azimuth lines were observed close to areas of observed heavy rainfall. This observation led to the computation and display of the so-called **gradient of the meridional water vapour flux** ($\nabla(qv)$) as well as the **gradient of the SE/NW water vapour flux** ($\nabla(qv_{se})$) described in chapter 2. In nearly all the case studies these vectors were observed to converge near areas of heavy rain. The next step resulted in the computation of the following scalar fields at both 1000 and 850 hPa levels:

Divergence of the gradient vector, of the water vapour flux, by the meridional wind component ($\nabla\bullet\nabla(qv)$) (Referred to as MC)

As above but with the SE wind component (($\nabla\bullet\nabla(qv_{se})$) (Referred to as SEC)

In all of the case studies **negative values of MC and or SEC (convergence) occurred** near areas of heavy rainfall. Both **MC** and **SEC** have units of **$kgkg^{-1}m^{-1}s^{-1}$** and provide information on the convergence of near surface water vapour required for heavy rainfall. The units differ from the conventional divergence of the water vapour flux (($\nabla\bullet(qV)$) (**$kgkg^{-1}s^{-1}$**) because in the case of MC or SEC the gradient of the flux component was used.

5.3.3 MC and SEC on 27 August 1970

On 27 August 1970 a cut-off low was responsible for heavy and widespread rainfall along the coast and interior of the Eastern Cape Province. The surface pressure analysis was typical of these systems with a strong high-pressure system lying south of the country in the typical "banana shape" pattern. At the 850 hPa level a low was situated over the interior of the Eastern Cape. In the upper air, at 300 hPa the cut-off low was centred over the Northern Cape Province. Figure 5.3.1 depicts the 24-hour rainfall distribution.

Considering the relative vorticity advection in the upper troposphere as well as the temperature advection at the 850 hPa level (not shown) eastward movement of the cut-off low can be expected if the quasi-geostrophic theory holds. Maximum vertical motion (not shown) occurred over Lesotho and southern Kwazulu-Natal, some 400 km northeast of where the actual rainfall happened. This means that any system, for determining heavy rainfall, based on the vertical motion alone, will fail. Figure 5.3.2 depicts the surface moisture flux vectors ($q\overline{V}$) as well as the magnitude of $q\overline{V}$.

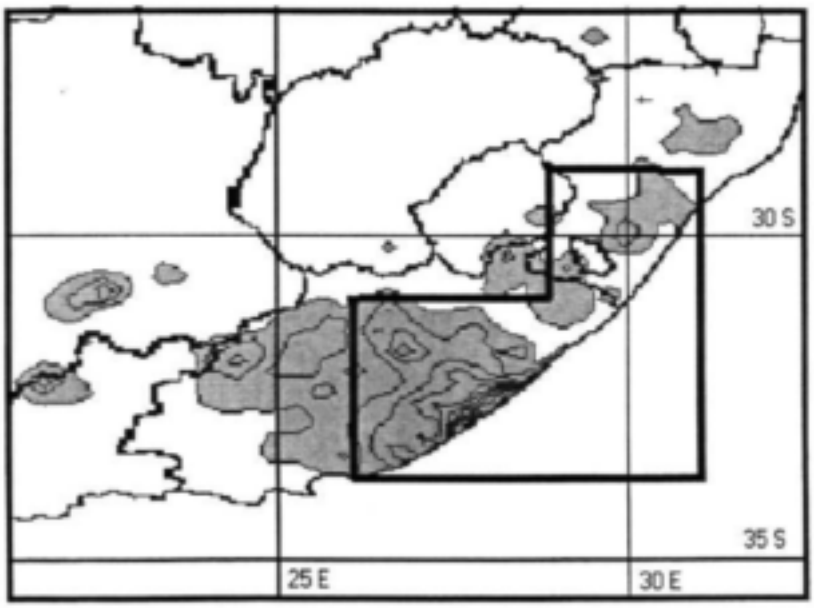

Figure 5.3.1: BARCOZ results on 27 August 1970. The blocks indicate the areas where heavy precipitation are predicted. The shaded areas are observed rainfall with the first isohyet at 20 mm. Up to 20 mm rain is possible outside the 20 mm isohyet.

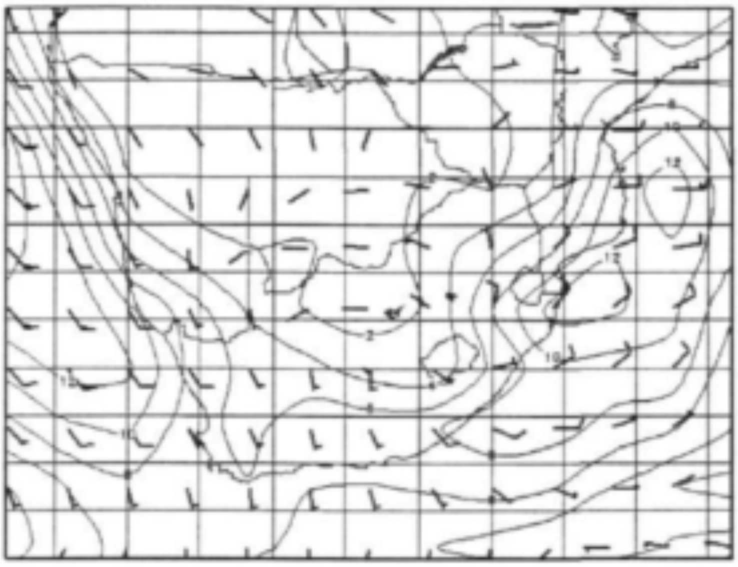

Figure 5.3.2: Moisture flux vectors (barbs) and the magnitude of the moisture flux (solid lines) on 27 August 1970 at 1200 UT.

Comparing the rainfall map and the moisture fluxes shows that this field fails completely to link up with the area of heavy rainfall. This was the case in the majority of the other case studies. Positive fluxes of moisture into the area of heavy rain generally existed but this parameter simply does not indicate where heavy rain is probable.

However Figure 5.3.3 is a composite figure depicting the water vapour flux by the meridional component of the 1000 hPa wind component (qv) and the gradient vector ($\overline{\nabla}$(qv)) (arrows) of this scalar quantity. It is immediately obvious that both qv and the vector $\overline{\nabla}$(qv) possess considerable more structure relevant to the rain area than was the case with the moisture flux ($q\overline{V}$) (Figure 5.3.2). Positive values of scalar qv means that v>0 (south wind) and that water vapour is transported northward. Figure 5.3.4 shows the divergence of the gradient of the water vapour flux with the meridional wind component ($\overline{\nabla} \bullet (\overline{\nabla}$ (qv)), referred to as **MC.** Figure 5.3.5 is the same as Figure 5.3.4 but in this case for **SEC** (($\overline{\nabla} \bullet (\overline{\nabla} (qv_{SE})$).

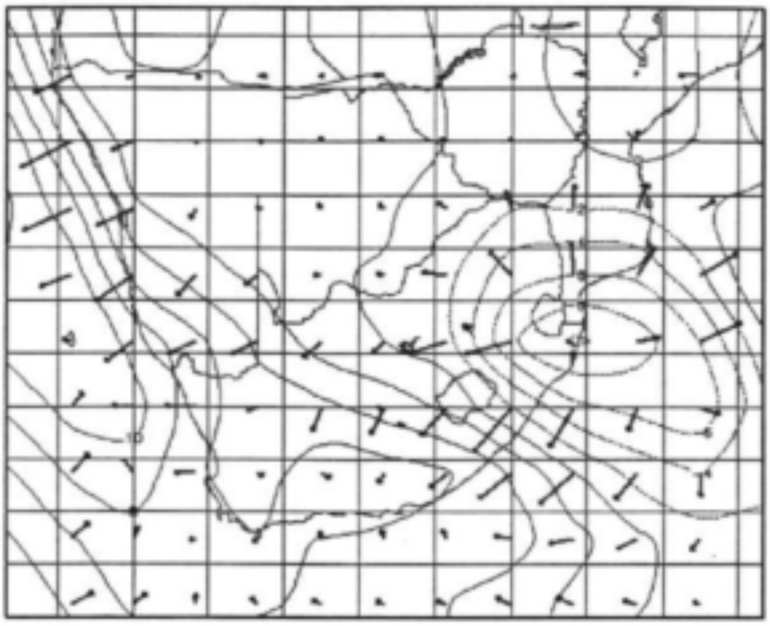

Figure 5.3.3: Flux of water vapour with the meridional wind component (qv), (lines) and the gradient (arrows) $\overline{\nabla}$ (qv), on 27 August 1970 at 1200 UT.

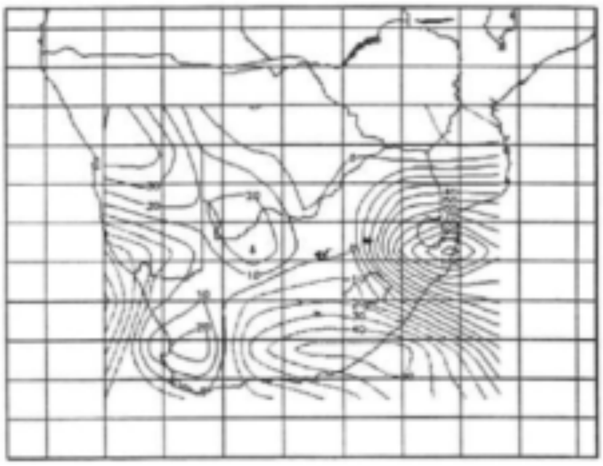

Figure 5.3.4: Divergence of the gradient of the meridional water vapour flux (MC) on 27 August 1970.

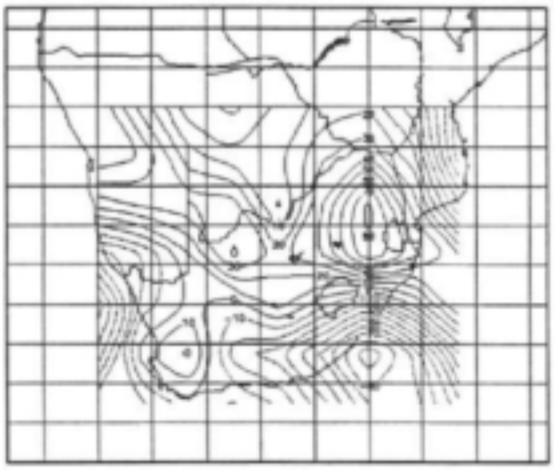

Figure 5.3.5: Divergence of the gradient of the southeast component water vapour flux (SEC) on 27 August 1970.

Careful analysis of these figures reveals that considerable convergence of water vapour takes place over and near the area with heavy rainfall. It is also clear from these figures that convergence of water vapour also exists along the Northern Cape Province western- and the Namibian south coastal regions but where no rain occurred. Water vapour convergence is a requirement for heavy rain, which will only materialize if large-scale upward motion is also present to transport the water vapour upward, resulting in adiabatic expansion, cooling, condensation and the development of rainfall.

5.3.4 Development of single field Masks for baroclinic weather systems.

Single field masks were developed from the overlays, some of which where dealt with in paragraph 5.3.2. They isolate areas where several significant dynamical features, generally thought to promote rainfall, co-exist. A mask differs from an overlay in that only if the prescribed conditions exist will it generate a field. The area designated by the mask indicates where all the atmospheric variables co-exist. In this section the masks isolate areas where strong upper wind divergence, mid-tropospheric upward motion, surface moisture fluxes and/or convergences co-exist. Masks were developed and tested in the case studies for the following combinations, referred to as **Masks**:

1. *Wind convergence at the 850 hPa level, average 300-200 hPa wind divergence and MC<0.*
2. *Same as 1 but with SEC < 0.*
3. *Vorticity advection 300-200 hPa > 0 and MC < 0*
4. *MC < 0 and $\omega < -0.1$ Pa s^{-1} at **both 700- and 600 hPa** levels*
5. *As 4 but with SEC < 0 and $\omega < -0.1$ Pa s^{-1}*
6. *As 5 but with **SEC*10E13 < -10** and ω **< -0.2 Pa s^{-1}***

Table 5.3.4 details the results of the single field masks, which were able to isolate heavy rain "near" to where it actually occurred in at least 7 of the 14 case studies. The comparison between the area isolated by the Mask and the area with heavy rainfall was determined by visual comparison. Unfortunately this process is somewhat subjective. Statistical evaluation will be detailed below. However the maps displayed here are precisely what the operational forecaster will have available. A classification of YY was generally assigned if the area isolated by the Mask included the area with heavy (observed) rainfall and generally had the same shape, even if larger, than the observed rainfall. The classification YN was assigned if the Mask generally identified an area of heavy rainfall near to or overestimated the area of heavy rainfall. A YN classification can be considered useful but with a risk of being somewhat misleading. A YY classification on the other hand is judged to be very useful and a feature previously unavailable to local meteorologists.

If table 5.3.4 is considered it is obvious that only Masks 1, 4, 5 and 6 made the YY grading at least 8 times. In all of the Masks the factor MC or SEC form one component of the mask. Mask 6 was identified as the baroclinic heavy rainfall identification system for coastal rain (BARCOZ).

Table 5.3.4: Evaluation of the ability of selected *single field masks* to isolate areas of heavy *Coastal Rainfall.* The classification YY YD, FF and FD is the same as in table 5.3.1.

Date	Mask 1	Mask 2	Mask 3	Mask 4	Mask 5	Mask 6
1 September 1968	FD	YN	FD	YN	YY	YY
2 September 1968	FF	FF	FD	YY	YY	YY
25 August 1970	YY	YY	YY	YY	YY	YY
26 August 1970	YY	YY	YY	YY	YY	YY
27 August 1970	YY	YN	YY	FF	YY	YY
28 August 1970	FD	FF	FD	FD	YY	YY
20 August 1979	YN	YN	YY	YY	YN	YN
21 August 1979	YN	YN	YN	YY	YN	YY
25 January 1981	YN	YN	YN	YY	YY	YY
26 September 1987	YY	YN	YN	YY	YY	YY
27 September 1987	YY	YN	YN	YY	YY	YY
28 September 1987	YY	YY	YN	YN	YY	YY
29 September 1987	YY	YY	YN	YN	YY	YY
7 July 1996	YY	YY	YY	YY	YN	YY
No: YN / YY	3 / 8	7 / 5	6 / 5	3 / 9	3 / 11	1 / 13

Figure 5.3.6a-d displays the areas delineated by BARCOZ (rectangles) together with the corresponding recorded rainfall for the case studies (a) 28 August 1970, (b) 7 July 1996, (c) 1 September 1968 and (d) 2 September 1968. The BARCOZ results for 27 August 1970 is depicted in Figure 5.3.1 and did very well. It captured the heavy rains centred on East-London, inclusive of most of the rains occurring over KwaZulu-Natal. It did miss some of the heavy rains extending westwards over the Eastern Cape Province. BARCOZ extended the heavy rainfall far eastwards on 28 August 1970 (Figure 5.3.6(a)). Considering that the NCEP data points are some 250 km apart this is nevertheless an encouraging result, as it would have shown the

eastward movement of the system. This is significant because the East-London area had more than 700 mm of rain in a few days. The next map, Figure 5.3.6(b) shows how well BARCOZ captured the heavy rain over KwaZulu-Natal on 7 July 1996. Considering the Port Elizabeth flood event (Figure 5.3.6(c)) it is clear that BARCOZ did well again. It isolated the heavy coastal rain and isolated an area over the Transkei coast, where only moderate rain fell (table 5.3.5). It missed some of the heavy rain north of Algoa Bay probably because of the large horizontal scale of the NCEP data. On the following day, 2 September 1968, BARCOZ did rather well again, capturing the heavy rain over the eastern parts of the Eastern Cape Province.

Table 5.3.5: Average rainfall (mm) and percentages for the areas identified by BARCOZ. (% gt 0 = percentage of rainfall stations reporting more than 0mm of rain, % gt 10= more than 10mm of rain, % gt 20= more than 20mm of rain, % gt 50=more than 50mm of rain). The asterisk indicates days, which were classified as tropical, and the shaded rows depicts days when BARCOZ forecast over the interior.

Date	Average (mm)	% gt 0	% gt 10	% gt 20	% gt 50
1 September 1968 (Area 1)	43	85	70	56	29
1 September 1968 (Area 2)	5	75	17	2	0
2 September 1968	39	91	88	70	30
25 August 1970	26	71	55	41	15
26 August 1970	42	90	81	67	32
27 August 1970	47	92	66	48	31
28 August 1970	5	86	5	0	0
19 August 1979	21	74	46	34	14
20 August 1979	34	80	61	47	26
21 August 1979	81	100	100	100	49
24 January 1981	39	87	69	55	30
25 January 1981	55	98	78	65	40
24 September 1987	1	10	3	0	0
25 September 1987	8	52	28	10	2
26 September 1987	30	86	70	53	19
27 September 1987	62	94	88	77	41
28 September 1987	41	76	54	42	23
29 September 1987	14	53	26	16	9
19 February 1988*	26	84	67	52	16
20 February 1988*	63	88	80	76	54
21 February 1988*	10	53	28	17	2
11 March 1988*	7	54	23	11	1
13 February 1996*	35	87	82	64	23
14 February 1996*	29	86	73	58	20
15 February 1996*	16	50	38	30	12
7 July 1996	24	68	56	39	16
	31	76	56	43	21

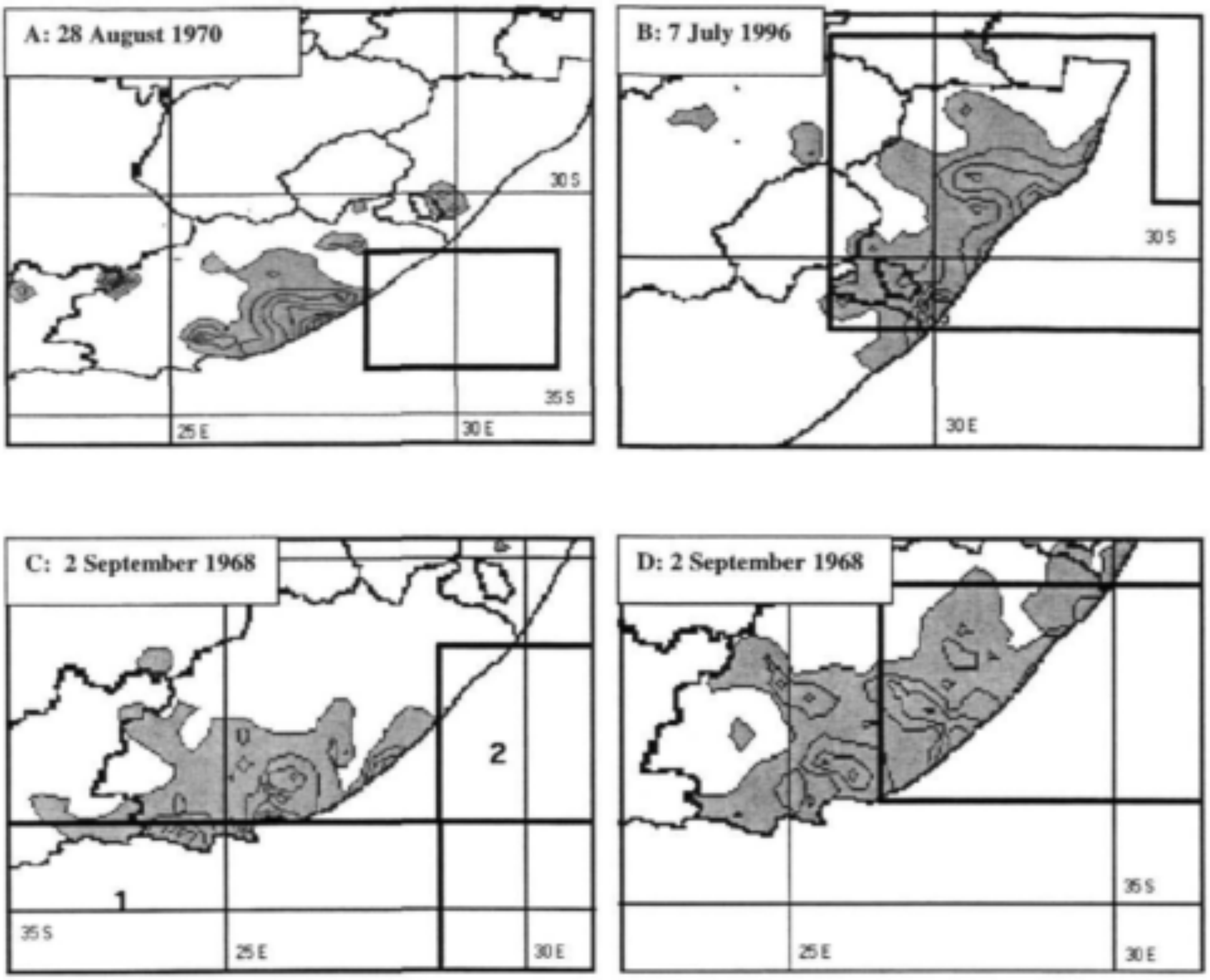

Figure 5.3.6: BARCOZ results on (A) 28 August 1970, (B) 7 July 1996, (C) 1 September 1968 and (D) 2 September 1968. The blocks indicate the areas where heavy precipitation is predicted. The shaded areas are observed rainfall with the first isohyet at 20 mm. Up to 20 mm rain is possible outside the 20 mm isohyet.

5.3.5 BARCOZ statistical results

Table 5.3.5 lists some statistics of rainfall within the areas delineated by BARCOZ. The table lists the statistics for 25 case study days. BARCOZ was also tested on days which were classified as tropical as was detailed in chapter 4. These days are indicated by an asterisk. The average rainfall within the BARCOZ areas is listed in table 5.3.5 together with the percentages of rainfall stations reporting more than 0, 10, 20 and 50 mm of rain. On 8 of the days BARCOZ indicated areas with heavy rainfall, when in fact the area average rainfall turned out to be less than 20 mm. On 12 of the days the average rainfall was more than 30 mm, on 8 occasions more than 40 mm of rainfall occurred in the BARCOZ area and on 4 days the average rainfall was more than 50 mm. On 21 August 1979 the average rainfall in the BARCOZ area was 81 mm. However, on this day only a very small area was identified over South Africa and only 4 rainfall stations were available for the computation of the average rain. On 27 September 1987 the average rainfall was 62 mm. On this day an extensive heavy rainfall area was identified over the KwaZulu-Natal coast, extending into the eastern interior. 41% of the stations in the area reported more than 50 mm of rain. Generally BARCOZ had a 70% success rate in identifying areas where the average rainfall was greater than 20 mm. Depending on the hydrological state of a catchment an average rainfall greater than 20 mm can result in serious flooding. On 15 of the 25 days 80% or more of the stations reported some rainfall in the BARCOZ identified area.

The average rainfall in the BARCOZ area on 20 February 1988 was 63 mm and 54% of the stations had more than 50 mm of rain. This day was classified as tropical in chapter 4. Considering these results together with the THERIS results in table 4.6.1, it is suggested that BARCOZ and THERIS together would have given a very good indication of the heavy rainfall on this day, with THERIS identifying the continental tropical rainfall and BARCOZ capturing the rainfall along the coastal areas.

5.3.6 Concluding remarks

The research described in this chapter has succeeded in finding two basic atmospheric circulation parameters which when viewed together with the vertical motion were very successful in isolating areas of heavy rainfall. The two, MC and SEC are new parameters. They are related to the more conventional convergence of the water vapour flux, which is in common use by South African weather forecasters. The authors are convinced that even forecasters with only very basic understanding of atmospheric dynamics will be able to understand and appreciate these new parameters.

The Masks, especially BARCOZ, supply the kind of rainfall prognosis that could mean much to the experienced weather forecaster, flood management managers as well as disaster prevention authorities.

The dynamical criteria of BARCOZ were sometimes also met over the interior of South Africa. When BARCOZ identified the heavy rainfall area over the interior, the average rainfall was generally low. These days are identified on table 5.3.5 by the shaded rows. Additional refinement of BARCOZ is required to improve identification of heavy rainfall areas over the interior.

CHAPTER 6
VERIFICATION TECHNIQUES

One of the greatest problems faced by the meteorologist and especially the weather forecasters is to determine how good their rainfall predictions are. The problem is compounded by the fact that weather systems, even if they are predicted well, possess so many small-scale structures that the rainfall they generate reaches the ground distributed almost randomly. The systems also move and develop, thereby changing their rainfall producing characteristics. In this chapter the efforts to establish the accuracy of rainfall forecasts are detailed.

6.1 Verification of rainfall forecasts for the Vaal Dam Catchment, Summer 1994 to 1998.

The six forecasting offices of the South African Weather Service (SAWS) can receive, in total, up to 200 000 calls a month. Many of these calls inquire about the rainfall outlook for anything from a few hours to a week ahead. Edwards (2000) stated that the SAWS had adopted a policy, many years ago, to issue worded rainfall forecasts using the terms isolated, scattered and general rain. In a worded rainfall forecast a glossary of words and phrases are used to describe the expected rainfall. During the 1980's increasing demands were made on the Directorate of Weather Forecasting by television services in particular, as well as by the many newspapers, to produce rainfall forecasts graphically. The decision was taken to delineate areas where rainfall is predicted on a map of southern Africa. At about this time percentages were assigned to the terms isolated, scattered and general rain. These were isolated 20% to 30%, scattered 40% to 70% and general 80% to 100%. However a rainfall percentage forecast compiled by the SAWS for a specific area does not represent the probability of rainfall occurrence, but rather the rainfall distribution over the area. At present, rainfall forecasts, using percentages to indicate distribution, have become the norm in South Africa. Scholz (2002) stated that a large number of the telephonic requests for rainfall predictions, received in the Central Forecasting Office (CFO), require that the rainfall prediction is issued in terms of such a percentage. At present no information exists on how reliable these forecasts are. However the quality of a forecast can best be determined through statistical and other verification schemes.

6.1.1. Data and Statistical aspects

A detailed discussion on verification methods used in meteorology is available in Murphy and Epstein (1967), Murphy and Winkler (1984), Murphy et al. (1985), Murphy and Winkler (1987), Murphy (1995), Sanders (1963) and Stanski et al. (1989). Verification is only useful if it leads to some decision considering the product being verified. In meteorology, verification has two goals: an administrative goal, to monitor the overall quality of a forecast and track any changes in the quality, and a scientific goal, to identify strengths and weaknesses of a forecast so as to direct research and development (Stanski et al. 1989).

In this section the goal was to determine the accuracy of the rainfall percentages as forecasted, subdivided into specific rainfall classes. This was achieved by using the SAWS 24h rainfall forecast maps, which are valid for the Vaal Dam catchment and for the five summer rainfall seasons (October to March) of 1994 to 1998. The rainfall forecast maps are considered subjective because no exact or reliable numerical method exists to determine rainfall distribution and depth from atmospheric circulation fields, actual or prognostic. It is also widely accepted within the forecasting community that predictions of rainfall, distribution and depth from general circulation models are unreliable at the spatial scale of the SAWS rainfall districts. Therefore these rainfall forecasts are subjective in the sense that they depend largely on the interpretation and experience of the individual forecaster (Sanders, 1963). The forecast and rainfall observation data are of a categorical nature and are evaluated by using the contingency tables designed by Stanski et al. (1989). In this paper no attempt is made to verify the depth of rain forecast. The aim is rather to verify the rainfall distribution classes.

6.1.2 The Vaal Dam Catchment

The Vaal Dam is the primary supplier of potable water to the heartland of the South African economy (Department of Water Affairs and Forestry, 1991). More than 25% of the country's people are dependent on water stored in the Vaal Dam. This dam lies in the eastern part of the much larger Vaal drainage region. The largest part of the Vaal Dam catchment lies in the Free State Province (60%) with the rest lying in Gauteng and Mpumalanga Provinces. A rectangular area of approximately 261km by 287km can cover the Vaal Dam catchment (Fig. 6.1.1). The mean annual runoff (MAR) to the Vaal Dam is approximately 8% of the annual rainfall (Department of Water Affairs and Forestry, 1991).

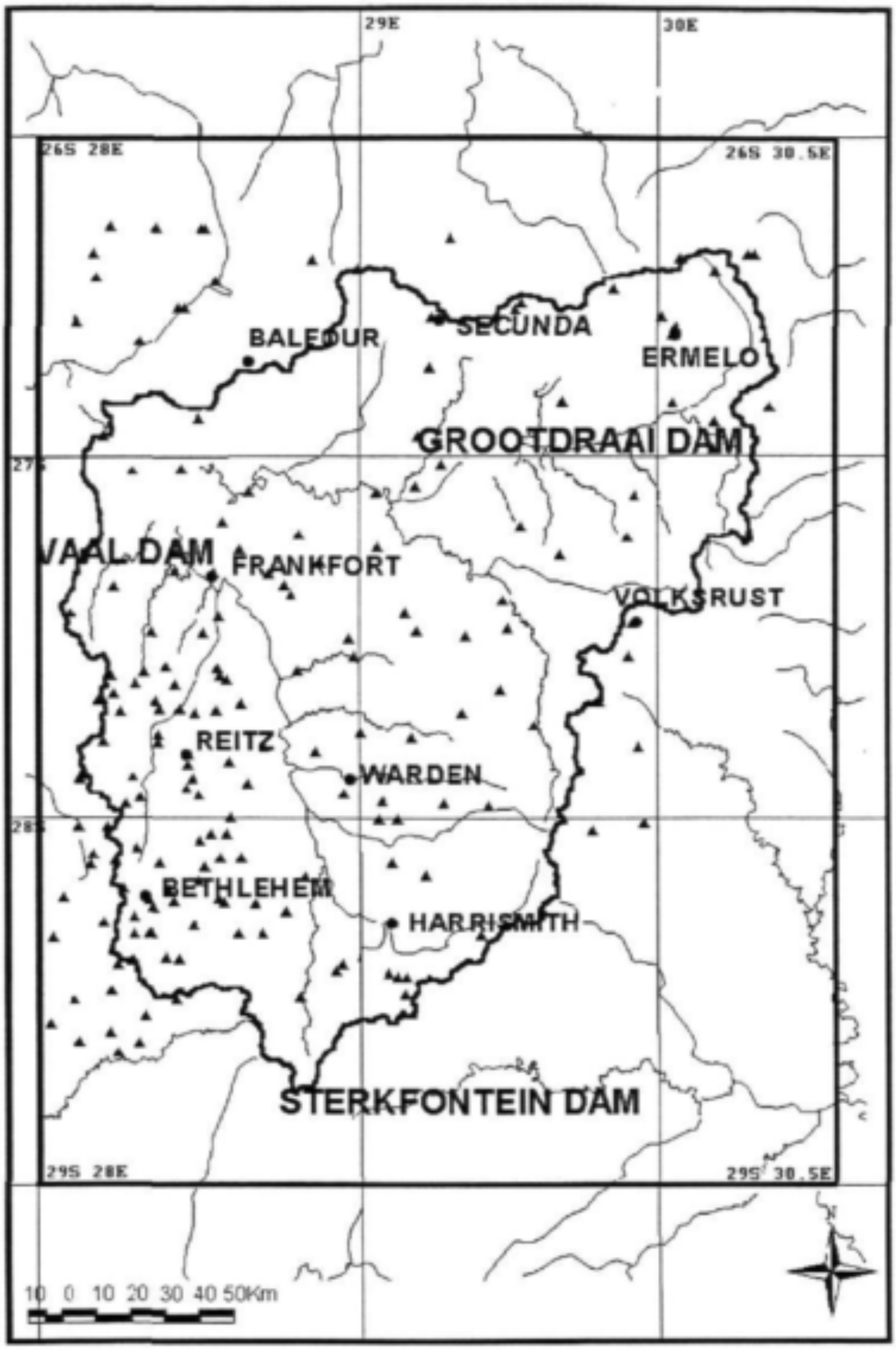

Figure 6.1.1: Rainfall stations (triangles) near and within the Vaal Dam catchment. The boundary of the Vaal Dam catchment is indicated by the solid line, and the rivers by thin lines. The area where rainfall stations were isolated is indicated by the smaller rectangle.

6.1.3 Methodology

It is important to note that complications occur when comparing the forecasts and rainfall gauge data, referred to here as observations. The period of validity of the forecast is from 00:00 to 24:00 SAST while the daily rainfall observation is valid from 08:00 to 08:00 SAST the next day, but by convention assigned as rainfall which fell on the first (previous) day. This means that there is a 16h period in which the rainfall observational and forecast periods overlap. The rainfall forecast starts 8h before the rainfall observation and also ends 8h before the rainfall observation period ends. There is approximately 180 rainfall station in the Vaal Dam catchment (triangles in figure 6.1.1).

In this report the percentage of the stations reporting more than 0.0 mm rain per day was calculated for each 24h day. The percentages were computed using the weighting average method of Tennant (1999), where the geographical position of each station relative to the other stations is taken into consideration. Marx et al. (2002) provided detailed information on the computation of the weighted mean and this is also detailed in chapter 2. This weighting function was applied to all the rainfall stations in the Vaal Dam catchment on a daily basis.

Two different methods were used to perform the forecast evaluation.

Contingency tables compare the distribution classes of the forecast and observation. The classes as classified by the authors are no-rain; isolated rain; scattered rain and widespread rain. In terms of percentages these classes are no-rain (0 to 15%); isolated rain (16 to 35%); scattered rain (36 to 75%) and widespread rain (76 to 100%). Using this classification, several skills and scores can be determined. These scores include the percentage correct forecasts (PCF), the false alarm ratio, the threat score as well as the Heidke skill score as described by Stanski et al. (1989).

Due to the large number of forecasts, which were classified as scattered rain, the question was raised whether it would be statistically justified to use this class without further subdivision. The decision was taken to use this class unchanged because of its common use by the South African weather forecasters and its wide acceptance by the general public. Analysis of the rainfall gauge data indicated that rainfall classified as widespread rain occurred only 8% of the time. This severely limits the significance of statistical parameters calculated for widespread rain. Because of the importance of this class (widespread rain) for hydrological forecasting it was decided to use this class without any modification.

The second evaluation method used in this paper is the hit rate. Eleven rainfall stations, with continuous records, within the Vaal Dam catchment area were selected. Rainfall data from the 11 stations were used to determine whether rain had occurred at the station when it was forecast but irrespective of the category (class). The true skill score (TSS) is a measure of the association between the forecast and observation (Stanski et al.,1989). TSS is perfect when it is equal to +1 and at its worst when it is equal to -1.

6.1.4 Research Results

Figure 6.1.2 depicts the PCF over the Vaal Dam catchment for the summer seasons 1994 to 1998. For the entire period the PCF was less than 50%. The best results were found for the 1995/1996 and 1998 summer seasons. Banitz (2001) postulated that persistence forecasting played a role in the forecasting skill for heavy rainfall during February 2000. It is conceivable that persistence forecasting also contributed to the higher accuracy of forecasts during the 1995/1996-rainfall season. This summer was characterised by above normal rainfall over the study area (De Coning, 1997, De Coning et al., 1998 and Edwards, 1997).

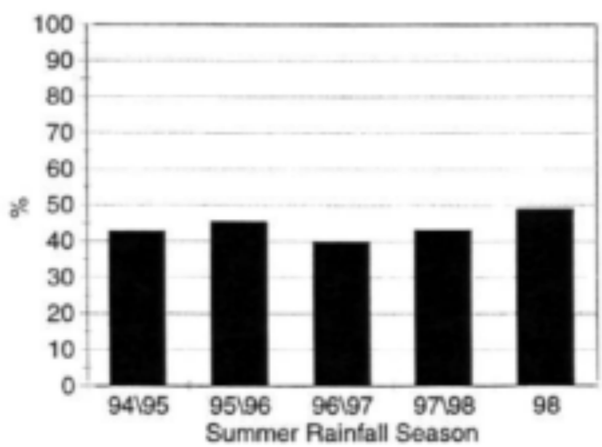

Figure 6.1.2: Percentage of correct forecasts (PCF) over the Vaal Dam catchment for the summer rainfall seasons 1994 to 1998

Figure 6.1.3 shows the PCF but in this case considering the different classes of rainfall. Analysis of figure 6.1.3 indicates that the forecasts produced by the SAWS were generally less than 50% correct. Notable exceptions occurred with the 'no-rain' class during the 1995/1996 and 1998 summer seasons, the 'isolated rain' class in the 1998 early summer months and the 'scattered rain' class during the 1997/1998-summer season. However, when it came to 'widespread rain', the forecast accuracy for the Vaal Dam catchment was very poor. Results were less than 25% correct with two seasons as low as 12%.

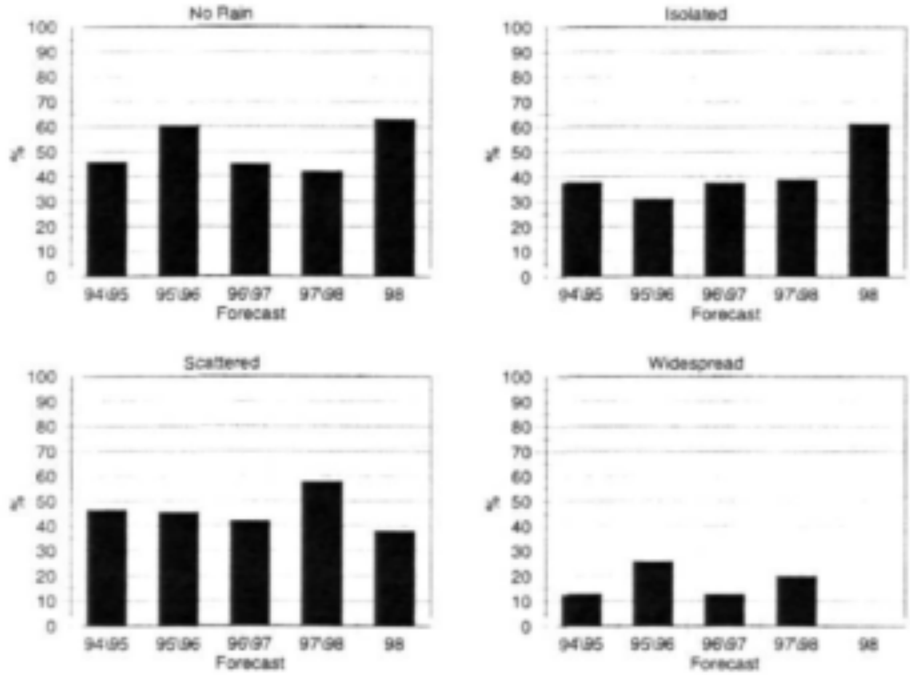

Figure 6.1.3: Percentage of correct forecasts (PCF) over the Vaal Dam catchment for the summer rainfall seasons 1994 to 1998 for the four individual rainfall classes. The observation class is indicated at the top of each histogram.

Figure 6.1.4 indicates the percentages of what was forecast for the actual observed rainfall classes. In figure 6.1.4 the observed rain class is shown at the top of each histogram while the forecast for the specific class is indicated at the bottom. When 'no-rain' occurred 'no-rain' was forecast 49% of the time, 'isolated rain' was forecast 29% of the time and 'scattered rain' 21% of the time (Fig 6.1.4a). Good forecasting is indicated by high percentages for the corresponding observation class. This was only partially achieved with the 'no-rain' and 'scattered rain' observation classes. For the 'no-rain' observation, 49% of the forecasts were 'no-rain' (Fig

6.1.4a) while when 'scattered rain' was observed, 47% of the forecasts were 'scattered rain' (Fig 6.1.4c). The observed 'isolated rainfall' class shows that the forecasters tend to predict 'scattered rain' rather than 'isolated rain' (Fig 6.1.4b). Considering the observed 'widespread rain' class, it is also clear that the forecasters tend to be conservative and would rather predict 'scattered rain' (Fig 6.1.4d). Figure 6.1.4 suggests that for the Vaal Dam catchment region, the preferred class of rainfall forecast is 'scattered rain' whenever any rain event is expected.

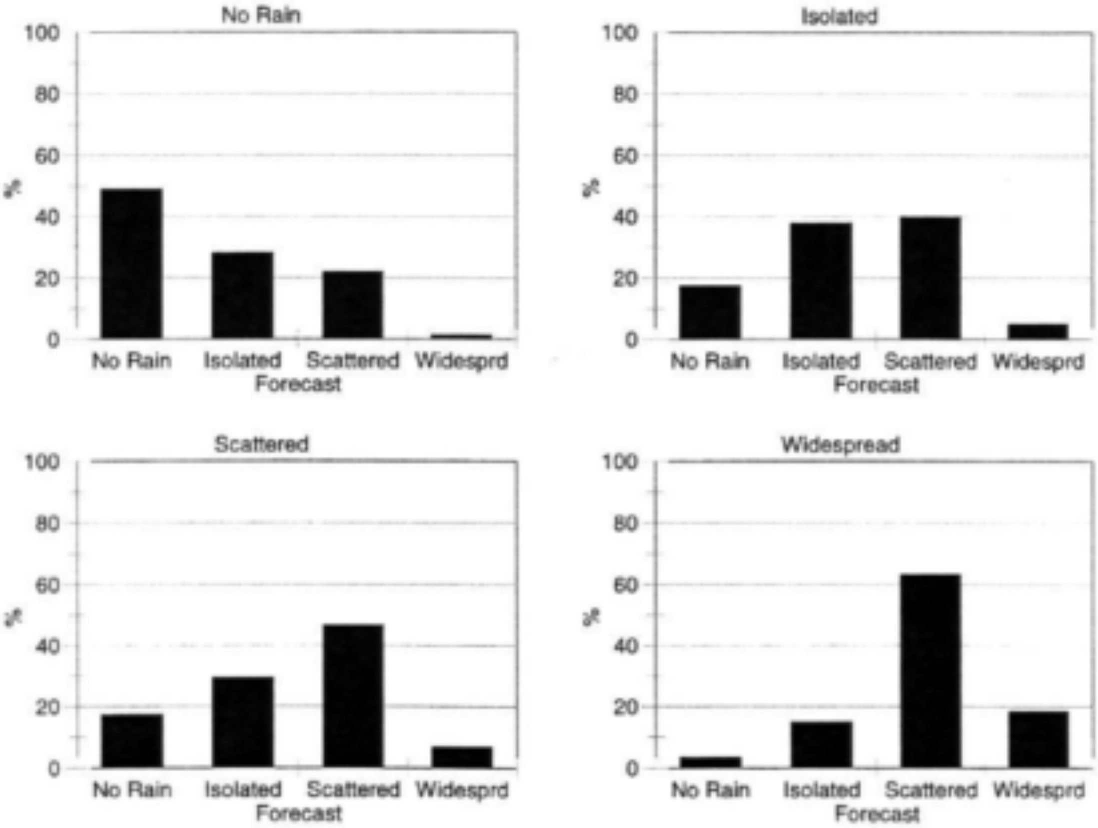

Figure 6.1.4: As figure 6.1.3 but for the percentages of forecasts issued in each class.

Figures 6.1.5a (6.1.5b) are pie charts indicating the percentage of forecasts (observations) made in each class for the whole period. Again most rainfall forecasts (35%) fall in the 'scattered rain' class while 'scattered rain' actually occurred only 25% of the time. 'No-rain' was observed most often (45%), but it was forecast only 31% of the time. The 'isolated rain' observation, which occurred 21% of the time, was forecast 29% of the time. 'Widespread rain' occurred 8% of the time, but is only forecast 5% of the time.

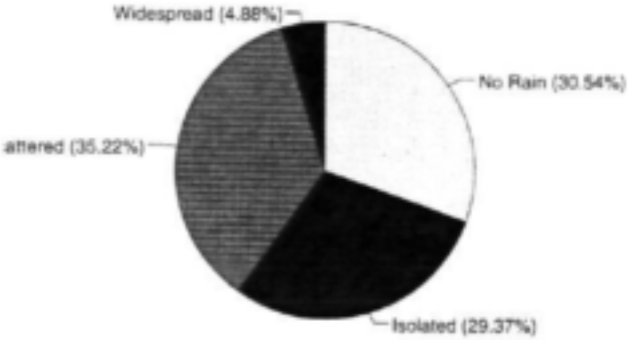

Figure 6.1.5a: The number of forecasts, expressed as a percentage, in each class over the Vaal Dam catchment for the summer rainfall seasons 1994 to 1998.

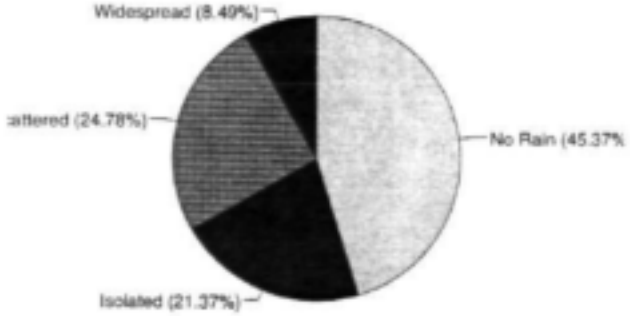

Figure 6.1.5b: As figure 6.1.5a but for the number of observations in each class.

Log-linear modelling (Fienberg, 1980) was also performed on the contingency table for the whole study period. This method was used to test the statistical association between each of the rainfall categories. Table 6.1.1 lists the results of this analysis. These values are odds-ratio values, which is a measure that describes the degree of association. Calculations showed that absolute values greater than 2.38 were significant. The ratio of the log-linear parameter estimate with its standard error indicated that a significant relationship exists between the 'no-rain' forecast and the 'no-rain' observation (9.141). The relationship between the 'isolated rain' forecast and the 'isolated rain' observation is close to significant (2.141), but the 'isolated rain' forecast is also associated with the 'no-rain' observation (2.134). The 'scattered rain' forecast produced unexpected results. A very weak and negative association exists between the 'scattered rain' forecast and the 'scattered rain' observation, but a significant relationship exists between the 'scattered rain' forecast and the 'widespread rain' observation (3.431). This indicates that the 'widespread rain' observation is usually associated with the 'scattered rain' forecast. The 'widespread rain' forecast shows a significant relationship with the 'widespread rain' observation.

Table 6.1.1: Ratio of the log-linear parameter to its standard error for the observed and forecasted rainfall classes in the Vaal Dam catchment during the summer rainfall seasons, 1994 to 1998. An asterisk marks significant values.

	No rain	**Isolated**	**Scattered**	**Widespread**
No Rain	9.141 *	2.134	-3.572 *	-4.869 *
Isolated	0.189	2.141	-1.061	-0.825
Scattered	-0.12	-0.345	-0.094	0.376
Widespread	-4.107 *	-2.34	3.431 *	6.144 *

With respect to the hit rate at the 11 rainfall stations in the region, table 6.1.2 indicates that a rain event was missed only 3% of the time. On average, rain was correctly predicted 52% of the time, while 45% of the time rain was forecast, rain did not occur. The average TSS for the 11 stations reveals a positive association between the forecasts and observations (0.2518). These results, however, are not as good as those obtained by the SAWS (Banitz, 2001). Remembering that time discrepancies exist between the forecast and the observation times, the hit rate results suggest that the forecast of rainfall is only some 50% reliable at any specific station in the Vaal Dam catchment.

Table 6.1.2: Hit rate for eleven rainfall stations in the Vaal Dam catchment for the summer rainfall seasons of 1994 to 1998.

Stations	Latitude (° S)	Longitude (°E)	Rain observed - not forecasted (%)	Correctly forecasted (%)	Rain was not observed but rain was forecasted (%)	True Skill Score (TSS)
1	27.18	29.63	4.01	50.43	45.56	0.2252
2	27.12	29.85	4.01	50.29	45.7	0.2256
3	26.85	29.15	2.44	52.01	45.56	0.291
4	26.77	30.12	4.76	55.41	39.83	0.2611
5	26.37	28.93	2.88	48.08	49.04	0.2424
6	26.5	29.18	3.58	57.8	38.63	0.3117
7	26.28	30.2	3.43	50.43	46.14	0.246
8	28.6	28	3.58	49.21	47.21	0.2201
9	27.87	28.08	3.74	52.99	43.26	0.2575
10	27.2	28.58	4.13	47.94	47.94	0.1973
11	28.12	28.35	2.39	52.62	44.99	0.2916
Average			**3.54**	**51.56**	**44.9**	**0.2518**

6.1.5 Concluding remarks

The SAWS evaluated rainfall forecasts for 19 districts covering most of the country and found their forecasts to be reliable (Banitz, 2001). Choosing a relatively small area, such as the Vaal Dam catchment, and verifying the rainfall distribution classes gave a PCF of less than 50%. However the statistical results are clearly dependent on the chosen verification method and it is clear that no single verification measure provides complete information about the quality of a forecast (Stanski et al., 1989). Considering the verification of the rainfall distribution classes, the best forecasts were made during the 95/96-summer season. The best forecast classes were 'no-rain' and 'scattered rain'. It was also found that when a rain event was expected 'scattered rain' was the preferred forecast. Log-linear modelling identified the same trends. No trend in the accuracy of the forecasts could be detected in the data over the rather short study period. The second hit rate method indicates that although a rain event was rarely missed (3%), rain was forecast close to 45% of the time when no rain was observed.

Widespread rain occurred only 8% of the time and was forecast poorly with the PCF ranging between 12 and 25%. Widespread rain was observed close to double the number of times it was forecast and scattered rain is often forecast when widespread rain in fact occurred. Widespread rain occurs on average only 15-days per summer rainfall season. Due to the rareness of a widespread rain event it is probable that forecasters have less skill in identifying the systems responsible and isolating geographical areas where widespread rainfall is probable. Areas of widespread rain often contain regions with heavy rain, which may cause flooding. It is therefore imperative that forecasting techniques are developed to aid the forecaster in identifying and accurately predicting this rain class. Considering the many discrepancies between data and forecast periods as well as the meteorological factors, the results do indicate that forecasting methods used for identifying rainfall classes need to be re-examined. It is therefore recommended that an ongoing evaluation be initiated with timely feedback to the forecasters in order to assist in the improvement of rainfall forecasts.

6.2 The Verification of Precipitation of a Numerical Weather Prediction Model

The precipitation forecast generated by a numerical weather prediction model is considered to be one of the potentially most useful products the model can provide. The SAWS currently runs a Limited Area Model (LAM) referred as the Eta model. Case studies on heavy rainfall events over South Africa involving the Eta model found that the model is generally well equipped to identify the geographical distribution of heavy rainfall but can underestimate the amount of rainfall by 50%. (De Coning et al., 1998, Dyson and Van Heerden, 2001). Before the onset of this project in 1999 no objective verification system to determine the accuracy of the Eta model's rainfall forecast existed in South Africa. The aim of this research was to develop verification methods by using, amongst others, the statistical measures currently in use in the Bureau of Meteorology (BOM) in Australia (Ebert and McBride, 1997). Two verification methods were investigated:

1. The 24-hour rainfall totals simulated by the Eta model were evaluated against the daily rainfall provided by the MRL5 Radar situated close to Bethlehem.
2. The 24-hour rainfall totals simulated by the Eta model were evaluated against the daily gauge rainfall over South Africa.

6.2.1 Radar Description

The MRL-5 radar is a dual-wavelength radar that operates on both the S- and X-bands. It is situated approximately 20 km northwest of Bethlehem at 28°05′ S, 28°10′ E. The central Free State, southern Gauteng, southwest Mpumalanga, northwest Kwazulu-Natal, southeast North West Province and Lesotho fall within the range of the radar. The rainfall data derived from this radar proved to be reliable and stable in capturing major rain events (Terblanche et al., 1994, Terblanche, 1996 and Van Heerden and Steyn, 1999).

Terblanche and Mittermaier, (2001), stressed the importance of weather radar data for forecasting due to its real-time nature and the high temporal and spatial resolution of storms and rainfall events over large areas. They expressed the opinion that radar data forms one of the components needed to provide accurate area rainfall estimates.

6.2.2. Verification of Numerical Weather Prediction Models

Many statistical measures exist to quantify the errors in the NWP forecast. Stanski et al. (1989) and Wilks (1995) provide two useful reviews of verification methods. Both categorical (conditional) and continuous statistics are necessary to gain a total picture of the performance of a forecast (Ebert and McBride, 1997). Verification statistics of the model data should be compared to verification statistics of persistence (observed rainfall from the previous forecast period) and climatology (long-term mean rainfall, or the most probable value) to determine the quality of the model precipitation forecasts (Ebert and Mcbride, 1997). If the model forecast outperforms persistence and climatology, it is considered to be useful.

To verify the model precipitation forecast, it is necessary to first determine the model's ability to predict the location and time of a precipitating system. Maps of the observed and predicted rainfall, and the maps showing the difference between the forecast and observations are used here to answer questions of model accuracy. A mapped forecast can appear correct, while the verification statistics are quite inadequate. This can be due to errors in the location of the rain maxima. Deficiencies in the model's physical parameterisation can also result in the rain to be correctly located, but its magnitude or extent may be incorrect (Ebert and Mcbride, *1997)*. The errors in a forecast are often difficult to determine when the verification is done on the regional scale especially when a weather system does not fit precisely into a set region.

6.2.3 Verification of Eta model precipitation using Radar Rainfall.

6.2.3.1 Data

Two data sets were used these were the Bethlehem MRL-5 radar rainfall and the Eta model precipitation prognostic field. The horizontal resolution of the MRL-5 rainfall data is one 60th of a degree, approximately 1.5km (1 pixel). The Eta model precipitation prognosis has a horizontal resolution of half a degree or approximately 48 km. A large discrepancy therefore exists in resolution between the two data sets. The rainfall value at a single grid point of the Eta model represents the averaged rainfall for a rectangular area of 30' by 30' surrounding the grid point. The radar data was averaged onto the same grid by adding the radar rainfall pixel totals, in the rectangle, and dividing it by their number. One Eta grid point covers approximately 900 radar pixels. The geographical position of the radar (dark gray) and Eta data is shown in figure 6.2.1. The light grey areas, where the two data sets overlap, consist of 33 Eta grid points.

6.2.3.2 Results

The verification method was tested on data of the 9th February 2000. Figures 6.2.2 and 6.2.3 represent the Eta model precipitation forecast and radar rainfall, respectively. Figure 6.2.2 shows that the Eta model predicted rainfall in excess of 10 mm in the northwest. The maximum rainfall forecast in any rectangle was 21 mm, while over the remainder of the area insignificant or no rainfall was forecast. The radar (Fig. 6.2.3) indicated rainfall over the central parts of the area. The maximum radar rainfall was 67 mm.

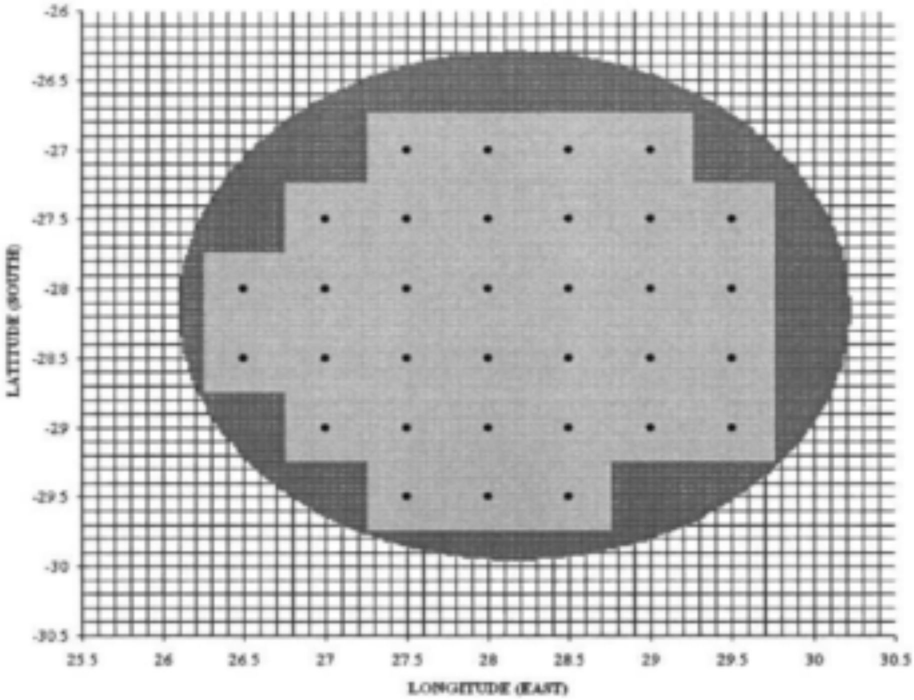

Figure 6.2.1: The geographical position of radar (dark grey) coverage and Eta data. The light grey area indicates where the data sets overlap.

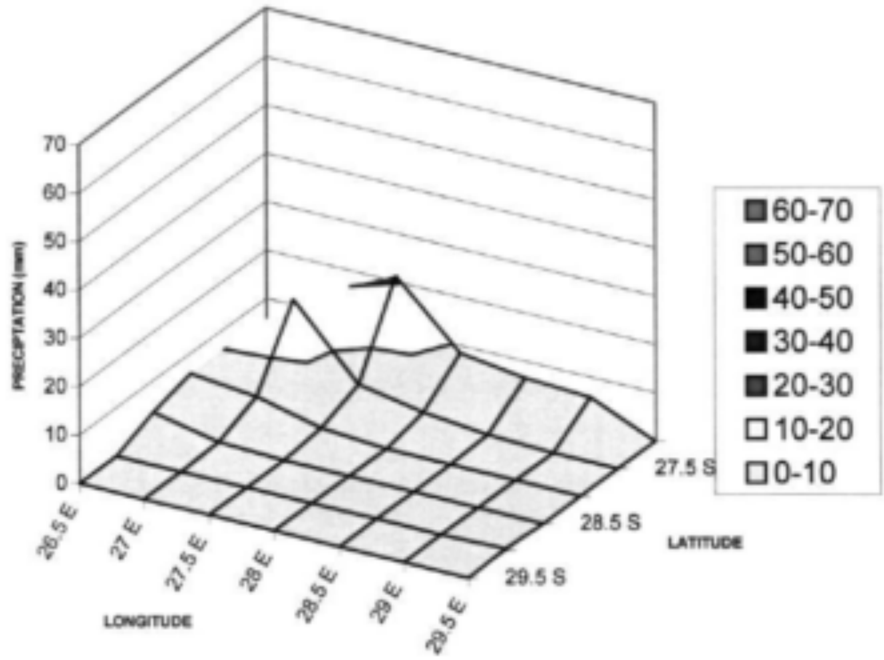

Figure 6.2.2: The Eta model precipitation forecasts in millimeters on the 9th of February, 2000. Contour intervals of 10 mm.

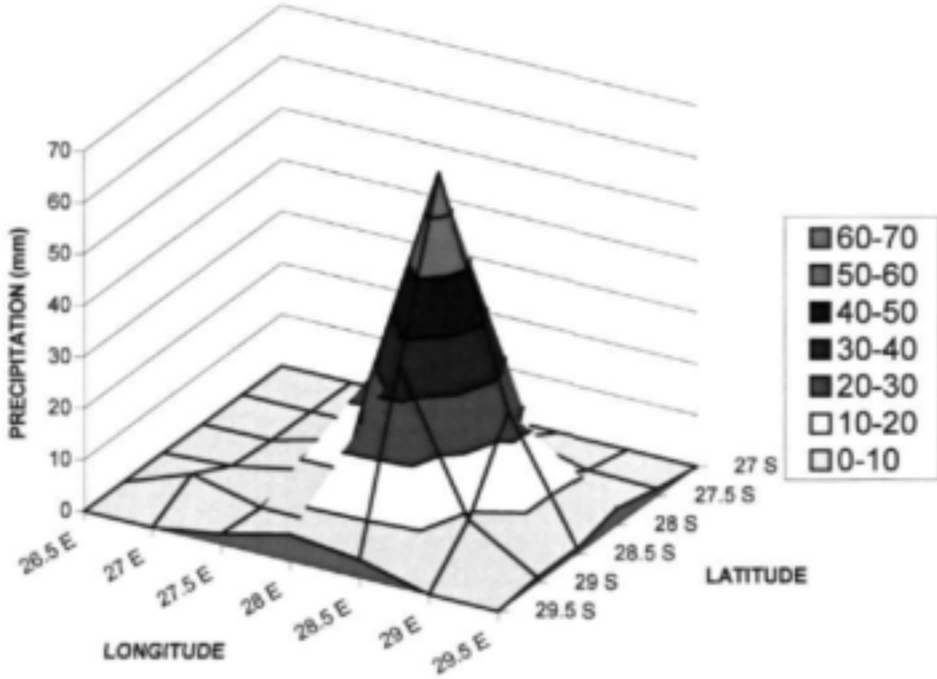

Figure 6.2.3: Same as figure 6.2.2 but for the radar rainfall.

Table 6.2.1 is an example of the statistical scores that can be computed. On the 9th of February 2000 all 33 rectangles recorded some radar rainfall while Eta predicted rainfall at only 16 rectangles. The average radar rainfall over the entire area was just over 7 mm while the Eta model predicted 5 mm (if only non-zero values are used in the computation of the average rain). However, as figures 6.2.2 and 6.2.3 indicate the rainfall predicted by the Eta model was some 200 km northwest to where the radar indicated it actually occurred.

Table 6.2.1 lists the comparative statistics between the model precipitation forecast and the radar rainfall as well as categorical statistics derived from the contingency table. The bias score was 33%, which confirms that the model under predicted for this day. The probability of detection was 27% and therefore rainfall was predicted at fewer rectangles than where it actually occurred. The false alarm ratio of 20% means that at only 20% of the rectangles where Eta predicted rainfall, did it not occur. The area under investigation is rather small (33 rectangles) and the method was tested on one day only. However in this research the emphasis is placed on the verification method and the results for the 9th of February are included to show the potential of this method if it is to become operational and implemented over the entire of South Africa.

A method to determine if the weather systems responsible for the rainfall were on sub grid scale is to compute the wetted area ratio (WAR) for the radar rainfall. The WAR is the ratio between the pixels indicating rainfall (> 2.5 mm) and the total amount of pixels (Mittermaier and Terblanche, 2000). Mittermaier and Terblanche (2000) concluded that if the WAR is small, the development is most likely on sub-grid-scale. On the 9th of February 2000 the average WAR over the research area was 0.098 (table 6.2.1). This would confirm that the weather systems causing the rainfall were indeed on sub-grid-scale.

Table 6.2.1: Continuous and categorical statistics for the 9th of February, 2000.

CONTINUOUS STATISTICS

NUMBER OF GRIDPOINTS	=	33	
AVERAGE WAR OF GRIDPOINTS	=	0.120	
BLOCK WAR	=	0.098	
		RADAR	ETA
NUMBER OF GRIDPOINTS RAINING		33	16
AVERAGE RAIN (0 mm excl. in model)		7.429 mm	5.188 mm
AVERAGE RAIN (0 mm incl. in model)		7.429 mm	2.515 mm
VARIANCE		13.109 mm	4.991 mm
MAX RAIN		67.502 mm	21.125
mml			
COVARIANCE	=	-13.755	
MEAN ERROR	=	-4.914 mm	
MEAN ABSOLUTE ERROR	=	8.701 mm	
ROOT MEAN SQUARE ERROR	=	15.761 mm	
CORRELATION COEFFICIENT	=	-0.210	

CATEGORICAL STATISTICS

		Predicted	
		No Rain	Rain
Observed	No Rain	1	2
	Rain	22	8

RATIO OF CORRECT FORECASTS TO TOTAL NUMBER	= 0.273
BIAS SCORE	= 0.333
PROBABILITY OF DETECTION	= 0.267
FALSE ALARM RATIO	= 0.200
CRITICAL SUCCESS INDEX	= 0.250
EQUITABLE THREAT SCORE	= -0.048
HEIDKE SKILL SCORE	= -0.100
HANSEN AND KUIPERS SCORE	= -0.400

The radar reflectivity on the 9th of February was studied by using the Thunderstorm Identification, Tracking, Analysis, and Nowcasting (TITAN)) system (Terblanche, 1996). Stratiform cloud occurred during the morning with convective development taking place during the afternoon. The maximum diameter of the convective development in the afternoon was only 5 km. Confirming that the rainfall developed from sub-grid-scale cloud systems.

6.2.4 Verification of Eta data using gauge rainfall.

In this part of the report Eta model precipitation forecasts are compared against rainfall data obtained from the South African Weather Service's rain gauges. Only the 190 daily reporting SAWS rainfall stations, available in real time are used. The 24-hour Eta rainfall forecast, which corresponds with the rain gauge observation period, is evaluated for both the 00 UTC and 12 UTC model runs. Eta provides two precipitation forecasts; the total precipitation (Zhao and Carr, 1997) and convective precipitation (Betts and Miller, 1986; Janjic, 1994). Both these products are evaluated.

Two verification methods developed for NCEP by Ghelli and Lalaurette (2000) are employed here. The approach is to ensure that the Eta precipitation forecast and the rain gauge data have the same format. The first method, defined as 'upscaling', calculates the average rainfall observation value in a model grid box. This is done by computing the average rainfall of all rainfall stations, which fall into the geographical area represented by a grid point in the Eta model. The average values or '*super observations*', as defined by NCEP, are assigned to the particular model grid point.

The second method is the Cressman method (Colle et. al., 1999). In this approach a model rainfall total is computed to correspond with the geographical position of the observed rainfall data. Four surrounding model grid points are used to interpolate a model rainfall value *P* at the position of every station.

$$P = \frac{\sum_{n=1,4} W_n P_n}{\sum_{n=1,4} W_n}$$

P_n is the model rainfall value at the grid point and n=1,4. W_n is the weight given to the surrounding grid point values (Cressman,1959).

$$W_n = \frac{R^2 - D_n^2}{R^2 + D_n^2}$$

D_n is horizontal distance from the model grid point to the observation and R is the model horizontal grid spacing. This method is referred to as the '*station observations*'

For both of the methods a 2x2 contingency table (Yes/No) was calculated for 6 different rainfall thresholds. The thresholds are 0.1mm, 1mm, 2mm, 4mm, 8mm and 16 mm per 24 hours. For the 0.1mm threshold any rainfall total greater than 0.1mm (observed or predicted) would fall into the "Yes" category of the contingency table while rainfall of less than 0.1 mm falls into the "No" category of the contingency table. The same method applies for the other 5 thresholds. The yes/no nature for each category is then tested at each point, which will explain the model's behaviour at the different thresholds. For example, at low thresholds, it explains the model's behaviour for light rain events or the area coverage of rain (Ebert and McBride, 2000). At higher thresholds it explains the model's behaviour at peak values.

Verification scores include those used by ECMWF (2000), namely, the Frequency Bias Index (FBI), the Equitable Threat Score (ETS) and the Hansen-Kuiper Score (TSS). Additionally, another three scores were calculated, namely, the probability of detection (POD), the false alarm ratio (FAR) and the hit rate (ACC). The bias is calculated for both methods and is displayed graphically.

6.2.4.1 Results

A great number of graphs and statistical measures are available when applying the methods described above. In order to demonstrate this method, results for the December-January-February (DJF) 2001/2002 rainfall season will be detailed.

Figure 6.2.5a depicts the FBI for DJF of the 2001/2002-rainfall season for the station observations as well as the super observations. The FBI is a measure of the frequency of occurrence of a forecast relative to the observation. If the forecast is perfect the FBI would be equal to 1- that is, the event is forecast exactly as often as observed. For a FBI greater (less) than 1 the event is over-forecast (under-forecast). For both the super observations and station observations and for all 6 thresholds investigated here there exists a tendency to over-forecast (Fig 6.2.5). The FBI is largest, 2, for the 2mm threshold and is close to perfect for the 16mm threshold. In order to demonstrate how well the Eta model performed at specific locations over South Africa four stations were selected for comparison they are Pretoria, Cape Town, De Aar and Durban. The FBI at the four stations is depicted in figure 6.2.5b. As was the case in figure 6.2.5a there is again a tendency to over-forecast. The FBI is close to perfect for the 0.1mm threshold but the error increases as the threshold increases. The largest error consistently occurred at Cape Town with an FBI of 35 for the 16mm threshold. The smallest error occurred at Durban and the FBI for the 16mm threshold was significantly less at 8.

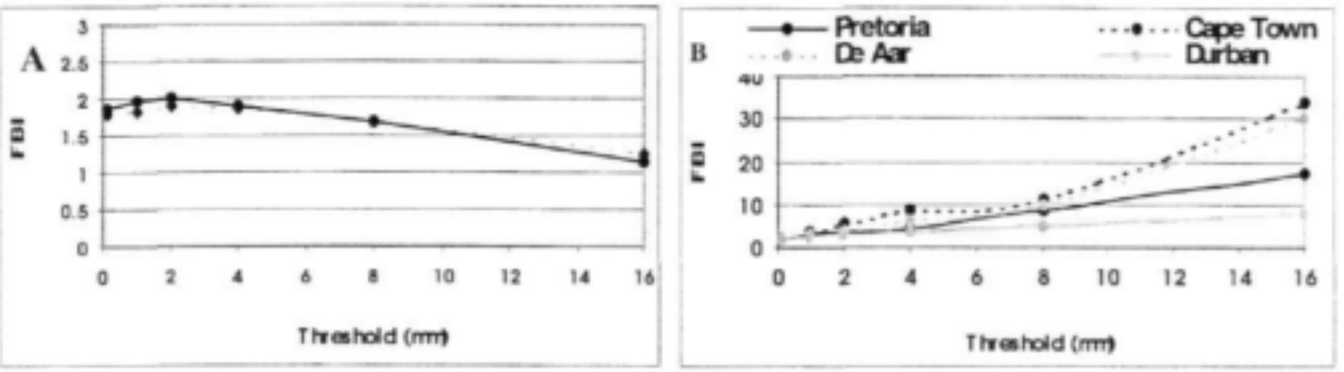

Figure 6.2.5: The Frequency Bias Index (FBI) for December-January-February 2001/2002 for (a) the station observations (solid line) and super observation (dotted line) and (b) four selected stations.

The ETS for the station observations and super observations for the 6 rainfall thresholds are depicted in figure 6.2.6. A perfect forecast will give an ETS equal to 1. The ETS is generally less than 0.3. There is a decreasing trend as the threshold increases and the ETS is just more than 0.1 for the 16mm threshold.

The true skill score (TSS) is a measure of the association between the forecast and observation and is perfect when it is equal to +1 and at its worst when it is equal to -1. Figure 6.2.7a shows that the TSS for the 0.1mm threshold is close to 0.5 for both the super observations and station observations. As was the case with the ETS, the quality of the forecast again decreases proportionally with increasing rainfall threshold. For the 16mm threshold the TSS is just larger than 0.2. Figure 6.2.7b depicts the TSS at the four selected stations. At Cape Town and De Aar the TSS varied between 0.6 and 0.8. At Durban the TSS for the 0.1 mm threshold was 0.4 and decreased to 0.3 for the 16mm threshold. At Pretoria the worst TSS occurred at the 0.1mm threshold and increases slightly to the 16mm threshold.

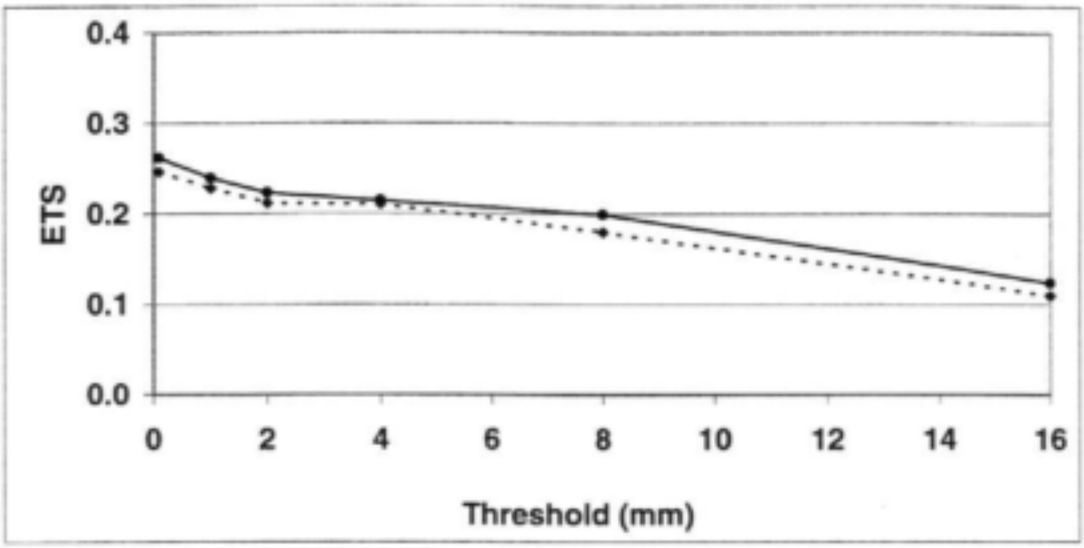

Figure 6.2.6: The Equitable Threat Score (ETS) for December-January-February 2001/2002 for the station observations (solid line) and super observation (dotted line)

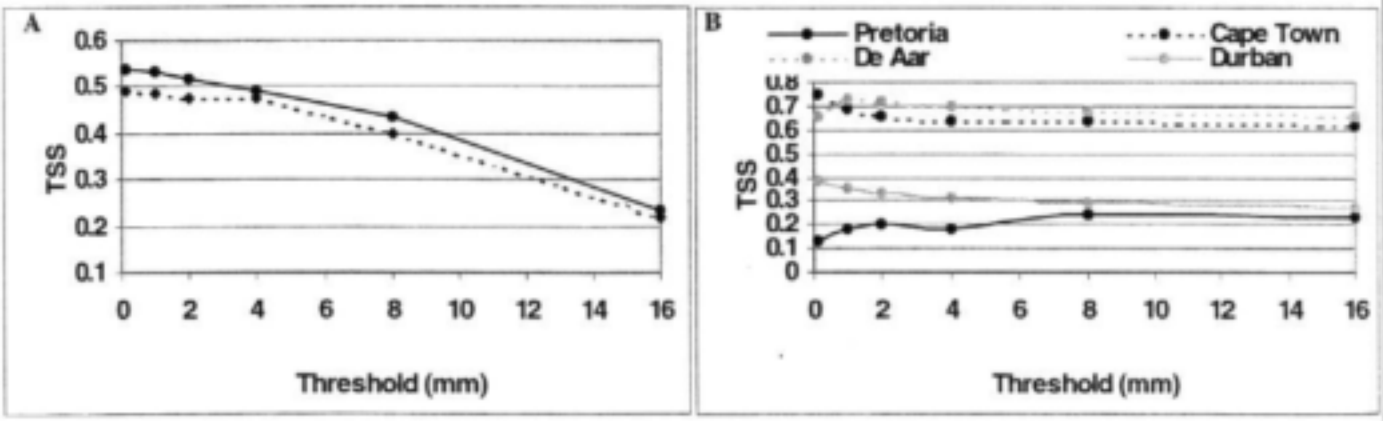

Figure 6.2.7: The Hansen-Kuiper Score (TSS) for December-January-February 2001/2002 for (a) the station observations (solid line) and super observation (dotted line) and (b) four selected stations.

The POD is a measure of the ability of the forecast to correctly predict rainfall (if rainfall occurred, did the model in fact predict rainfall). A perfect POD is equal to 1. Figure 6.2.8 depicts the POD for the station and super observations. The Eta model faired very well in identifying rainfall larger than 0.1mm. The POD nevertheless decreases for increasing rainfall threshold. For rainfall larger than 16mm the POD was only 0.3. The POD at the 4 selected stations also rendered excellent results. The Eta rainfall forecast was close to perfect at all 4 stations considering rainfall larger 8mm. For the 0.1mm, 1mm, 2mm and 4mm rainfall thresholds the POD varied between 8.5 and 1 (not shown). These results indicate that if any rainfall occurred the Eta model was quite capable to identify the rainfall event. However, these results should be viewed together with the false alarm ratio (FAR), which measures the tendency of the model to predict rainfall when no rainfall was in fact observed. The FAR varies between 0 and 1 where 0 would indicate the perfect forecast. Figure 6.2.9 depicts that the FAR for rainfall larger than 0.1mm was just more than 0.5. The FAR increases for increasing rainfall threshold. At the 16mm rainfall threshold the FAR increases to 0.8. Considering figures 6.2.8 and 6.2.9 together it would seem that although the Eta model is quite capable to identify a rainfall event the model also tends to predict rainfall when in fact no rainfall occurred.

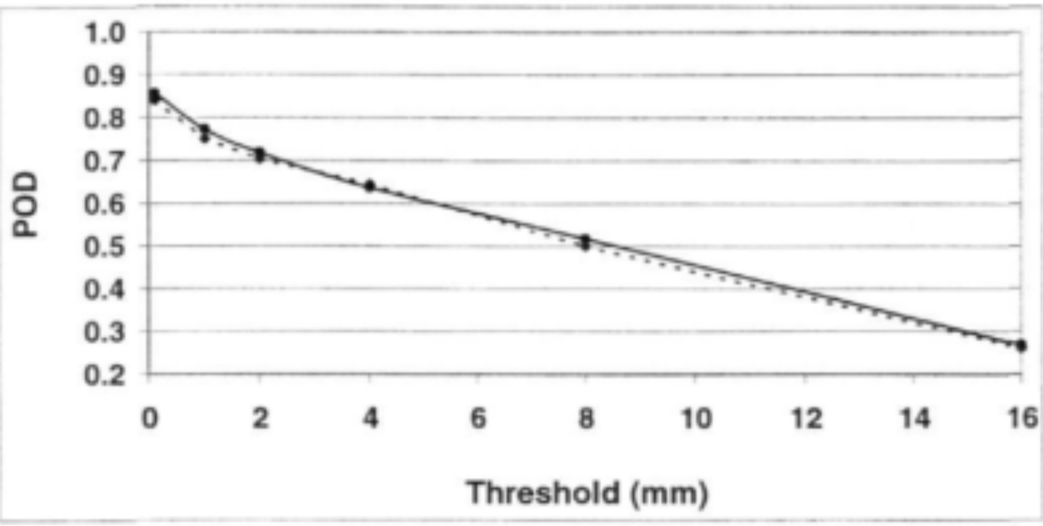

Figure 6.2.8: The Probability Of Detection (POD) for December-January-February 2001/2002 for the station observations (solid line) and super observation (dotted line).

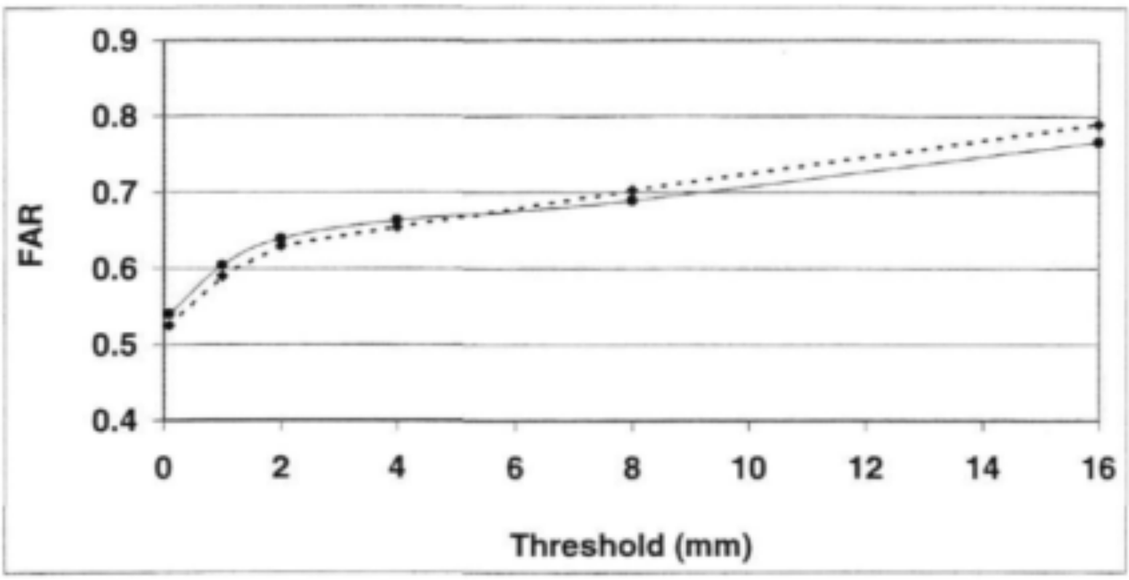

Figure 6.2.9: The False Alarm Ratio (FAR) for December-January-February 2001/2002 for the station observations (solid line) and super observation (dotted line)

Figure 6.2.10a depicts the results for the ACC, which is a ratio of the correct forecast to the total number of forecasts. The ACC for rainfall larger than 0.1mm is 0.7. There is an increasing trend with increasing threshold. For rainfall larger than 8mm the ACC is 0.9 and for the 16mm threshold the ACC is greater than 0.9. The ACC at four selected stations during the DJF rainfall season is depicted in figure 6.2.10b. At Cape Town and De Aar the results are very good and vary between 0.6 and 0.8 for all the rainfall thresholds. At Durban and Pretoria the results are less favourable. The best results nevertheless occur for the 0.1mm threshold and decreases to the 16mm threshold where the forecast was only some 30% correct at Durban and Pretoria.

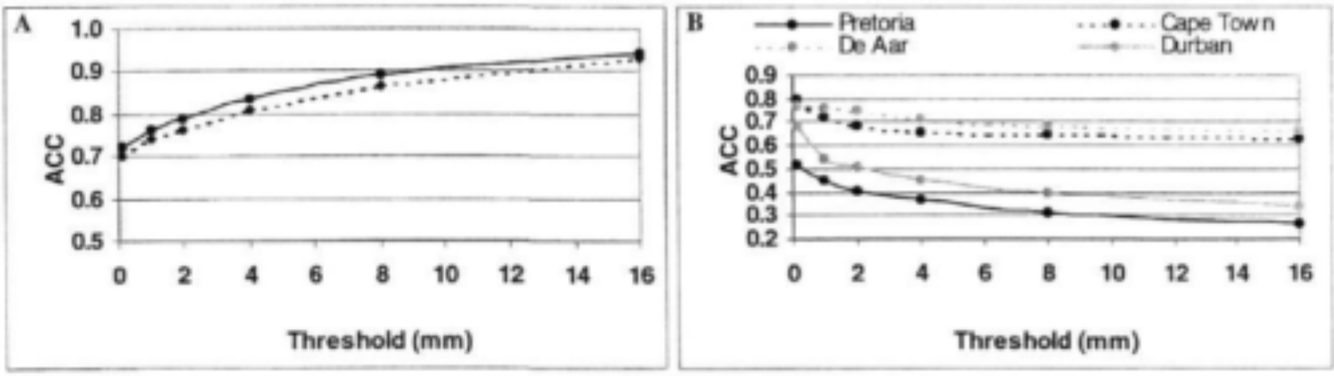

Figure 6.2.10: The Hit Rate (ACC) for December-January-February 2001/2002 for (a) the station observations (solid line) and super observation (dotted line) and (b) four selected stations

In order to determine if a trend exists in the accuracy of the forecast over time the ACC for the 0.1mm threshold is depicted in figure 6.2.11a and b. In figure 6.2.11a the station and super observations are depicted for every month from September 2001 to February 2002. These results indicate that the Eta precipitation forecast for rainfall larger than 0.1mm was consistently higher or close to 70% correct. In figure 6.2.11b the ACC for the 0.1mm threshold is depicted at the four stations. The Eta forecast at the four stations over the 6- month period was generally higher than 60% correct. Pretoria was the exception, during both December (40%) and February (50%).

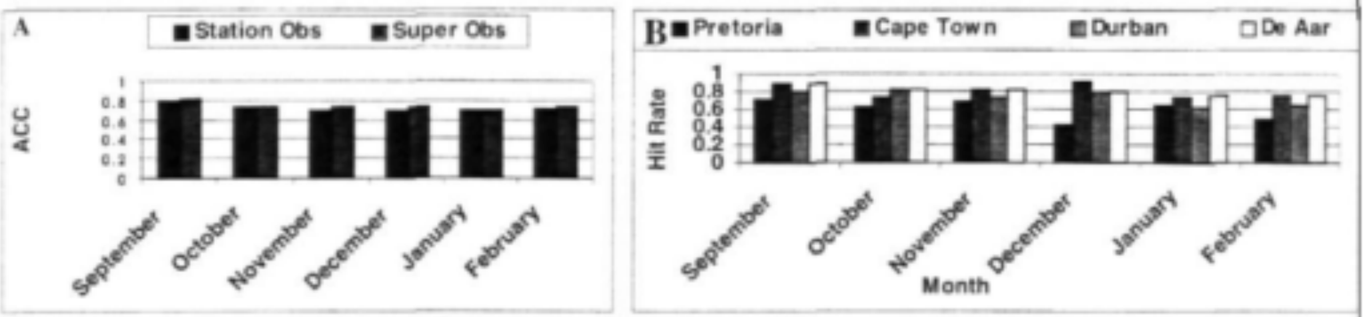

Figure 6.2.11: The Hit Rate (ACC) for September 2001 to February 2002 for the 0.1mm threshold for (a) the station observations and super observation and (b) at four selected stations.

Difference maps can provide the user of rainfall forecasts with some idea of the accuracy of the Eta model precipitation on a daily basis. Using the so-called *super observation* method difference maps are created by subtracting the station-averaged rainfall from the Eta forecast. An example of the difference map is shown in figure 6.2.12. Difference maps can also be created for the station observation method.

6.2.5 Concluding Remarks

The second method described here, where the Eta data is verified against gauge rainfall became operational at the SAWS in September 2001. This is the first objective verification system in South Africa. Modelers, forecasters and water managers can use the results obtained from the verification. For the first time the Eta model's performance can be quantified on the regional level as well as at specific stations.

The verification results during the December-January-February rainfall season of 2001/2002 can be summarised as follows

- The Eta model tended to over-forecast rainfall for all the rainfall thresholds
- The probability of detection for the 0.1mm rainfall threshold is very high (0.9) but the forecasting skill decreases as the rainfall threshold increases
- When considering the hit rate on the regional level the rainfall prediction is more than 70% correct for all rainfall thresholds.
- The hit rate results at the four selected stations for the 0.1mm threshold is equally impressive, with the forecast generally being more than 60% correct for the 6 months from September to February.

These results indicate that the Eta model is capable of identifying a rainfall event but the actual quarterly distribution of rainfall is not captured equally well.

Figure 6.2.12 provides some information on the distribution of rainfall stations over southern Africa. The grey indicates areas where no gauge rainfall is available for comparison with the Eta rainfall. This figure indicates that for the largest area of the Eta domain no gauge rainfall is available. It is therefore recommended that the verification system be expanded to include the approximately 1500 rainfall stations for which data became available around two months later. Radar and satellite rainfall maps should also be included in the operational rainfall verification system.

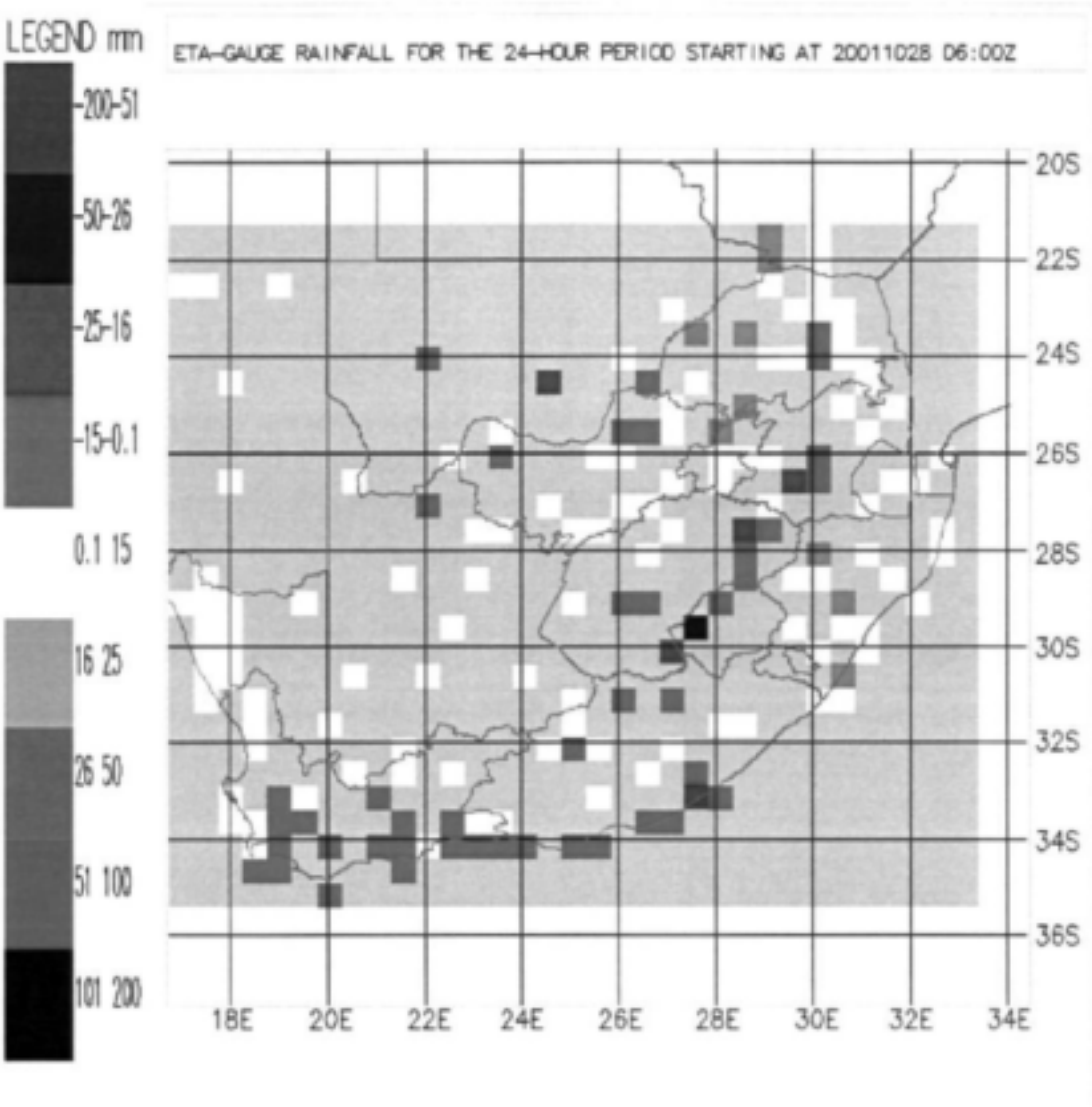

Fig 6.2.12: Eta rainfall minus gauge rainfall for the 24h period starting at 0600Ut on 28 October 2001.

CHAPTER 7
TECHNOLOGY TRANSFER

7.1 Heavy rainfall identification system

The model for the identification of tropical weather systems (MITS) is available in a so-called macro which operates on PCGRIDDS. PCGRIDDS is a display package which is currently in operational use in the forecasting offices of South Africa. A full operational implementation of MITS in the SAWS can be easily achieved but will require some intervention from the information technologists at the SAWS. However, the dynamical criteria applied by MITS is readily available from the prognostic fields from Numerical Weather Prediction models (NWP) and can therefore also be operated in forecasting offices in the SADC community. Countries to the north of South Africa's border may find this product especially useful due to the high frequency of tropical weather systems in the summer months.

The tropical heavy rainfall identification system (THERIS) is also available for implementation on PCGRIDDS. However, PCGRIDDS is not ideal to display THERIS results. There are two reasons for this. Firstly the horizontal resolution capability of PCGRIDDS makes it impossible to incorporate all the Eta model grid points (50km) and in this way information is lost. Secondly the operational version of the Eta model on PCGRIDDS has prognostic fields available at 6-hourly intervals only, while in fact Eta produces a prognostic field every 3-hours. The full capability of the Eta model can not be exploited on PCGRIDDS. To compensate for this, software programs were developed which operate on the entire Eta data set. A single matrix, containing all the THERIS areas, is generated in this way. This result is then displayed on a map of South Africa using a Geographical Information System (GIS). An example of a THERIS forecast generated in this way, is depicted in Figure 7.1.1

BARCOZ the baroclinic coastal heavy rainfall identification system, can not be implemented on PCGRIDDS. The new variable SEC can not be programmed to operate on the PCGRIDDS software and the only way to make these results available is through the method described above.

Using the THERIS and BARCOZ results a single field can be generated every day where all areas of expected heavy rainfall are indicated. By using the capabilities of a GIS this map could be published on the world wide web on a daily basis where any user will have access to the information. The software programs already exist and a full operational implementation is imminent depending on continued collaboration between the SAWS and the project team from the University of Pretoria.

Another product which is now available is the 24-hour Eta rainfall map. This map provides the Eta prognostic rainfall for the period starting 0600UT on day 1 to 0600UT on day 2. An example of the Eta rainfall map is depicted in Figure 7.1.2 and is also available for publication on the world wide web on a daily basis.

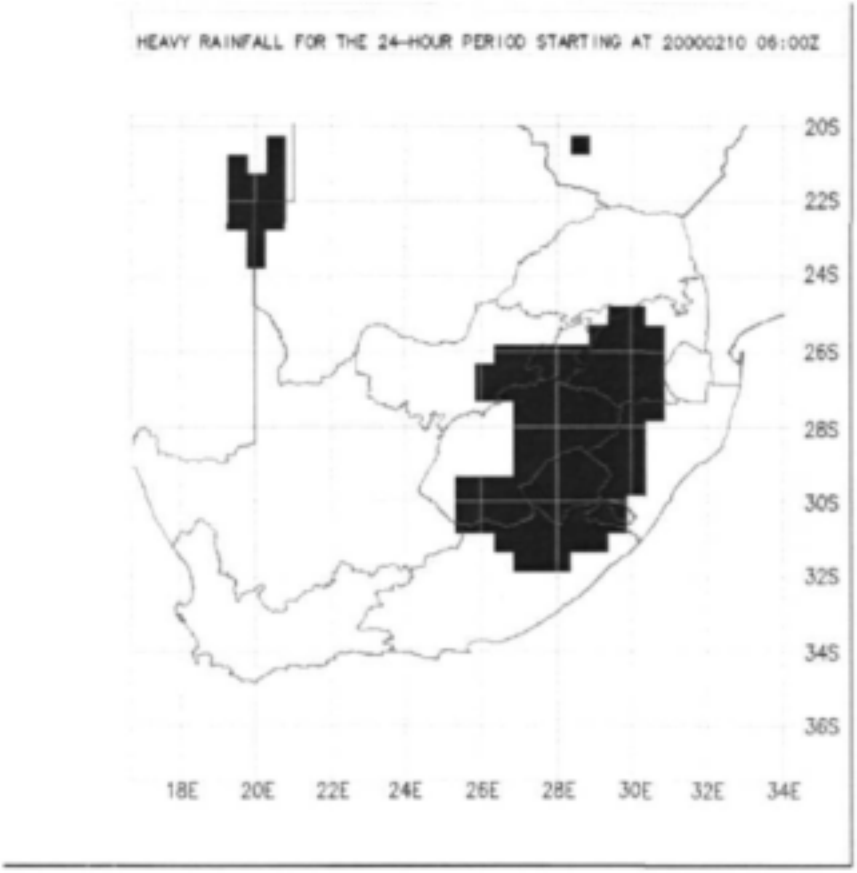

Figure 7.1.1: THERIS results on the 10 February 2000.

Versions of MITS and THERIS have been demonstrated to some of the forecasters of the SAWS Central Forecasting Office (CFO). The project team is ready to do an installation of the complete system, on request from the CFO. To ensure that the heavy rainfall systems are utilized to their full potential it is very important that the underlying meteorological principles are explained to the forecasters. A few training sessions would achieve this aim and the project team will gladly assist, on SAWS request. A letter requesting the system to be demonstrated to Weather Forecasters and installed at the SAWS is attached.

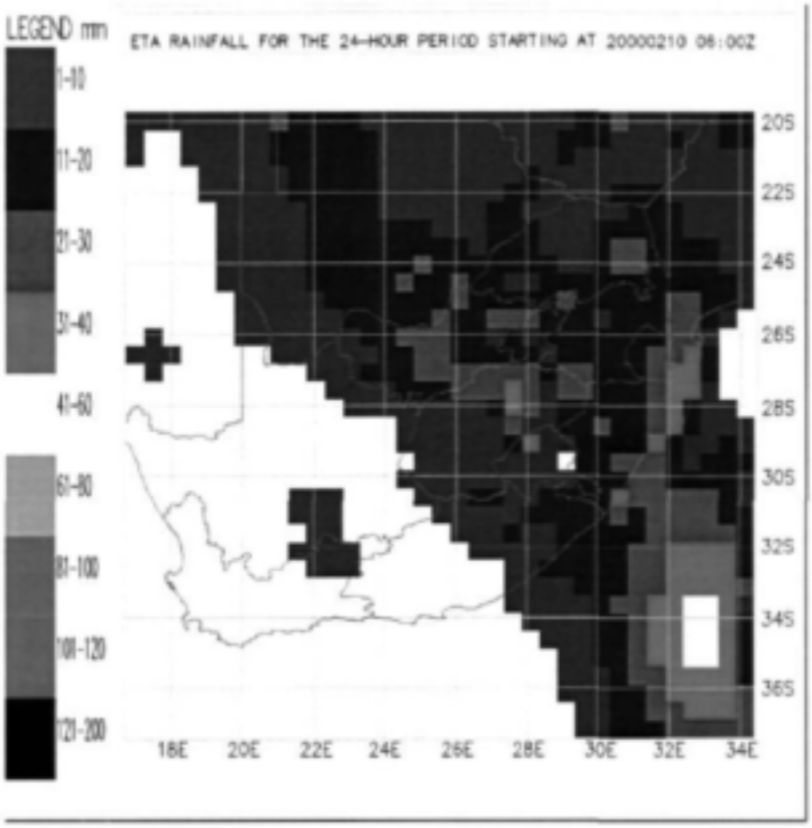

Figure 7.1.2: Eta rainfall for the 24-hour period starting at 0600UT on 10 February 2000.

The system can be made available to anyone who has access to NWP prognoses provided that all the necessary variables at the proper vertical layers are available in real time. Most of the Weather Services of the SADC countries will probably qualify. The project team can assist in making the product available to SADC provided the WRC lends its support. Dissemination of the system to the DWAF Hydrological Services as well as private forecasting groups awaits WRC approval.

The system can also be used as a research and training tool. It was used with considerable success during the University of Pretoria post-graduate forecasting course. However dissemination to other training schools is not recommended unless the personnel have considerable experience in weather forecasting.

7.2 Verification of the Eta model's precipitation forecast.

Research on the verification of the precipitation of the Eta model resulted in the verification system becoming operational at the SAWS in September 2001. The quality of the Eta model's precipitation can now be quantified statistically and objectively. It is recommended that the verification method be expanded to include all available rainfall data inclusive of radar- and satellite-derived rainfall fields. Results of the quality of the Eta rainfall prognosis should also be made available daily.

This product is a side benefit from the project. The project team member, Ms Marx, is now employed by the SAWS. It is proposed that the SAWS provide her with the opportunity to complete this task.

CHAPTER 8
CONCLUSIONS

For the convenience of the reader the main aims of the project as well as the secondary aims as agreed to by the WRC Steering Committee will be briefly detailed below followed by a report on how these aims were met.

8.1 Aims of the Project

The main aim of this project was to research the atmospheric circulation in order to determine the forcing mechanisms of widespread heavy rain and in this way pave the way for the preparation of a Quantitative Precipitation Forecast (QPF). Availability of a real time QPF would be a tremendous benefit for weather forecasting, dam and river flow hydrological management, disaster management organizations, road and air traffic authorities, industry and the general public. It was also envisaged that the QPF might become an important input into the River Flow Project by improving forecasting techniques and developing a new forecasting system for the period 6 to 48 hours ahead.

In order to achieve these goals, secondary aims of the project were defined. Some of them became major research concerns in themselves:

- A model for the identification of tropical weather systems (MITS) was constructed followed by the tropical heavy rainfall identification system (THERIS).
- A system for the identification of heavy rainfall along the coastal zone forced by baroclinic weather systems (BARCOZ) was developed.
- Research on the reliability of rainfall forecasts over the Vaal Dam catchment as well the quality of rainfall prognoses from the Eta model was completed.
- Independent and ongoing research on the classification and identification of widespread rainfall and the weather systems that cause them, became part of this project.
- Display of the results of the heavy rainfall identification schemes by a Geographical Information System (GIS) and availability for publication on the world wide web.

8.2 General concluding remarks and recommendations

This project can list three major research achievements. New ground was broken and for the first time, in southern Africa, a system exists which can delineate areas where heavy rainfall can be expected with a considerable degree of accuracy. All the components of these systems are based on well-proven meteorological dynamics but depend on the accuracy of the data fields generated by the analyses or prognoses using NWP models. This heavy rainfall identification and forecasting system consists of computer programs combining and applying atmospheric dynamic concepts to the data. These programs are able to synthesize many variables and parameters derived from the data. To integrate all this information in the short time available is otherwise beyond the capacity of a meteorologist.

The first part of the system, referred to as MITS (model for the identification of tropical weather systems), now enables meteorologists to determine whether a synoptic system can be classified as tropical. It also delineates the area where convective rainfall may develop. Tropical systems produce copious rainfall over South Africa's northern provinces as described in this report as well as in various publications to which reference has been made. MITS will also be extremely useful to South Africa's northern neighbours.

THERIS (tropical heavy rainfall identification system) is another powerful component, which isolates heavy rainfall forced by tropical weather systems. THERIS is novel, unique and was designed with the operational meteorologist in mind. The case studies, using THERIS, showed that this system performed well on NCEP analysis data as well as NWP prognoses. THERIS can be installed and run anywhere provided digital forecast data from a NWP is available. THERIS will also work well north of South Africa.

BARCOZ (baroclinic rainfall system for the coastal zone) provides the means to isolate the areas where heavy rainfall is expected from typical South African weather systems. Most important amongst these were the cut-off low-pressure systems held responsible for the majority of serious floods over the coast and adjacent inland areas. These systems were fairly well understood but BARCOZ will aid the forecasters to pinpoint the area where the rainfall will be maximised. The research also found new parameters, the convergence of the gradient of the moisture flux with the southeastern (meridonial) component of the wind, referred to as SEC (MC). Conventional dynamical parameters such as upward motion overestimated the area and placement of the heavy rain. Inclusion of the SEC/MC put matters right.

During the development of these systems it became apparent that synoptic scale data do not have the resolution to resolve some of the severe and important smaller scale rainfall events. The systems were very successful in isolating areas of heavy rain but were unable to explain severe events such as the Port Elizabeth flood or the very heavy rainfall along the escarpment. To accurately predict these severe events, more sophisticated models and data fields are required with horizontal resolution of kilometres rather than hundreds of kilometres.

However the systems developed (THERIS, BARCOZ) are powerful and provide tools to the meteorologist not available before. Urgent operational implementation is recommended. An invitation was extended to the Project Team by the SAWS to install these products operationally (Attachment 1).

Research to test the accuracy of SAWS rainfall forecasts over the Vaal Dam catchment indicated that forecasters tended to err on the safe or conservative side. A side benefit is that the SAWS is looking at the way rainfall forecasts are worded and compiled. This part of the project also evaluated the Eta model rainfall prognoses statistically. Verification was against rainfall figures computed from radar reflectivity data as well as rain gauge data. Verifying the Eta model with gauge data became operational at the SAWS in September 2001. For the first time in South Africa, it became possible to measure the quality of the Eta model rainfall prognoses objectively. Over the 6-month operational, period results show that the model tends to over-predict the rainfall. The model faired well with identifying rainfall areas but the rainfall totals are not simulated equally well. It is recommended that the verification method be expanded to include all available rainfall data.

Ongoing research on the geographical and spatial characteristics of widespread rain indicated that the period and amplitude of the annual number of these systems changed, probably during the long period with above normal rainfall of the 1970's. The research also indicated that the occurrence of these systems and the southern oscillation index (SOI) is uncorrelated. The research found a statistically significant increase in the number of one-day heavy rainfall events but a decrease in the number of multi-day events.

However the preparation of a proper quantitative precipitation forecast proved not to be possible in this project. Uncertainty about the accuracy of the NWP rainfall prognosis prevented the creation of a reliable first guess rainfall field. In future improved NWP generated rainfall fields could serve as a basis in the creation of a QPF.

Research results to pinpoint heavy rainfall from baroclinic systems, but well inland, was disappointing. It is speculated that summer continental baroclinic systems are modified by daytime convection and develop many features typical of tropical systems. The tropical temperate trough (TTT) may be an example of a mixed tropical, baroclinic system, producing considerable rainfall, yet not easy to detect with either THERIS or BARCOZ. The project was too short and not enough data on continental systems were available to develop a heavy rainfall detection system suitable for the TTT and other continental baroclinic systems. However results from BARCOZ, analysing particularly active baroclinic systems, indicate that the convergence of water vapour and vertical motion remains fundamentally important. Preliminary results also indicate further research on these systems should consider atmospheric stability and related factors.

The project personnel are now in the position to install the operational version of MITS, THERIS and BARCOZ in the SAWS Central Forecasting Office or elsewhere. This version will produce a single field incorporating THERIS and BARCOZ. MITS will also be available to the forecasting staff. Virtually no training is required. It is advisable however that a demonstration package be prepared to detail the scientific basis of these systems. This package can also serve as a training package.

SAWS personnel are requested to assist the project staff in the implementation and maintenance of an evaluation process to determine the value of the system.

Finally it is our belief that the output fields of this system should be disseminated to the Department of Water Affairs, Flood Management Group for independent evaluation. In time perhaps also to some civil authorities and Disaster Prevention Groups.

8.3 The way forward

Research during this project determined that the horizontal resolution of current operational NWP models, in use by the South African Weather Service, is too large to resolve smaller scale severe events. The rainfall prognoses of these models are as yet not good enough to use as a QPF. Regional models with a horizontal scale of kilometres should improve the situation.

MITS, THERIS and BARCOZ will, in the mean time, provide new and powerful guidance. These systems will in turn also improve as the model horizontal resolution improves.

The role of the high South African topography plays a decisive role in rainfall enhancement. This also holds for tropical systems where the slope of the terrain often determined the area of high rainfall. A future project will research this factor.

The operational implementation, support and evaluation of MITS, THERIS and BARCOZ will require the ongoing support and dedication of the SAWS.

The project team should be supported in efforts to install these systems in SADC countries.

CHAPTER 9
CAPACITY BUILDING

Opportunities for Capacity Building provided by this project have been utilised in the following ways.

9.1 Individuals

Ms L L Dyson was responsible for the concept and the research that eventually lead to the development of both MITS and THERIS. This work culminated in a MSc (Meteorology) degree, awarded with distinction. There is consensus that the MITS and THERIS systems are ready for operational implementation in the SAWS Central Forecasting Office. Ms Dyson, a major role player in the post-graduate forecasting course presented by the University of Pretoria and Lecturer in Meteorology, has utilised opportunities to disseminate the experience gained during this project, in this way extending capacity building beyond just herself.

Ms H G Marx (nee Pienaar) was responsible for most of the research on the evaluation of SAWS rainfall forecast as well as the model rainfall prognoses. This she did in part fulfilment of the requirements for a BSc Meteorology degree in 1999 and a BSc (Hons) Meteorology degree in 2000. A direct result of the research is that the SAWS are currently in the process of re-assessing the way that rainfall forecasts are worded. Ms Marx's research work went considerably beyond the requirements for the degree and enabled her to develop research skills now used to the benefit of the SAWS.

Under the auspices of this project Ms L Clark (2000) and Mr L Masimini (2001) each completed a compulsory research assignment in part fulfilment of a BSc (Meteorology) degree. Both Ms. Clark and Mr Masimini are continuing their research and may pursue research careers.

Table 9.1 lists at least 15 students, 12 from previously disadvantages communities who have completed their BSc (Hons) degrees at the University of Pretoria between 1999 and 2001. The students were exposed to the MITS, THERIS and BARCOZ systems and they were taught the atmospheric dynamics behind them. The systems will remain components of the forecasting course, thereby ensuring that future forecasters benefit from the project.

Table 9.1: Students exposed to the MITS, THERIS and BARCOZ systems

Name	Degree	Gender	Previously Disadvantaged	Country
L.L. Dyson	MSc (2000)	Female	No	SA
H. G. Pienaar	1. BSc (Meteorology) 1999 2. BSc (Hons) Meteorology 2000	Female	No	SA
L. Clark	BSc (Meteorology) 2001	Female	No	SA
L. Masimini		Male	Yes	SA
X. Mabusela	BSc (Hons) Applied Sciences (2000)	Male	Yes	SA
S. Mthethwa		Male	Yes	SA
J. Matsapola		Male	Yes	SA
E. Khoza		Female	Yes	SA
MF Mahahabisa		Female	Yes	Lesotho
MC Nkosi	National Higher Diploma in Meteorology (2001)	Male	Yes	SA
AC Moloto		Male	Yes	SA
EK Sebego		Male	Yes	SA
H Al-Brashdi	BSc (Hons) Weather Forecasting (2001)	Male	No	Sultanate of Oman
R Al-Nadhir		Female	No	
S Al-Zakwani		Female	No	
Q Jacobs		Male	No	SA
M Motsepe		Male	Yes	SA
MW Msimanga		Male	Yes	SA
T Ngobeni		Male	Yes	SA

In 2000, M F Mahahabisa from the Kingdom of Lesotho completed the forecasting course. During 2001 Mr. H Al-Brashdi, Ms. R Al-Nadhir and Ms. S Al-Zakwani, all from the Sultanate of Oman, completed their BSc (Hons) degree in weather forecasting. The research results have therefore also found application outside the borders of South Africa on a regional (SADC) and international level. Mr. T Ngobeni, a South African who completed his degree in 2001, has enrolled for his MSc (Meteorology) degree, at UP, and is undertaking research to identify the circulation features responsible for heavy rainfall developing in the tropical temperature trough. The benefits of presenting the FORFLOOD research results as part of the Weather Forecasting Honours course are therefore beginning to bear fruit

9.2 Institutions

The University of Pretoria has benefited from this project in numerous ways. The financial assistance has ensured the employment of research assistants, who played an invaluable role in the success of the project. The research results obtained have influenced the course content of subjects presented at the honours level considerably and have helped to maintain an internationally recognised standard. This in turn has ensured a continued growth in the student numbers at the honours level and establishment of contact with weather services in Southern Africa and abroad.

The research results emanating from this project have also directly profited the SAWS. The weather forecasting students (potential SAWS employees) completing the honours course have been trained in the latest available techniques. Several research products (MITS, THERIS, BARCOZ and GIS generated rainfall charts) could find a practical application in the SAWS. The evaluation of the Eta model rainfall prognosis has become operational at the SAWS recently and this project has contributed to the research to establish the evaluation system.

CHAPTER 10

CONFERENCES AND ARTICLES

1999

1. Dyson L.L., Poolman E.P. and van Heerden J. (1999). Classifying synoptic systems responsible for heavy rainfall over South Africa using thermodynamic and kinematic parameters. *15th Annual conference of the S. Afr. Soc. Atmos. Sci.*
2. Pienaar H.G. and Dyson L.L. (1999) Verification of rainfall forecasts for the Vaal catchment in recent summers. *15th Annual conference of the S. Afr. Soc. Atmos. Sci.*
3. Poolman E.P. (1999). Heavy Rain Events over South Africa. *15th Annual conference of the S. Afr. Soc. Atmos. Sci.*

2000:

1. Dyson L.L. (2000). The meteorological events that gave rise to the February 2000 floods. *Preprints of the 2000 Conference on Floods, Bridges and People.* 11-12 May 2000, Univ. of Pretoria, S. Afr.
2. Van Heerden J. and Dyson L.L. (2000). Flood producing rainfall over the northeastern interior of South Africa during February 2000. *16th Annual conference of the S. Afr. Soc. Atmos. Sci.*
3. Dyson L.L. (2000). Heavy Rainfall and Flooding in February 2000: The Human Impact. *16th Annual conference of the S. Afr. Soc. Atmos. Sci.*
4. Poolman E.P. (2000). Tropical rainstorm Eline as simulated by the ETA numerical weather prediction model. *16th Annual conference of the S. Afr. Soc. Atmos. Sci.*
5. Pienaar H.G. and Dyson L.L. (2000). The verification of precipitation of a numerical weather prediction model. *16th Annual conference of the S. Afr. Soc. Atmos. Sci.*
6. Clark L. and Dyson L.L. (2000). Weather systems associated with general rainfall over the Vaal Dam catchment *16th Annual conference of the S. Afr. Soc. Atmos. Sci.*

2001

1. Dyson L.L and van Heerden J. (2001). The heavy rainfall and floods over the northeastern interior of South Africa during February 2000. *S. Afr. J. Sci.* **97** 80-86p
2. Van Heerden J and Dyson L.L. (2001). The 1 September 1968 Port Elizabeth floods revisited. Can we do be better now? *17th Annual conference of the S. Afr. Soc. Atmos. Sci.*

3. Dyson L.L and Van Heerden J (2001). A tropical heavy rainfall identification system. *17th Annual conference of the S. Afr. Soc. Atmos. Sci.*
4. Dyson L.L. (2001). Rainfall forecasts, what do they mean? (2001). *Short course on flood risk analyses.* 1-3 August 2001, Univ of Pretoria, S Afr.

2002

1. Marx H.G., Dyson L.L. and van Heerden J. (2002). Verification of Rainfall Forecasts for the Vaal Dam Catchment for the Summer Rainfall Seasons of 1994 to 1998. *Article accepted by Water SA*
2. Dyson L.L and van Heerden (2002) A Model for the Identification of Tropical Weather Systems. *Water SA,**28** No. 3, 249-258p* .

CHAPTER 11
REFERENCES

Alexander W.J.R., and Van Heerden J. (1991). Determination of the risk of widespread interruption of communications by floods. *Department of Transport Research Project* **RDAC 90/16.**

Andrews D.G (2000). *An introduction to atmospheric physics.* Cambridge University Press. 229 pp

Banitz E (2001) Evaluation of short-term weather forecasts in South Africa. *Water S.A.* **27 No. 4** 489-498

Betts A.K. (1986) A new convective adjustment scheme. Part I: Observational and theoretical basis. *Quart. J. Roy. Meteor. Soc.*, **112,** 677-691.

Betts A.K., and Miller M.J. (1986) A new convective adjustment scheme. Part II: Single column tests using GATE wave, BOMEX and arctic air-mass data sets. *Quart. J. Roy. Meteor. Soc.*, **112,** 693-709.

Bradley A.A. and Smith J.A. (1994). The hydrometeorological environment of extreme rainstorms in the southern plains of the United States. *J. of Appl. Met.,* ***33,*** *1418-1431.*

Colle B.A., Westrick K.J. and Mass C.F. (1999). Evaluation of MM5 and Eta-10 Precipitation Forecasts over the Pacific Northwest during the Cool Season. *Wea. Forecasting*, Vol. **14**, p. 137-154

Cressman G. (1959). An operational objective analysis system. *Mon. Wea. Rev.*,Vol. **87,** p. 367–374.

Crimp S.J., van den Heever S.C., D'Abreton P.C., Tyson P.D. and Mason S.J. (1997). Mesoscale Modelling of Tropical-Temperate Troughs and Associated Systems over Southern Africa. *WRC Report* **595/1/97,** 395 pp.

De Coning E. (1997). Isentropic Analysis As A Forecasting Tool In South Africa. *Unpublished M.Sc. Thesis,* Univ. of Pretoria, S. Afr.

De Coning E., Forbes G.S. and Poolman E.P. (1998). Heavy precipitation and flooding on 12-14 February 1996 over the summer rainfall regions of South Africa: Synoptic and Isentropic analyses. *Ntl. Wea. Dig.* **22** 25-36.

De Villiers M.P. (1992). The role of orographic forcing on heavy precipitation over Natal. *Unpublished M.Dip. Thesis,* Tech. of Pretoria, S. Afr.

De Villiers M. P. (2000). Spring Rain Winter Cold
http://www.weathersa.co.za/stories/spring_rain2000.html

Department of Water Affairs and Forestry (1991) *Vaal Dam Pamphlet.* Issued by Communication Services, Department of Water Affairs and Forestry, Private Bag X313, Pretoria 0001.

Dunn L.B. and Horel J.D., (1994) Prediction of Central Arizona Convection. Part I: Evaluation of the NGM and Eta Model Precipitation Forecasts. *Wea. Forecasting.,* **9,** 495-507.

Dyson L.L. (2000). A dynamical forecasting perspective on synoptic scale weather systems over southern Africa. *Unpublished M.Sc. Thesis,* Univ. of Pretoria, S. Afr.

Dyson L.L and Van Heerden J. (2001). The heavy rainfall and floods over the northeastern interior of South Africa during February 2000. *S. Afr. J. Sci.* **97** 80-86p

Dyson L.L. and Van Heerden J (2002). A Model for the Identification of Tropical Weather Systems over South Africa. *Water SA,**28** No. 3, 249-258p* .

Ebert E.E. And McBride J.L. (1997). Methods for verifying quantitative precipitation forecasts: Application to the BMRC LAPS model 24-hour precipitation forecasts. *BMRC Techniques Development Report No.* ***2***, 87 pp

Ebert E.E. and McBride J.L. (2000). Verification of quantitative precipitation forecasts from operational numerical weather prediction models over Australia. *Wea. Forecasting,* Vol. **15,** p. 103-121

ECMWF (2000). Verifying precipitation forecast using upscaled observations. *ECMWF Newsletter* **87** *Spring 2000.* 9-17p

Edwards M (1997). Heavy Rain and Floods in South Africa January February 1996: Synoptic Review. Proceedings of the 1997 Fifth International Conf. on the Southern Hemisphere Meteorology and Oceanography. *Am. Meteorol. Soc.* 9-10p.

Edwards M (2000). Personal communication. Manager: Aviation Forecasting Services. South African Weather Service, Johannesburg International Airport.

Estie K.E. (1981). The Lainsburg flood disaster of 25 January 1981. *S. Afr. Weath.Bur. News Lett.* **383**, 19-32.

Fienberg S.E. (1980). *The analysis of cross-classified categorical data.* MIT Press, Cambridge, MA, 198 pp.

Forsdyke A.J. (1949). Weather forecasting in tropical regions. *Geophys. Mem.* **82** British Meteor. Office, 82 pp.

Ghelli A. and Lalaurette F (2000). Verifying precipitation forecasts using upscaled observations. *ECMWF Newsletter Nr.* ***87*** *– Spring 2000,* p. 9-17

Gordon A., Grace W., Schwerdtfeger P. and Byron-Scott R. (1998). *Dynamic Meteorology. A Basic Course.* Arnold Publishers. 325 pp.

Hammon O. and Wilson C. (1993). Poor precipitation forecasts from the limited area model. *Fore Res Dev Tech Report* ***74****, 1993.*

Harrison M.S.J. (1983). A generalised classification of South African summer rain-bearing synoptic systems. *J. Climatology* **4**, 547-560.

Harrison M.S.J., (1986). A synoptic climatology of South African rainfall variations. *Unpublished PhD Thesis*, University of Witwatersrand, 341 pp.

Harrison M.S.J. (1988). Rainfall and precipitable water relationships over the central interior of South Africa. *S. Afr. Geographical J.* **70** No. 2 100-111

Hayward L.Q. and Van den Berg H.J.C. (1968). Die Port Elizabeth-Stortreens van 1 September 1968. *S. Afr. Weath. Service Newslett.* **234,** 157-169

Holton J.R. (1992). *An Introducion to Dynamic Meteorology*. Academic Press. 511 pp.

Houze R.A., Smull B.F. and Dodge P. (1990). Mesescale organization of springtime rainstorms in Oklahoma. *Mon. Wea Rev., **118**, 613-654.*

Huschke R.E. (1959). *Glossary of Meteorology*. Am. Meteorol. Soc. 638 pp.

Janjic' Z.I. (1984). Non-linear advection schemes and energy cascade on semi-staggered grids. *Mon. Wea. Rev.*, **112,** 1234-1245.

Janjic' Z.I. (1990). The step-mountain coordinate: Physical package. *Mon. Wea. Rev.*, **118,** 1429-1443.

Janjic' Z.I. (1994). The step-mountain eta coordinate model: Further developments of the convection, viscous sublayer, and turbulence closure schemes. *Mon. Wea. Rev.*, **122**, 927-945

Jury M.R., Lindesay J.A. and Wittemeyer I. (1993). Flood episodes in central South Africa from satellite and ECMWF data. *S. Afr. J. Sci.*. **89**, 263-269.

Karoly D.J. and Vincent D.G. (1998). Meteorology of the Southern Hemisphere. **27** N0. 49. *Am. Met. Soc.* 410 pp

Kovacs Z.P.J., Du Plessis D.B., Bracher P.R., Dunn P. and Mallory G.C.L. (1985). Documentation of the 1984 Domoina Floods. *Department of Water Affairs Technical Report* **122.**

Landman W.A. (1997). A study of rainfall variability of South Africa as revealed by multivariate analysis. *Unpublished MSc Thesis.* Univ. of Pretoria, S. Afr

Lindesay J.A. and Jury M.R. (1991). Atmospheric controls and characteristics of a flood event in central South Africa. *Int. J. of Clim.* **11**, 609-627.

Marx H.G., Dyson L.L. and van Heerden J. (2002). Verification of Rainfall Forecasts for the Vaal Dam Catchment for the Summer Rainfall Seasons of 1994 to 1998. *Article accepted for publication, Water SA*

Mesinger F. (1984). A Blocking technique for representation of mountains in atmospheric models. *Riv. Meteor. Aeronautica,* **44,** 195-202.

Mesinger F., Janjić Z. Ničković S., Gavrilov D., and Deaven D. (1988). The Step-mountain Coordinate: Model description and performance for cases of Alpine lee cyclogenesis and for a case of an Appalacian redevelopment. *Mntly. Wea. Review* **116** 1493-1518.

Mittermaier M.P. AND Terblanche D.E. (2000). The integration of daily rain gauge and radar rainfall estimates for the Liebenbergsvlei catchment, north-eastern Free State. *(Submitted to S. Afr. J. Sci.)*

Murphy A.H. (1995). A coherent method of stratification within a general framework for verification. *Mon. Weather Rev.* **123** 1582-1588.

Murphy A.H. and Epstein E.S. (1967) Verification of probabilistic predictions: A brief review. *J. Appl. Meteorol.* **6** 748-755.

Murphy A.H. and Winkler R.L. (1984). Probability forecasting in meteorology. *J. Am. Stat. Assoc.* **79** 489-499.

Murphy A.H., Hsu W., Winkler R.L. and Wilks D.S. (1985). The use of probability in subjective quantitative precipitation forecasts: Some experimental results. *Mon. Weather Rev.* **113** 2075-2089.

Murphy A.H. and Winkler R.L. (1987). A general framework for forecast verification. *Mon. Weather Rev.* **115** 1330-1338.

Poolman E.P. and Terblanche D. (1984). Tropiese siklone Demonia en Imboa. *S. Afr. Weath. Service News Lett.* **420,** 37-45

Preston-White R.A. and Tyson P.D. (1993). *The Atmosphere and Weather of Southern Africa.* Oxf. Univ. Press. 374 pp.

Rautenbach C. J. de W. (1996). The construction of a data point concentration dependent weight function for interpolation to rainfall grid fields. *Die S. Afr. Tydskrif vir Natuurwetenskap en Tegnologie.* **4**, 168-171

Riehl H. (1979). *Climate and Weather in the Tropics.* Academic Press. 611 pp.

Rogers R.R. and Yay M.K. (1989). *A short Course in Cloud Physics.* Pergamon Press. 293 pp.

Sanders F. (1963). On subjective probability forecasting. *J. Appl. Meteorol.* **2** 191-201

Scholz E.P. (2000). Personal communication. Assistant Director: Weather Forecasting. S. Afr. Weath. Bur., Private Bag X97, Pretoria 0001.

Schulze B.R. (1965). General Survey. Climate of South Africa. WB28. S. Afr. Weath. Bur., Private Bag X97, Pretoria 0001.

Schulze G.C. (1989). Seasonal variations in summer rainfall over the summer rainfall areas of South Africa. *Unpublished MSc dissertation.* University of Pretoria.

Stanski H.R, Wilson L.J. and Burrows W.R. (1989). Survey of common verification methods in meteorology. World Weather Watch Technical Report no.**8** *WMO/TD No.385.*

Strydom P.H. and Nel C. (1996). Die Weer van Julie 1996. *S. Afr. Weath. Service Newslett.* **568,** 22-26

Sutcliffe R.C. (1953). The formation of new anticyclones. *Met Mag* **82** 163-175

Taljaard J.J. (1985). Cut-off lows in the South African region. *S. Afr. Wea. Bur. Technical Pap.* **14**, 153 pp. S. Afr. Weath. Bur., Private Bag X97, Pretoria, 0001

Taljaard J.J. (1986). Change of rainfall distribution and circulation patterns over southern Africa in summer. *J. Climatology* **6**, 579-592.

Taljaard J.J. (1994). Atmospheric Circulation Systems, Synoptic Climatology and Weather Phenomena of South Africa. Part 1: Controls of the weather and climate of South Africa. *S. Afr. Weath. Bur. Technical Pap.* **27**, 45pp. S. Afr. Weath. Bur., Private Bag X97, Pretoria, 0001

Taljaard J.J. (1996). Atmospheric Circulation Systems, Synoptic Climatology and Weather Phenomena of South Africa. Part 6: Rainfall in South Africa. *S. Afr. Weath. Bur. Technical Pap.* **32**, 98pp. S. Afr. Weath. Bur., Private Bag X97, Pretoria, 0001.

Tennant W.J. (1999). Personal Communication. Research Group for Seasonal Climate Studies (RGSCS), S. Afr. Weath. Bur., Pretoria.

Tennant W.J. and van Heerden J. (1994). The influence of orography and local sea-surface temperature anomalies on the development of the 1987 Natal floods: a general circulation model study. *S. Afr. J. Sci.* **90**, 45-49.

Terblanche D.E. (1996). A Simple Digital Processing Method to simulate linear and quadratic responses from a radar's logarithmic receiver. *J. Tech.*, **13(2)**, 533-538.

Terblanche D.E. (1996). Digital Signal Processing of Data from Conventional Weather Radar: The Displace Method. *Unpublished Ph D Thesis* University of Pretoria, 86pp.

Terblanche D.E., Hiscutt F.O. and Dicks D.J., (1994). The upgrading and performance testing of the Bethlehem weather radar. *S. Afr. J. Sci.*, **90**, 588-595.

Terblanche D.E. and Mittermaier M.P. (2001). A state-of-the-art weather radar networking system for South Africa. metsys.weathersa.co.za/radardetail.html

Thompson B.W. (1957). Some reflections on equatorial and tropical forecasting. *East Africa Meteor. Dept.* **7** 14pp

Triegaardt D.O., Terblanche D.E., van Heerden J. and Laing M.V. (1988). The Natal floods of September 1987. *S. Afr. Weath. Bur. Tech. Paper* **19**, 62 pp. S. Afr. Weath. Bur., Private Bag X97, Pretoria 0001.

Triegaardt D.O., van Heerden J. and Steyn P.C.L. (1991). Anomalous precipitation and floods during February 1988. *S. Afr. Weath. Bur. Tech. Paper* **23**, 25 pp. S. Afr. Weath. Bur., Private Bag X97, Pretoria 0001.

Van Heerden J. and Hurry L. (1987). *South Africa's weather patterns.* Acacia. 95 pp

Van Heerden J. and Steyn P.C.L. (1999). Weather radar measurement of rainfall as well as hydrological and other applications of weather radar. Draft final report to WRC.

Van Heerden J. Terblanche D.E. and Schulze G.C. (1988). The southern oscillation and South African summer rainfall. *J. Climatol., **8**, 577-597.*

Wallace J.M. and Hobbs P.V. (1977). *Atmospheric Science. An Introductory Survey.* Academic Press. 467 pp.

Wilks D.S. (1995). *Statistical Methods in the Atmospheric Sciences. An Introduction.* Academic Press, San Diego, 467pp.

Zhao, Q, and Carr F.H. (1997). A prognostic cloud scheme for operational NWP models. *Mon. Wea. Rev.*, **125**, 1931-1953.

Other related WRC reports available:

Weather radar measurement of rainfall for hydrological and other purposes

J van Heerden & PCL Steyn

This project was initiated soon after the installation, near Bethlehem, of an MRL-5, Russian-built dual-band (S, X) weather radar. The purpose was to investigate the acquisition of quantitative rainfall data by the radar at temporal and spatial scales (and resolution) suitable for hydrological applications. To facilitate this, a high-density network of 20 recording rain gauges, covering an area of approximately 20 km^2, was established about 60 km east of the MRL-5 radar. Measurements permitted radar and gauge-derived rainfall estimates to be compared on an areal and on a pixel-by-pixel basis. Comparisons revealed that radar had good potential of providing accurate rainfall information, both at wide-ranging spatial (down to pixel, i.e. 1 km^2 resolution) and temporal (season down to event) scales. Studies on a large number of individual rainfall events supported the use of the conventional Marshall-Palmer Z-R relationship for converting the radar reflectivity factor (Z) to rain rate (R). There were, however, indications that event- and/or storm-based classification might be useful for assigning reliability ratings to radar-derived rainfall for different classes of events

Report Number: 693/1/99 **ISBN 1 86845 538 6**

TO ORDER: Contact **Rina** or **Judas** -	Telephone No:	012 330 0340
	Fax Number:	012 331 2565
	E-mail:	publications@wrc.org.za

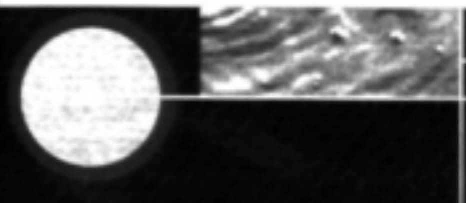

Water Research Commission
Private Bag X03, Gezina, 0031, South Africa
Tel: +27 12 330 0340, Fax: +27 12 331 2565
Web: http://www.wrc.org.za

1868459373